Scuola Internazionale Superiore di Studi Avanzati - Trieste

Beyond the Standard Model with Orbifold Field Theories

Thesis submitted for the degree of

Doctor Philosophiæ

Candidate:
Andrea Wulzer

Supervisor:
Marco Serone

October 2005

SISSA – Via Beirut 2-4 – 34014 TRIESTE – ITALY

Beyond the Standard Model with Orbifold Field Theories

Thesis submitted for the degree of

Doctor Philosophiæ

Candidate:
Andrea Wulzer

Supervisor:
Marco Serone

October 2005

Contents

Introduction

The Standard Model of Electroweak and Strong interactions (SM) is an extremely successfull theory describing all known processes of high energy physics. Its validity has been confirmed by a huge amount of experiments, which have tested the SM predictions at an impressing level of accuracy. Most likely, however, the SM cannot provide a final description of Nature, and it has to be interpreted as an effective description, valid up to a certain scale Λ_{SM}, of a more fundamental (and yet unknown) theory. Leaving aside the recent developments in neutrino physics and in cosmology, which however provide very interesting indications of new physics beyond-the-SM, there are several theoretical reasons for which the SM should not be Fundamental. First of all, it does not incorporate a satisfactory description of Quantum Gravity, so that its cut-off Λ_{SM} is upper–bounded by the Planck mass $M_P \sim 10^{19}$GeV. Secondly, the origin of its many parameters, such as the Yukawa couplings, with large hierarchies among each other, is completely unexplained. Moreover, the structure of $SU(2) \times U(1)_Y$ quantum numbers in the hadronic and leptonic sectors is suggestive of a more fundamental Grand-Unified Theory (GUT) in which quarks and leptons and their (Strong and Electroweak) interactions are treated on an equal footing. The occurrence, in the SM, of a rough running coupling unification at a scale $M_{GUT} \sim 10^{15}$GeV, and of a more precise unification at $M_{GUT} \sim 10^{16}$GeV in its Minimally Supersymmetric extention (MSSM) suggest $\Lambda_{SM} \leq 10^{15-16}$GeV.

There is an argument, however, suggesting that the SM cut–off cannot be as high as the Planck or GUT scale, but it should be at much more low energies, namely in the TeV range, so that new physics should be discovered in the next–future experiments to be performed at the LHC collider. This argument can be formulated as follows. If the SM is seen as an effective field theory, its parameters, though affected by divergences and therefore not predicted by the model, should satisfy a naturalness criterion. Namely, their size should be of the same order of magnitude of the quantum corrections they receive when the divergence is regulated by the physical cut–off Λ_{SM}. This is the same as assuming the theory to become non–

perturbative at the cut–off scale. Basically, one requires the high energy unknown physics not to influence too much the low energy one which is described by the effective theory. If this requirement is not satisfied, an "unnatural" cancellation should be imposed among high and low energy physics contributions, resulting in a "fine tuning" of the bare parameter versus its quantum correction, which should cancel and give rise to the small physical value. In the SM, the one-loop correction to the squared Higgs mass m_H^2 is given by

$$\delta m_H^2 = \frac{3G_F}{\sqrt{2}\pi^2}\left(m_t^2 - \frac{1}{2}m_W^2 - \frac{1}{4}m_Z^2 - \frac{1}{4}m_H^2\right)\Lambda_{SM}^2\,, \qquad (0.0.1)$$

in terms of Fermi constant $G_F \sim 10^{-5}\text{GeV}^{-2}$, the W and Z gauge bosons masses and the mass of the top quark $m_t \sim 174\text{GeV}$, which is the only fermion giving a sizable contribution. Since it receives quadratically divergent one–loop contributions, the natural size of the Higgs mass is roughly of the order of Λ_{SM}, so that Λ_{SM} cannot be as high as M_{GUT} or M_P. With such an high value of m_H, indeed, the SM would not be internally consistent, or at least it will become non–perturbative near the TeV scale. A value of $m_H \leq$ TeV is indeed required for the four gluons scattering process not to violate the Unitarity bound. One then concludes that $m_H \sim \Lambda_{SM} \sim$ TeV. The impossibility of Λ_{SM} to be M_P if m_H (whose size is in the end fixed by the Electro–Weak Symmetry Breaking (EWSB) scale $v = 246\text{GeV}$) is in the TeV range is usually indicated as the "Hierarchy Problem" of the SM. The hierarchy one refers to is in this case the 15 orders of magnitude difference among m_H and M_P.

After the completion of the ElectroWeak Precision Test (EWPT) program, a more modest, but more concrete and experimentally motivated version of the problem of hierarchies, the so–called "Little Hierarchy Problem" [1] (see also [2]) has been formulated. From EWPT, in which quantum effects are precisely measured, an upper bound for m_H can be extracted from the contributions of virtual Higgses to the observables. If data are analyzed in the pure SM, one has $115\text{GeV} \leq m_H \leq 250\text{GeV}$, the lower bound coming of course from direct production. The same set of data, however, can also be used to give upper bounds on the scale of new physics Λ, whose effects can be parametrized in terms of an effective Lagrangian

$$\mathcal{L}_{eff} = \mathcal{L}_{SM} + \sum_{i,p} \frac{c_{i,p}}{\Lambda^p}\mathcal{O}_i^{4+p}\,,$$

containing operators of dimension higher than four whose adimensional coefficients, as implied by naturalness, are assumed to be of order one and $\Lambda \sim \Lambda_{SM}$. One finds, for various dimension six operators, $\Lambda \geq 10\text{TeV}$ [1]. [1] Assuming $m_H \leq 200\text{GeV}$, as suggested by data, Eq. (0.0.1) can be rewritten as

$$\delta m_H^2 = (115\text{GeV})^2 \left(\frac{\Lambda_{SM}}{400\text{GeV}}\right)^2 ,$$

since all the contributions but the top one can be neglected. If Λ_{SM} is identified with Λ, then, one has a one order of magnitude mismatch, a little hierarchy, between m_H^2 and its one–loop correction δm_H^2. Since the hierarchy problem comes in the Higgs sector, which is responsible for EWSB and, by the way, is still experimentally unproven, it suggests us to look for an alternative mechanism to break the SM Electroweak symmetry.

Overcoming the (big or little) hierarchy problem of the SM has been in the last decades one of the main tasks and guiding lines of model building Beyond-the-SM. Recent experimental results, however, indicating the cosmological constant λ not to be exactly zero, but 15 orders of magnitudes smaller than m_H, seem to demonstrate that the fine–tuning exists in Nature. It has then been suggested to abandon the Hierarchy paradigm in favor of an "anthropic" selection [3] of the many vacua the theory is assumed to possess [4]. It is commonly believed, however, that explaining the size of λ could be a Quantum Gravity problem, on which few can be said, while the quantum stability of m_H should be ensured by some (more experimentally and theoretically accessible) TeV–energy new physics.

Clearly, the problem of hierarchies comes into the SM due to the presence of a fundamental scalar Higgs field. For vector bosons and fermions, indeed, there are symmetries (respectively, the gauge and the chiral one) protecting their masses from quadratic divergences. Most of the attempted solutions, indeed, are based on changing the nature of the Higgs field which may not be fundamental (as in Technicolor models [5]) or may be part of a multiplet of fields which also contains fermions (Supersymmetry) or gauge bosons (Gauge–Higgs Unification), so that its mass is protected by chiral or gauge symmetries. The Higgs has also, more recently, been supposed to be a pseudo–Goldstone boson [6] which takes mass at two–loop order only (Little Higgs [7, 8]) or not to exist at all (Higgsless theories [9]). Supersymmetry (SUSY), and in particular the MSSM, is at present one of the best candidate for physics beyond-the-SM. It reproduces without problems the EWPT data and, thanks to the well–known boson–fermion cancellation, the one–loop correction to

[1] Nothing forbids, in perturbative extensions of the SM, the coefficients $c_{i,p}$ to be smaller then one. This is what happens, for instance, in the MSSM, and permits the SUSY scale to evade this bound.

the lightest Higgs mass m_H reads [2]

$$\delta m_H^2 \sim \frac{G_F m_t^2}{\sqrt{2}\pi^2} m_{ST}^2 \log \frac{\Lambda_{SB}}{m_{ST}}\,, \qquad (0.0.2)$$

where m_{ST} is a suitable average of the stop masses and Λ_{SB} is the supersymmetry breaking scale at which some mechanism of SUSY breaking and transmission generate the masses of superpartners. Note that the quadratic SM divergence is cut–off at the stop mass scale m_{ST} and m_H is only logarithmically sensitive to the high energy physics, so that the hierarchy problem is solved. The problem comes now, however, from the Higgs being too massive, $m_H \geq 115\text{GeV}$, and not too light as in the SM. A famous tree–level relation of the MSSM states that the lightest Higgs should be lighter than the Z boson and to overcome this bound one has to rely on quantum corrections which increase m_H as compared to m_Z. The increasing is however only logarithmic in m_{ST} while Eq. (0.0.2) is quadratically sensitive to it. This reintroduces a fine–tuning in Eq. (0.0.2). More detailed analysis confirm this simple argument and show that a factor 20 cancellation must occur in the Higgs mass. This is the little hierarchy of the MSSM, whose size is the same as the SM one.

Motivated by the above considerations, many efforts have been performed in the last years to find alternatives to supersymmetry for solving the (little or big) hierarchy problem. In this context, models with large extra dimensions (ED) have been extensively studied. In this scenario, as suggested by string theory which somehow "predicts" ED, extra space-like dimensions are supposed to exist beside the four ordinary ones. The extra dimensions, clearly, should be small enough (compactified) or somehow hidden not to conflict with observations. There are several different ways in which ED can be employed to stabilize the EWSB scale. In the ADD scenario [10], for instance, flat extra dimensions with sub–millimeter compactification radiaii, in which gravity only can propagate, were proposed to explain the weakness of gravity (*i.e.* the big value of M_p) through the fact that it is "diluted" in the ED. Another intersting possibility is to consider truncated AdS_5 spaces [11] and solve the Plank-Weak hierarchy through the exponential red-shift factors which come from the AdS_5 metric. Notably, realistic models for EWSB can be formulated in this set–up [12], which also possess an extremely interesting interpretation, based on the AdS/CFT correspondence [13], in terms of a strongly-interacting $4D$ theory, then realizing a computable version of the composite Higgs

[2]This an extremely simplified discussion, which can be found in [2]; $\tan\beta \ll 1$ is assumed and the influence on stop masses of gluino exchange have been neglected.

idea. Large flat ED, but not as large as in the ADD scenario, can be also used for model-building in a slightly different manner, exploiting the possibility of breaking symmetries in the compactification. In so doing, the scale of symmetry breaking is stabilized at the compactification scale $1/R$. This possibility [14] (see also [15] for a simple, interesting, model) was first advocated to break supersymmetery, so that a compactification scale $1/R \sim \mathrm{Te}V$ was needed. The possibility was also discussed [16] to use ED, with $1/R \sim M_{GUT}$, for breaking GUT groups.

In the context of $\mathrm{Te}V$ Extra–Dimensions, a very interesting possibility for stabilizing the EWSB scale is provided by the so–called Gauge–Higgs Unification (GHU) mechanism, which was proposed long ago [17, 18, 19] and recently received renewed interest, in both its non–supersymmetric [7, 20, 21, 22, 23, 24, 25] and supersymmetric [26, 27] versions. In GHU models, the SM scalar Higgs doublet comes from the extra–dimensional components of the gauge fields associated to an extended electroweak symmetry propagating in the ED. The EWSB scale is stabilized by the ED gauge invariance or, stated in a different way, by the fact that the scalar Higgs field is part of the ED gauge multiplet, whose mass is protected from large high energy contributions. Note that gauge theories in ED have dimensionful couplings, so that they become non–perturbative at an energy scale Λ which is typically of the order of $10/R$. The $\mathrm{Te}V$ ED models, such as the GHU ones, are then effective descriptions of a more fundamental (maybe String) theory, and their validity is upper–bounded from the 10 $\mathrm{Te}V$ energy scale. Moreover, they do not include any modified description of gravity, so that they cannot address the Big hierarchy problem. However, they can solve the little one if, as in the GHU case, the EWSB scale is insensitive to the high energy cut–off Λ. Of course, these models are less ambitious then other extentions of the SM, since their validity is upper–bounded at a not so high scale. Note that, however, a realistic model of this kind would contain all the new physics effects which could be tested with the LHC energies.

The original GHU model [17] was, in modern language, a six dimensional gauge theory compactified on the 2–sphere S^2, with a suitable gauge flux for breaking the original group down to the SM one. The intent was not only to obtain the Higgs scalar field from the six dimensional gauge bosons, but also to realize $SU(2)$ and $U(1)_Y$ couplings unification, by considering rank two simple Lie groups in six dimensions. By inspection, the exceptional $\mathbf{G}_2$ group was found to be the more realistic possibility, giving rise to a tree–level prediction for the weak mixing angle $\sin^2\theta_W = 1/4$, which was compatible, at that time, with the experimental results. At present, of course, such a value of θ_W is ruled out, so that one must rely on sizable quantum corrections for obtaining Electro–Weak unification in this way. Moreover, a negative Higgs mass term is present at tree–level in the Manton's model, so that the Higgs mass and the EWSB scale are directly related to the inverse radius of the sphere. This would result, with the present–day experimental data, in an unacceptably small compactification scale. Due to the experimental failure (and the difficulties in obtaining a realistic fermion content), GHU models were abandoned for a long time. As we will better discuss in the following, the introduction of new (stringy–inspired) tools in the ED context gave a new twist and perspective to the GHU construction. At present, the simplest framework in which this idea can be implemented are five–dimensional ($5D$) $SU(3)$ gauge theories compactified on the $S^1/\mathbf{Z}_2$ orbifold [28]. These models have been studied in great detail and shown [24] to posses all qualitative features which are needed to construct realistic extentions of SM. They fail, however, at the quantitative level, since they predict too a small Higgs boson mass, smaller than the W boson one. Basically, this failure is due to the smallness of the Higgs quartic coupling, which is indeed one–loop generated in these models.

One of the main topics treated in this thesis, along the lines of [25] (see also [29]), is the possibility of obtaining realistic values for the Higgs mass from $SU(3)$ GHU models in $6D$, compactified on the $T^2/\mathbf{Z}_N$ orbifolds. In $6D$, indeed, the possibility opens up of having a tree–level quartic coupling for the Higgs, while in $5D$ models it is one–loop generated, so that the Higgs–W mass–ratio is expected to be higher in the $6D$ case as compared to the $5D$ one. In the following, $6D$ $T^2/\mathbf{Z}_N$ models, based on an $SU(3)$ gauge group which is broken to $SU(2) \times U(1)_Y$ by the orbifold projection, are explored. Orbifold projections are found to exist (for the $T^2/\mathbf{Z}_{3,4,6}$ cases only) which leave a single Higgs doublet in the low–energy theory. In the single Higgs cases, the aforementioned tree–level quartic coupling has a very strong effect. Assuming EWSB to occur, the Higgs mass in these models is predicted at tree–level to be twice the W–boson one

$$m_H \;=\; 2\, m_W\,,$$

which is an encouraging result. Differently from the $5D$ case in which the Higgs potential is completely finite, however, divergences can be found in the Higgs mass term, due to the appearance of a "tadpole" operator [23, 30], localized at the orbifold fixed points, which is proportional to the component of the gauge field–strength in the hypercharge direction. The appearance in the quadratic part of the field–strength of a bilinear term in the Higgs field, which is also responsible for the arising of the quartic coupling in the tree–level action, makes the tadpole contribute to the

Higgs mass term. Since it is generated at one loop with a quadratically divergent coefficient, the tadpole operator may destabilize the Higgs mass and reintroduce an hierarchy problem. It turns out, by performing an explicit one loop calculation, that the tadpole operator always arises in single–Higgs models and even an accidental cancellation of the leading divergence in its coefficients cannot be achieved. The tadpole, then, cannot be locally cancelled, but a global cancellation of its integral over the ED can be realized in the $SU(3)$ $T^2/\mathbf{Z}_4$ model. In this case, similarly to what happens for a globally vanishing FI term in $5D$ supersymetric theories [31], its presence does not trigger EWSB and does not affect the mass of the Higgs field. In complete analogy with $6D$ supersymmetric theories with localized FI terms [32], the Higgs wave function is distorced by the presence of the tadpole and displays localization or delocalization at the fixed points.

In the framework of GHU models and, more generally, in the context of extra–dimensional field theories, orbifold compactification [33] is a particularly useful tool. It provides, indeed, a simple way to get $4D$ chirality and symmetry breaking. On orbifolds, moreover, localized $4D$ fields are commonly introduced in any number at the fixed points and this flexibility in the $4D$ field content is a further reason for which orbifolds are so popular. Localized $4D$ states (we will focus on spinors in the following) are generally thought to have a stringy origin, as twisted states arising on a brane located at the fixed point, even though the existence of a stringy UV completion of the ED model, with the appropriate content of localized states, is in general doubtful. Alternatively, in a purely field theoretical context, extra–dimensional fermions with localized profile were shown to arise [34] from topological defects. More recently, in an higher dimensional field theory context, localization of fields in both flat and warped space has been considered [35], [31, 32, 36].

In this thesis, the possibility is discussed of getting localized $4D$ chiral fermions in a very natural manner, as an effect of the resolution of the orbifold singularities [37, 38]. Orbifolds, indeed, are singular spaces, the singularities being located at the orbifold fixed points. As also suggested by string theory, orbifolds should be always seen as smooth "resolving" spaces, in the particular limit in which the gravity and/or gauge connection backgrounds approach a singular profile. In [37, 38], resolved versions of the $\mathbb{C}/\mathbf{Z}_N$, $T^2/\mathbf{Z}_N$ and $S^1/\mathbf{Z}_2$ orbifolds are constructed and a $6D$ chiral fermion field compactified on the resolved space. The wave functions in the internal space of the $4D$ chiral zero–modes arising from the $6D$ fermion (all of them but the ones which are constant and correspond to the usual orbifold ones) are found to be peaked around the resolved singularities and to become completely localized in the orbifold limit. Moreover, due to an ambiguity in defining the resolving space, many (but not all) brane fields distributions are found to originate from a single ED field, so that they have a "unified" origin. In the following, the "allowed" bulk–brane field distributions one can get in this manner are classified. We believe that, due to aforementioned interpretation, the brane field spectra we will work out are distinguished, and "favored", since they admit such a simple resolution. As already mentioned, fermion localization have been shown in the literature to arise on topological defects in various way, so that other localized fermion spectra can clearly be obtained. The localization phenomenon observed here is somehow analogous, as it is induced by the presence of a background field with non trivial profile along the extra dimensions. What is peculiar of our case is that this background is precisely the one needed for resolving the orbifold singularity and there is no need of introducing extra fields or extra dynamics.

This thesis is organized as follows. In the first two introductive chapters several topics on extra dimensional field theories are discussed. The idea is not, of course, to provide a complete introduction to the subject but, on the contrary, to discuss, in a hopefully ordered and self–consistent manner, some of the concepts and technical instruments that will be employed in Chapters 3 and 4. For what concerns Chapter 1, it is devoted to compactification on smooth spaces, and particularly on the simple S^1 circle and T^2 torus. Those spaces are defined in Sect. 1.2 and 1.3. Scherk–Schwarz compactification and symmetry breaking is also discussed. As an introduction to the Kaluza–Klein compactification procedure and to fix notations, complex scalar compactification on a general d–dimensional compact manifold $\mathcal{C}_d$ is studied in Sect. 1.1. When considering GHU models, we will be dealing with gauge theories in extra dimensions. For this reason, we discuss this subject in detail, focusing our attention, in particular, on the structure of linearly and non–linearly realized gauge symmetries which are present in the resulting $4D$ theory, and on the gauge–fixing procedure which is required to perform quantum computations. This is discussed in Sect. 1.4 and 1.5 for the S^1 and T^2 cases, respectively. Sect. 1.6, finally, is devoted to fermion fields. When studying spinors on resolved orbifolds, we will need the general discussion, proposed in Sect. 1.6.2, of fermions compactified on a general $2D$ manifold $\mathcal{C}_2$. In chapter 2, orbifold compactification is considered. After a general discussion of orbifolds and their capability of breaking symmetries, the simple $S^1/\mathbf{Z}_2$ and $T^2/\mathbf{Z}_N$ orbifolds are introduced, respectively, in Sect. 2.1 and 2.3. Gauge theories on $S^1/\mathbf{Z}_2$ and $T^2/\mathbf{Z}_N$ are considered in Sect. 2.2 and 2.5. In Sect. 2.4, the wave function basis on $T^2/\mathbf{Z}_N$ is derived, while Sect. 2.6 contains a general discussion of Feynman rules on orbifolds. The prescription is found for obtaining orbifold Feynman rules out of the covering space ones. This technique turns out to be extremely useful when performing quantum computations in orbifold field theories. Chapter 3 is devoted to the previously discussed 6D GHU models, along the lines of [25]. Fermion localization from orbifold resolution is discussed, as in [37, 38], in Chapter 4. Finally, two short technical appendices on Jacobi theta function and $2D$ spaces with $O(2)$ isometry are included.

Chapter 1

Smooth Extra Dimensions

Field theories with more than three spatial dimensions were introduced long ago [39], as a tool for obtaining an unified description of gravity and gauge interactions. Many attempts have been performed [40] to make, through compactification, $4D$ gauge symmetries arise from the general coordinate transformation invariance of the parent ED theory. Due to the failure of this original program, ED field theories were forgotten for many years, until the invention of string theory, which gave a new perspective, and a renewed interest, to this subject. In string theory, indeed, extra–dimensions are required by consistency and the existence of an energy range in which the physics is extra–dimensional and the field theory description still appropriate seems possible, or even favored. Moreover, several technical tools (like orbifolds), introduced in the context of string theory, result extremely useful when applied to the old ED ideas, and permit to obtain (semi–)realistic models. In these first two chapters, we review several concepts and technical tools which are commonly used for model–building in ED. In the first one, compactification on smooth spaces is considered while orbifolds are discussed in the second one.

1.1 Scalar Field

In this chapter we will consider quantum field theories in a D–dimensional ($D = 4 + d$) space–time described by the coordinates $X^M = (x^\mu, y^i)$, with $M = 0, \dots, D$, $\mu = 0, \dots, 3$ and $i = 1, \dots, d$. We restrict to factorized spaces of the form $\mathcal{M}_4 \times \mathcal{C}_d$, where $\mathcal{M}_4$ is the ordinary $4D$ Minkowski space–time and $\mathcal{C}_d$ is a compact orientable d–dimensional manifold, so that the line element assumes the form

$$ds_D^2 = G_{MN} dX^M dX^N = \eta_{\mu\nu} dx^\mu dx^\nu - ds_d^2 \,, \tag{1.1.1}$$

where $ds_d^2 = g_{i,j}dy^i dy^j$ is the line element on $\mathcal{C}_d$. The D–dimensional metric G has $(+,-,\dots,-)$ signature, so that $\eta = \mathrm{diag}(+,-,-,-)$ and g is euclidean. In the following, we will mainly be dealing with the cases $d = 1$ and $d = 2$. As an example of the compactification procedure, consider a complex scalar field $\Phi(x,y)$ in D dimensions, with Lagrangian

$$\mathcal{L}_D(x,y) = \sqrt{G}\left(D_M\Phi^\dagger D^M\Phi - m^2\Phi^\dagger\Phi + \mathcal{L}_D^{int}(\Phi)\right) ,$$

where $G = |\det\{G_{MN}\}|$, and the indices are raised and lowered with the D–dimensional metric G_{MN}. In order to get the effective $4D$ theory, the field must be expanded as

$$\Phi(x,y) = \sum_n \phi_n(x) f_n(y) , \tag{1.1.2}$$

where the $4D$ fields ϕ_n are the relevant degrees of freedom for the 4 dimensional effective description and the f_n's are some kind of Fourier basis on $\mathcal{C}_d$. The $4D$ effective Lagrangian is obtained by integrating $\mathcal{L}_D$ in the extra dimensions. For the quadratic part, one has:

$$\begin{aligned}&\mathcal{L}_4(x,x) = \int_{\mathcal{C}_d} dy \mathcal{L}_D(x,y) = \\ &\sum_{n,k}\left[\partial_\mu\phi_n^\dagger\partial^\mu\phi_k \int_{\mathcal{C}_n} dy\sqrt{g} f_n^\dagger f_k - \phi_n^\dagger\phi_k \int_{\mathcal{C}_n} dy\sqrt{g}\left(m^2 f_n^\dagger f_k - f_n^\dagger D^i D_i f_k\right)\right] ,\end{aligned} \tag{1.1.3}$$

where $g = |\det\{g_{ij}\}|$, and the covariant derivative is now the d–dimensional (dD) one, constructed with the dD Levi–Civita connection. The indices are raised and lowered with the dD euclidean metric g. The wave functions f_n are chosen to be the solutions to the d–dimensional Klein–Gordon equation

$$D_i D^i f_n + {m_n}^2 f_n = 0 , \tag{1.1.4}$$

for all allowed values of m_n. Note that the f_n's form a complete set for functions on $\mathcal{C}_d$, and m_n^2 is never negative, since $D_i D^i$ is a negative definite hermitean operator. From Eq. (1.1.4), the orthogonality of two wave functions with different mass trivially follows, since

$$(m_k^2 - m_n^2)\int_{\mathcal{C}_d} dy\sqrt{g} f_n^\dagger f_k = \int_{\mathcal{C}_d} dy\sqrt{g}\left[f_k D_i D^i f_n^\dagger - f_n^\dagger D_i D^i f_k\right] = 0 ,$$

while independent wave functions with equal mass can always be made orthogonal since the Klein–Gordon equation is linear. By suitably choosing the normalization, one has

$$\int_{\mathcal{C}_d} dy\sqrt{g} f_n^\dagger f_k = \delta_{n,k} ,$$

so that Eq. (1.1.3) assumes the very simple diagonal form

$$\mathcal{L}_4(x) = \sum_n \left[\partial_\mu \phi_n^\dagger \partial^\mu \phi_n - (m^2 + {m_n}^2)\phi_n^\dagger \phi_n\right] , \tag{1.1.5}$$

and describes a Kaluza–Klein tower of massive scalars with mass

$${M_n}^2 = m^2 + {m_n}^2 .$$

The values assumed by m_n clearly depend on the detailed form of $\mathcal{C}_d$.

With the mode expansion (1.1.2), then, the Feynman propagator in the $4D$ momentum space assumes the very simple diagonal form

$$\langle (\phi_n(p))^\dagger \phi_k(p) \rangle = \frac{i}{p^2 - {m_n}^2 - m^2 + i\epsilon}\delta_{n,k} ,$$

which is simply obtained from the scalar propagator on the D–dimensional Minkowski space by replacing the D–dimensional squared momentum $P^2 = p_\mu p^\mu - p_i p^i$ with $p_\mu p^\mu - {m_n}^2$. For what concerns interactions, on the contrary, Feynman rules are complicated on our general space $\mathcal{C}_d$. For $\mathcal{L}_D^{int}(\Phi) = -\frac{\lambda_D}{4}|\Phi|^4$, for instance, one would get

$$\mathcal{L}_4^{int}(x) = -\frac{\lambda_D}{4} \sum_{n,k,l,m} (\phi_n)^\dagger (\phi_k)^\dagger \phi_l \phi_m \mathcal{K}_{n,k,l,m} , \tag{1.1.6}$$

and the Feynman rule of this quartic vertex is

$$-i\lambda_D \mathcal{K}_{n,k,l,m} = -i\lambda_D \int_{\mathcal{C}_d} dy \sqrt{g} \left[(f_n)^\dagger (f_k)^\dagger f_l f_m\right] ,$$

which is a complicated tensor to be computed case by case once the explicit form of f_n is known. The above formulas will drastically simplify on flat spaces on which translational invariance is preserved, such as the circle or the torus we will discuss below.

1.2 The circle S^1

The circle S^1 is simply obtained from the real line $\mathbb{R}$ by identifying points connected by $2\pi R$ translations: $S^1 = \mathbb{R}/t$ where t acts as $y \to y + 2\pi R$ on the coordinate y of $\mathbb{R}$. Clearly, the fundamental domain of S^1, *i.e.* the set of points in $\mathbb{R}$ which are not connected to each other by translations and from which any other point can be reached, is the line segment $[0, 2\pi R)$. Fields on S^1 are defined as fields on $\mathbb{R}$ which are left invariant by the translation transformation $\Phi(x, y) \to \Phi(x, y + 2\pi R)$.

Clearly, the Φ field does not need to be exactly invariant under t, but it can be invariant up to symmetry transformations. We can have:

$$\Phi(x, y + 2\pi R) = T\Phi(x, y)\,, \tag{1.2.1}$$

where T belongs to the (global or local) symmetry group acting on Φ. This is an example of the so–called Scherk–Schwarz compactification [41]. Note that periodicity conditions as in Eq. (1.2.1) can be used to break symmetries. It is clear, indeed, that Eq. (1.2.1) restricts the allowed symmetry transformations which can act on Φ, since they must preserve Eq. (1.2.1).

Equivalently, the Scherk–Schwarz twist matrix T in Eq. (1.2.1) comes from the fact that S^1 is a topologically non–trivial manifold, which, to be precise, needs two different charts to be described. The first, big one, is described by the segment $y \in (0, 2\pi R)$ while the second is infinitesimal and intersects with the big one at $y = 0$ and $y = 2\pi R$. Continuity of Φ when described in the infinitesimal chart coordinates implies, in the big–chart description, the field at $y = 0$ to be related with the one at $y = 2\pi R$. The possibility of choosing different transition functions, or symmetry transformations, among the charts in the two intersections makes the arising of T in Eq. (1.2.1) possible. A discrete ($\mathbf{Z}_2$) version of this argument is used to define the Möbius strip as the fiber bundle of segment on a circle.

The simplest example of Scherk–Schwarz compactification in which, however, no symmetries are broken, is when Φ is identified with the complex scalar field considered in the previous section, endowed with an $U(1)$ phase transformation symmetry. One has:

$$\Phi(x, y + 2\pi R) = e^{-2\pi i\alpha}\Phi(x, y)\,, \tag{1.2.2}$$

where α is, a priori, undetermined. Note that, from the definition, $\alpha \sim \alpha + 1$ and, since $\Phi \longrightarrow (\Phi)^\dagger$ is a symmetry, $\alpha \sim -\alpha$, so that we can restrict to $\alpha \in [0, 1/2]$. Let us now expand the field as in Eq. (1.1.2). Eq. (1.1.4) is trivially solved on $\mathbb{R}$. By imposing periodicity (1.2.2) and normalizing, one finds the S^1 wave functions

$$f_n(y) = \frac{1}{\sqrt{2\pi R}} e^{-i\left(\frac{\alpha}{R}+\frac{n}{R}\right)y}\,, \qquad m_n^2 = \left(\frac{\alpha}{R} + \frac{n}{R}\right)^2\,, \tag{1.2.3}$$

with $n \in \mathbb{Z}$. The shift $n \longrightarrow n + \alpha$ in the mass spectrum is the typical effect of a Scherk–Schwarz twist.

Note that a Scherk–Schwarz twist, when it is performed by means of a local gauge symmetry, can be reabsorbed by a non–periodic gauge transformation [42]. In the abelian case, one has

$$\Phi(x, y) \longrightarrow \Phi'(x, y) \equiv e^{i\alpha\frac{y}{R}}\Phi(x, y)\,. \tag{1.2.4}$$

In so doing, however, the 5th component of the gauge connection A_M also changes

$$A_y \to A'_y = A_y + \frac{\alpha}{g_5 R}, \qquad (1.2.5)$$

where g_5 is the $5D$ gauge coupling constant. A theory with twisted Φ as in Eq. (1.2.2) and zero background for the gauge connection should be then equivalent to a theory with periodic Φ and non trivial background $A_y = \frac{\alpha}{g_5 R}$. This is immediately checked from the general results of the previous section, which also apply when the covariant derivative has a gauge part also: $D = \partial - i g_5 A$. One has a modified Klein–Gordon equation and

$$f_n(y) = \frac{1}{\sqrt{2\pi R}} e^{-i\frac{n}{R}y}, \qquad m_n^2 = \left(\frac{\alpha}{R} + \frac{n}{R}\right)^2.$$

Note that, since α can be related to the vacuum expectation value (VEV) of A_y, its value is not, as it is in the case of a global symmetry, a free parameter to be chosen but, on the contrary, it will be fixed by the dynamics of the theory. Moreover, a constant VEV for A_y is a flat ($F = dA = 0$) gauge background and the only (non–local) gauge invariant operator which is sensible to it is the Wilson loop

$$W = e^{-i g_5 \int_0^{2\pi R} A_y dy}, \qquad (1.2.6)$$

wrapping around the circle. It is easy to generalize the above argument to a non abelian Scherk–Schwarz twist T, which is capable to break (non–linearly realize) part of the gauge group. In that case, a VEV for a non–abelian gauge boson comes from the gauge transformation which removes T from Eq. (1.2.1), and the gauge group is broken by this VEV. Again, the background is a Wilson line to be dynamically determined and the Scherk–Schwarz symmetry breaking is equivalent to a Wilson line breaking [43]. As we will better discuss in the following, this Wilson line interpretation will provide strong constraints [44] on the dynamics of the Scherk–Schwarz twist.

1.3 The 2–Torus T^2

In the plane $\mathbb{R}^2 \sim \mathbb{C}$ with euclidean metric, consider the translations $t_{1,2}$ in the directions of two non–parallel vectors $\vec{e}_{1,2}$. They act as

$$y^i \to y^i + e^i_{1,2},$$

on the coordinates y^i of $\mathbb{R}^2$ and, without loss of generality, we can take $\vec{e}_1 = (2\pi R_1, 0)$ and generic $\vec{e}_2$. The torus T^2 is defined from $\mathbb{R}^2$ by identifying points connected by the $t_{1,2}$ translations. Its fundamental domain is simply the parallelogram built on the $\vec{e}_{1,2}$ vectors. It will be useful to introduce a complex coordinate $z = \frac{1}{\sqrt{2}}(y^1 + iy^2)$ in which the non–vanishing entries of the metric are $g_{z\bar{z}} = g^{z\bar{z}} = 1$ and the translations $t_{1,2}$ act as

$$z \longrightarrow z + \frac{2\pi R}{\sqrt{2}} \qquad z \longrightarrow z + \frac{2\pi R}{\sqrt{2}} U \, ,$$

with $R = R_1$ and the modular parameter $U = \frac{(e_2^1 + ie_2^2)}{2\pi R}$. Fields on T^2 are subject to the generalized periodicity

$$\Phi(y^i + e^i_{1,2}) = T_i \Phi(y^i) \, ,$$

where $T_{1,2}$ are symmetry transformations and, since

$$\Phi(y^i + e^i_1 + e^i_2) = T_1 T_2 \Phi(y^i) = T_2 T_1 \Phi(y^i) \, ,$$

$[T_1, T_2] = 0$. $T_{1,2}$, clearly, are the equivalent on T^2 of the S^1 Scherk–Schwarz twist discussed in the previous section. Also in this case, non–abelian Scherk–Schwarz twists can break symmetries and are equivalent to Wilson line symmetry breaking. We will neglect this aspect in the following and set $T_{1,U} = 1$. Consider the field Φ to be a complex scalar as in Sect. 1.1. The wave functions f_n are more easily found by defining real coordinates $w_{1,2}$ as $z = \frac{1}{\sqrt{2}}(w_1 + Uw_2)$ on which t_i simply acts as $w_i \rightarrow w_i + 2\pi R$. In these coordinates, a basis for periodic functions is, up to normalization

$$f_{\vec{n}} \sim e^{i(\frac{n_1}{R}w_1 + \frac{n_2}{R}w_2)} \, ,$$

where $\vec{n} = (n_1, n_2)$ is a two–dimensional vector of integers labelling the wave function. When rewritten in complex coordinates using

$$w_1 = \frac{U\bar{z} - \bar{U}z}{\sqrt{2}i\text{Im}U} \, , \qquad w_2 = \frac{z - \bar{z}}{\sqrt{2}i\text{Im}U} \, , \tag{1.3.1}$$

and normalizing, the wave functions read

$$f_{\vec{n}} = \frac{1}{\sqrt{V}} e^{\frac{1}{\sqrt{2}}(\lambda_{\vec{n}} z - \bar{\lambda}_{\vec{n}} \bar{z})} \, , \tag{1.3.2}$$

where $V = (2\pi R)^2 \text{Im}U$ is the volume of T^2 and

$$\lambda_{\vec{n}} = \frac{n_2 - n_1 \bar{U}}{R\,\text{Im}U} \, , \qquad \bar{\lambda}_{\vec{n}} = \frac{n_2 - n_1 U}{R\,\text{Im}U} \, . \tag{1.3.3}$$

According to Eq. (1.1.4), the Kaluza–Klein masses on T^2 are given by

$$m^2_{\vec{n}} = |\lambda_{\vec{n}}|^2 = \frac{n_2^2 + n_1^2 |U|^2 - 2n_1 n_2 \text{Re}U}{(\text{Im}U)^2 R^2} \, . \tag{1.3.4}$$

As already mentioned, S^1 and T^2 compactifications preserve translation invariance in the extra dimensions. This is the reason why both wave functions in Eq. (1.2.3,1.3.2) can be rewritten as

$$f_{\vec{n}} = \frac{1}{\sqrt{V}} e^{-ip_{i,\vec{n}}y^i} , \tag{1.3.5}$$

where V is the volume of the space and the momentum is $p_{y,n} = \frac{n}{R}$ for the circle (or $p_{y,n} = \frac{n+\alpha}{R}$ for $\alpha \neq 0$) and $p_{z,\vec{n}} = \frac{i}{\sqrt{2}}\lambda_{\vec{n}}$, $p_{\bar{z},\vec{n}} = -\frac{i}{\sqrt{2}}\bar{\lambda}_{\vec{n}}$ for the torus. Consequently, if all ED fields are expanded in the $f_{\vec{n}}$ basis as

$$\Phi(x,y) = \sum_{\vec{n}} \phi_{\vec{n}}(x) f_{\vec{n}}(y) ,$$

Feynman rules for propagators and interactions of the $4D$ fields $\phi_{\vec{n}}$ are very easily extracted from those of the corresponding 5 or 6 dimensional theory on flat Minkowski space. One simply has to replace the ED component of the momentum vector $P_M = (p_\mu, p_i)$ with its quantized version $p_{i,\vec{n}}$ and to remember that indices are raised with the ED $(+,-,\ldots,-)$ metric so that $P^M = (p^\mu, -p^i)$. Moreover, a factor $1/\sqrt{V}$ must be added for any external leg while one V comes from the integration in the ED, together with a Kronecker delta imposing ED momentum conservation. The Feynman rule for the quartic coupling in Eq. (1.1.6), for instance, simply reads

$$-i\lambda_4 \delta_{\vec{n}+\vec{k},\vec{l}+\vec{m}} ,$$

with the effective $4D$ coupling $\lambda_4 \equiv \frac{\lambda_D}{V}$. Note that λ_D has energy dimension -1 in $D=5$ and -2 in $D=6$ so that λ_4 is adimensional. Clearly, the fact that λ_D has negative energy dimension means that the theory is not renormalizable, even though the $4D$ coupling is adimensional. From the $4D$ point of view, non–renormalizability arises as a consequence of the presence of an infinite number of fields.

1.4 Gauge theories on S^1

Consider now an abelian $5D$ gauge theory compactified on $\mathcal{M}_4 \times S^1$. The Maxwell $5D$ Lagrangian is

$$\mathcal{L}_5 = -\frac{1}{4} F_{MN}F^{MN} = -\frac{1}{4} F_{\mu\nu}F^{\mu\nu} + \frac{1}{2} F_{\mu y}F^{\mu}{}_{y} , \tag{1.4.1}$$

with $F_{MN} = \partial_M A_N - \partial_N A_M$ and $A = (A_\mu, A_y)$ is the $5D$ gauge connection. The fields are expanded as

$$A_\mu = \sum_n \frac{1}{\sqrt{2\pi R}} A_\mu^n(x) e^{-i\frac{ny}{R}} , \quad A_y = \sum_n \frac{1}{\sqrt{2\pi R}} A_y^n(x) e^{-i\frac{ny}{R}} , \tag{1.4.2}$$

where the $4D$ fields $A^n_{\mu,y}(x)$ are complex but subject to the condition $A^{-n}_{\mu,y} = \left(A^n_{\mu,y}\right)^\dagger$ since the $5D$ ones are real. By plugging this expansion into the Lagrangian and integrating on the circle, the effective $4D$ Lagrangian is found to be

$$
\begin{aligned}
\mathcal{L}_5 = \textstyle\sum_{n=-\infty}^{\infty} \Big[& -\tfrac{1}{4}F_{\mu\nu}{}^{n}\left(F^{\mu\nu n}\right)^\dagger + \tfrac{1}{2}\partial_\mu\left(A^n_y\right)^\dagger \partial^\mu A^n_y \\
& + \tfrac{1}{2}\left(\tfrac{n}{R}\right)^2 \left(A^n_\mu\right)^\dagger A^n_\mu + i\tfrac{n}{R}A^n_\mu \partial^\mu \left(A^n_y\right)^\dagger \Big] \\
= \mathcal{L}^0_4 + & \textstyle\sum_{n=1}^{\infty} \mathcal{L}^n_4 \,,
\end{aligned}
\tag{1.4.3}
$$

where we have separated the zero–mode Lagrangian $\mathcal{L}^0_4$, which simply describes a massless $4D$ real scalar A^0_y and an abelian real massless gauge field A^0_μ, from a sum of terms of the form

$$
\begin{aligned}
\mathcal{L}^n_4 = & -\tfrac{1}{2}F_{\mu\nu}{}^{n}\left(F^{\mu\nu n}\right)^\dagger + \partial_\mu\left(A^n_y\right)^\dagger \partial^\mu A^n_y \\
& + \left(\tfrac{n}{R}\right)^2 \left(A^n_\mu\right)^\dagger A^n_\mu \\
& - i\tfrac{n}{R}\left[\left(A^n_\mu\right)^\dagger \partial^\mu A^n_y - A^n_\mu \partial^\mu \left(A^n_y\right)^\dagger\right] .
\end{aligned}
\tag{1.4.4}
$$

To better interpret the result, define real fields as

$$
A^n_\mu = \frac{1}{\sqrt{2}}\left(X^n_\mu + iY^n_\mu\right) , \qquad A^n_y = \frac{1}{\sqrt{2}}\left(y^n - ix^n\right) , \tag{1.4.5}
$$

$\mathcal{L}^n_4$, omitting the index n for simplicity, reads

$$
\begin{aligned}
\mathcal{L}_4 = & -\tfrac{1}{4}X_{\mu\nu}X^{\mu\nu} - \tfrac{1}{4}Y_{\mu\nu}Y^{\mu\nu} \\
& + \tfrac{1}{2}\left(\tfrac{n}{R}\right)^2 X_\mu X^\mu + \tfrac{1}{2}\left(\tfrac{n}{R}\right)^2 Y_\mu Y^\mu \\
& + \tfrac{1}{2}\partial_\mu x \partial^\mu x + \tfrac{1}{2}\partial_\mu y \partial^\mu y \\
& - \tfrac{n}{R}X_\mu \partial^\mu x - \tfrac{n}{R}Y_\mu \partial^\mu y \,.
\end{aligned}
\tag{1.4.6}
$$

The above action is completely symmetric in $x \leftrightarrow y$, let us concentrate on the x part. It contains a mass term $M_X = n/R$ for the $U(1)$ gauge boson and a quadratic coupling of it with the real scalar x. It is then the action of a non–linearly realized (so–called spontaneously broken) $U(1)$ gauge symmetry. The field x clearly represents the pseudo–Goldstone boson which will be eaten by the gauge field when it will acquire a mass. When considering the simplest $4D$ abelian Higgs theory of a complex field ϕ which acquires a VEV $\langle\phi\rangle = \frac{v}{\sqrt{2}}$, exactly the same action comes out. If parametrizing $\phi = (\frac{v}{\sqrt{2}} + \rho)e^{i\frac{\theta}{v}}$ and neglecting the terms in ρ, we get, from the kinetic term of ϕ

$$
|\left(\partial_\mu - igA_\mu\right)\phi|^2 \;\; \rightarrow \;\; \frac{1}{2}\partial_\mu\theta\partial^\mu\theta + \frac{(gv)^2}{2}A_\mu A^\mu - gvA_\mu\partial^\mu\theta \,,
$$

which exactly matches Eq. (1.4.6) if gv is identified with $\frac{n}{R}$. In the $4D$ Higgs model, the field θ transforms non–linearly, as $\theta \to \theta + gv\beta(x)$ under the $U(1)$ symmetry transformation $A \to A + \partial\beta$. By expanding the $5D$ gauge parameter

$$\alpha(x,y) = \sum_n \alpha^n(x) \frac{1}{\sqrt{2\pi R}} e^{-iny/R} ,$$

which acts on the gauge $5D$ connection as

$$A_M(x,y) \to A_M(x,y) + \partial_M \alpha(x,y) ,$$

the $U(1)$ $5D$ local symmetry can be rewritten as an infinite product of non–linearly realized $U(1)^2_n$ $(n = 1, \ldots, \infty)$ $4D$ gauge symmetries acting on the fields X^n and Y^n as

$$\begin{array}{ll} X^n_\mu \to X^n_\mu + \partial_\mu \alpha^n_X , & x^n \to x^n + \frac{n}{R}\alpha^n_X , \\ Y^n_\mu \to Y^n_\mu + \partial_\mu \alpha^n_Y , & y^n \to y^n + \frac{n}{R}\alpha^n_Y , \end{array} \tag{1.4.7}$$

where $\alpha^n \equiv \frac{1}{\sqrt{2}}(\alpha_X + i\alpha_Y)$. For the zero–modes, we have $A^0_\mu \to A^0_\mu + \partial_\mu \alpha^0$ while A^0_y is invariant. The $4D$ $U(1)$ associated to α^0 is linearly realized and then unbroken.

As for any gauge symmetry, a gauge fixing is required to quantize the theory. In the $4D$ Higgs model it is convenient to use the so–called R_ξ gauges, in which a gauge–fixing term

$$\mathcal{L}^{g-f} = -\frac{1}{2\xi} \left(\partial_\mu A^\mu + \xi g v \theta\right)^2 ,$$

is added to the Lagrangian. Analogously, a gauge–fixing term

$$\mathcal{L}^{g-f} = -\frac{1}{2\xi} \left(\partial_\mu X^\mu + \xi \frac{n}{R} x\right)^2 - \frac{1}{2\xi} \left(\partial_\mu Y^\mu + \xi \frac{n}{R} y\right)^2 ,$$

will be required by the Lagrangian in Eq. (1.4.6). For $\mathcal{L}_0$, the usual $-\frac{1}{2\xi}(\partial_\mu A^\mu)^2$ will be added. One can easily check that the sum of all the $4D$ gauge–fixing terms which are required to quantize the $4D$ effective Lagrangian is reproduced by adding the $5D$ gauge–fixing term

$$\mathcal{L}^{g-f}_5 = -\frac{1}{2\xi} \left(\partial_\mu A^\mu - \xi \partial_y A_y\right)^2 , \tag{1.4.8}$$

to the $5D$ Lagrangian in Eq. (1.4.1). The unitary gauge is obtained by taking $\xi \to \infty$ in the above equation, which implies gauge–fixing $\partial_y A_y = 0$. This corresponds to take $x^n = y^n = 0$. The physical spectrum is clear from the above discussion, we have two infinite towers of massive vector bosons of mass $m_n = \frac{n}{R}$ $(n = 1, \ldots, \infty)$, one massless gauge fields A^0_μ corresponding to the unbroken $4D$ $U(1)$ symmetry and one real scalar A_y^0. All the Kaluza–Klein tower of A_y has been eaten by the vector bosons which have acquired mass. Note that A_y^0 taking a VEV, $\langle A_y^0 \rangle = \frac{2\pi\alpha}{\sqrt{2\pi R}g_5}$, corresponds to a constant gauge background $A_y = \frac{\alpha}{g_5 R}$ which, as in Eq. (1.2.5), is equivalent to a Scherk–Schwarz twist α. The dynamical determination of the Scherk–Schwarz parameter, then, is just the dynamical determination of the VEV of the $4D$ field A_y^0, which is given, as for any scalar field, by the minimum of the effective potential. Note that the tree–level effective potential of A_y^0 vanishes, so that one has to include one–loop corrections for α to be fixed. This is a trivial consequence the Wilson loop interpretation (1.2.6) of the Scherk-Schwarz twist.

The result in Eq. (1.4.8) is easily generalized to non–abelian theories. The gauge–fixing term

$$\mathcal{L}_5^{g-f} = -\frac{1}{\xi}\mathrm{Tr}\left[(\partial_\mu A^\mu - \xi\partial_y A_y)^2\right] , \qquad (1.4.9)$$

with $A_M = A_{M,a}t^a$, must be added to the Lagrangian. In that case, in order to perform quantum computations, the appropriate action for ghosts, consistent with Eq. (1.4.9), must be used. It is easily found to be

$$\mathcal{L}_5^{gh} = 2\mathrm{Tr}\left[\bar{c}\left(-\partial_\mu D^\mu + \xi\partial_y D_y\right)c\right] , \qquad (1.4.10)$$

where the ghost fields $c(x,y) = c_a t^a$ and $\bar{c}(x,y) = \bar{c}_a t^a$ are anticommuting $5D$ fields in the adjoint representation of the gauge group and D_M is the covariant derivative acting on them. From Eq. (1.4.9) and (1.4.10), all Feynman rules for the non–abelian gauge theory on S^1 could be derived. In the case $\xi = 1$, however, no additional computation is required. The usual Feynman gauge in $D = 5$ Minkowski space is indeed recovered and the Feynman rules on S^1 are easily extracted in this gauge from the text–book ones (see *e.g.* [45], whose conventions we will follow) by replacing the ED momentum $p_y \to p_{y,n} = \frac{n}{R}$ and multiplying by the appropriate power of $\sqrt{2\pi R}$. Note that in any cubic vertex a g_5 factor appears, while g_5^2 multiplies quartic verteces, so that all $\sqrt{2\pi R}$ factors are reabsorbed if defining the $4D$ effective gauge coupling

$$g_4 = \frac{g_5}{\sqrt{2\pi R}} . \qquad (1.4.11)$$

Note that g_4 is adimensional while g_5 has energy dimension $-1/2$ and makes the theory non–renormalizable. We will not explicitly discuss here the inclusion of $5D$ charged scalars and fermions in the theory, since this is trivial.

1.5 Gauge theories on T^2

Consider now an abelian $6D$ theory on the torus T^2. The gauge connection is $A_M = (A_\mu, A_z, A_{\bar z})$, with z, $\bar z$ complex coordinates as in Sect. 1.3. The action reads

$$\mathcal{L}_5 = -\frac{1}{4}F_{MN}F^{MN} = -\frac{1}{4}F_{\mu\nu}F^{\mu\nu} + F_{\mu z}F^{\mu}_{\ \bar z} - \frac{1}{2}|F_{z\bar z}|^2 . \tag{1.5.1}$$

The gauge field is expanded as

$$A_\mu = \sum_{\vec n} A_\mu^{\vec n}(x) f_{\vec n}, \qquad A_z = \sum_{\vec n} A_z^{\vec n}(x) f_{\vec n}, \qquad A_{\bar z} = \sum_{\vec n} A_{\bar z}^{\vec n}(x) f_{\vec n}, \tag{1.5.2}$$

with $f_{\vec n}$ as in Eq. (1.3.2). Note that, since the original $6D$ field A_μ is real, $A_\mu^{-\vec n} = \left(A_\mu^{\vec n}\right)^\dagger$ and, since $A_z = \frac{1}{\sqrt2}(A_1 - iA_2) = (A_{\bar z})^\dagger$, $A_z^{-\vec n} = \left(A_{\bar z}^{\vec n}\right)^\dagger$. The zero–modes are a real $4D$ gauge field A_μ^0 and a complex field $A_z^0 = (A_{\bar z}^0)^\dagger$. For describing the other modes we use the $A_\mu^{\vec n}$, $A_z^{\vec n}$ and $A_{\bar z}^{\vec n}$ fields, with $\vec n$ positive, as independent degrees of freedom. [1] It will be convenient to define, for each $\vec n > 0$, the complex scalar fields

$$G^{\vec n} \equiv \frac{1}{\sqrt2 |p_{z,\vec n}|}\left(p_{z,\vec n}A_{\bar z}^{\vec n} + p_{\bar z,\vec n}A_z^{\vec n}\right), \qquad S^{\vec n} \equiv \frac{1}{\sqrt2 |p_{z,\vec n}|}\left(p_{z,\vec n}A_{\bar z}^{\vec n} - p_{\bar z,\vec n}A_z^{\vec n}\right). \tag{1.5.3}$$

The $4D$ effective Lagrangian is

$$\mathcal{L}_4 = \mathcal{L}_4^0 + \sum_{\vec n > 0}\mathcal{L}_4 , \tag{1.5.4}$$

where,

$$\mathcal{L}_4^0 = -\frac{1}{4}F_{\mu\nu}{}^0 F^{\mu\nu 0} + \left(\partial_\mu A_z^0\right)^\dagger \partial^\mu A_z^0 ,$$

and

$$\begin{aligned}
\mathcal{L}_4^{\vec n} = &-\tfrac{1}{2}\left(F_{\mu\nu}{}^{\vec n}\right)^\dagger F^{\mu\nu\vec n} + \left(\partial_\mu G^{\vec n}\right)^\dagger \partial^\mu G^{\vec n} + m_{\vec n}{}^2 \left(A_\mu^{\vec n}\right)^\dagger A^{\mu\vec n} \\
&-i m_n\left[\left(A^{\mu,\vec n}\right)^\dagger \partial_\mu G^{\vec n} - A^{\mu,\vec n}\partial_\mu\left(G^{\vec n}\right)^\dagger\right] \\
&+\left(\partial_\mu S^{\vec n}\right)^\dagger \partial^\mu S^{\vec n} - m_{\vec n}{}^2\left(S^{\vec n}\right)^\dagger S^{\vec n} ,
\end{aligned} \tag{1.5.5}$$

with $m_{\vec n} = \sqrt2 |p_{\vec n,z}|$ as in Eq. (1.3.4). The zero–modes Lagrangian $\mathcal{L}_4^0$ simply describes an unbroken $U(1)$ gauge theory and one complex massless scalar field. The massive Lagrangian $\mathcal{L}_4^{\vec n}$, except for the kinetic term for the complex massive scalars $S^{\vec n}$, has exactly the same form as Eq. (1.4.4) when replacing A_y with G and $\frac{n}{R}$ with $m_{\vec n}$, so that it can be recast in the form of Eq. (1.4.6) with the suitable field redefinitions. It then describes two real $U(1)$ gauge bosons of a non–linearly realized

[1] We will say that $\vec n = (n_1, n_2)$ is positive when its first non–vanishing component is positive.

symmetry. The complex field $G^{\vec{n}}$ provides, for any $\vec{n}$, the two degrees of freedom the gauge bosons need to become massive. Note that, indeed, the $6D$ gauge transformations, having expanded the gauge parameter α as

$$\alpha(x,z) = \sum_{\vec{n}} \alpha_{\vec{n}}(x) f_{\vec{n}}(z) \,,$$

act on the scalars $A_z^{\vec{n}}$, $A_{\bar{z}}^{\vec{n}}$ as

$$\begin{aligned} A_z^{\vec{n}} &\longrightarrow A_z^{\vec{n}} - i p_{z,\vec{n}} \alpha_{\vec{n}} \,, \\ A_{\bar{z}}^{\vec{n}} &\longrightarrow A_{\bar{z}}^{\vec{n}} - i p_{\bar{z},\vec{n}} \alpha_{\vec{n}} \,. \end{aligned} \tag{1.5.6}$$

The scalar $S_{\vec{n}}$ is then invariant while the pseudo–Goldstone boson $G_{\vec{n}}$ is shifted as

$$G_{\vec{n}} \longrightarrow G_{\vec{n}} - i m_{\vec{n}} \alpha_{\vec{n}} \,.$$

By closely following the steps of the previous section, the gauge fixing term required by each $\mathcal{L}_4^{\vec{n}}$ is easily derived and the convenient gauge–fixing term to be added to the $6D$ Lagrangian is found to be

$$\mathcal{L}_6^{g-f} = -\frac{1}{2\xi} \left[\partial_\mu A^\mu - \xi \left(\partial_z A_{\bar{z}} + \partial_{\bar{z}} A_z\right)\right]^2 \,. \tag{1.5.7}$$

The result is trivially extended to the non–abelian case and the ghost action to be used is

$$\mathcal{L}_6^{gh} = 2\mathrm{Tr}\left\{\bar{c}\left[-\partial_\mu D^\mu + \xi\left(\partial_z D_{\bar{z}} + \partial_{\bar{z}} D_z\right)\right] c\right\} \,. \tag{1.5.8}$$

For $\xi \longrightarrow \infty$, as in the previous section, the unitary gauge is imposed. It now correspond to the condition $\partial_z A_{\bar{z}} + \partial_{\bar{z}} A_z = 0$, or $G_{\vec{n}} = 0$. The physical $4D$ field content consists on two towers of real vector bosons with mass $m_{\vec{n}}$ ($\vec{n} > 0$), one massless vector A_μ^0, one massless complex scalar A_z^0 and, differently form the S^1 case, one tower of massive complex scalars $S_{\vec{n}}$. Clearly, of the two Kaluza–Klein towers arising from the internal components of the $6D$ vector, only one has been eaten by the gauge bosons while the other is left as physical fields. In the following, $\xi = 1$ will be chosen, so that the ordinary $6D$ Feynman gauge is recovered. As discussed in the previous section, all Feynman rules are simply extracted, in this gauge, from the ordinary ones by replacing the extra–dimensional components of the momentum $p_{z,\bar{z}}$ with $p_{z,\bar{z},\vec{n}}$ and multiplying by the appropriate power of $\sqrt{V}$. The $4D$ effective gauge coupling is now defined as

$$g_4 = \frac{g_6}{\sqrt{V}} \,. \tag{1.5.9}$$

Again, $6D$ scalars or fermions can be trivially added to the gauge theory.

1.6 Fermion Field

1.6.1 Fermions on S^1

Be $\Psi(x,y)$ a $5D$ spinor compactified on $\mathcal{M}_4 \times S^1$. In 5 dimensions, spinors have 4 complex components as in $4D$. A basis can be used for the $5D$ gamma matrices

$$\Gamma^\mu = \gamma^\mu\,, \qquad \Gamma^y = i\gamma_5\,,$$

where γ^μ are the usual $4D$ gamma matrices and $\gamma_5 = i\gamma^0 \dots \gamma^3$ is the $4D$ chirality. In $5D$, of course, chirality cannot be defined and the minimal spinor to be considered is the Dirac one. The spinor Ψ can however be decomposed in $4D$ chiral components as

$$\Psi = \frac{(1-\gamma_5)}{2}\Psi + \frac{(1+\gamma_5)}{2}\Psi \equiv \Psi_R + \Psi_L\,,$$

where L, R components are defined so that $\gamma_5 \Psi_{L,R} = \pm\Psi_{L,R}$. The $5D$ action is

$$\begin{aligned}\mathcal{L}_5 = \overline{\Psi}\left(i\Gamma^M\partial_M - m\right)\Psi = \\ \overline{\Psi}_L\left(i\gamma^\mu\partial_\mu - m\right)\Psi_L + \overline{\Psi}_R\left(i\gamma^\mu\partial_\mu - m\right)\Psi_R \\ +\overline{\Psi}_L\left(\partial_y - m\right)\Psi_R + \overline{\Psi}_R\left(-\partial_y - m\right)\Psi_L\,.\end{aligned} \tag{1.6.1}$$

Trivial periodicity is assumed for Ψ around the circle. When expanding the fields as

$$\Psi_L(x,y) = \sum_n \frac{1}{\sqrt{2\pi R}}\psi_L^n e^{-i\frac{ny}{R}}\,, \qquad \Psi_R(x,y) = \sum_n \frac{1}{\sqrt{2\pi R}}\psi_R^n e^{-i\frac{ny}{R}}\,,$$

the $4D$ effective Lagrangian is found to be, after integration on S^1

$$\begin{aligned}\mathcal{L}_4 = \textstyle\sum_n &\Big[\overline{\psi}_L^n i\gamma^\mu\partial_\mu\psi_L^n + \overline{\psi}_R^n i\gamma^\mu\partial_\mu\psi_R^n \\ &-\overline{\psi}_L^n\left(i\tfrac{n}{R} + m\right)\psi_R^n - \overline{\psi}_R^n\left(-i\tfrac{n}{R} + m\right)\psi_L^n\Big] = \\ \textstyle\sum_n &\Big[\overline{\psi}_L^n i\gamma^\mu\partial_\mu\psi_L^n + \overline{\chi}_R^n i\gamma^\mu\partial_\mu\chi_R^n \\ &-\sqrt{m^2 + \left(\tfrac{n}{R}\right)^2}\left(\overline{\psi}_L^n\chi_R^n + \overline{\chi}_R^n\psi_L^n\right)\Big]\,,\end{aligned} \tag{1.6.2}$$

having defined

$$\chi_R^n = \frac{1}{\sqrt{m^2 + \left(\frac{n}{R}\right)^2}}\left(m + i\frac{n}{R}\right)\psi_R^n\,.$$

The $4D$ spectrum simply consists on couples of massive Dirac fermions $\lambda^n = \psi_L^n + \chi_R^n$ of mass $m_n = \sqrt{m^2 + \left(\frac{n}{R}\right)^2}$, $n = 1, \dots, \infty$, plus a zero–mode fermion of mass m.

Starting from the $5D$ Feynman propagator on $\mathcal{M}_5$, the same result could have been obtained. The $\langle \psi^n \overline{\psi}^n \rangle$ ($\psi^n = \psi_L^n + \psi_R^n$) correlator is found by replacing p_y with $p_{y,n} = \frac{n}{R}$ and reads

$$\langle \psi^n \overline{\psi}^k \rangle = \frac{i}{p^2 - \left(\frac{n}{R}\right)^2 - m^2} \left[\gamma^\mu p_\mu + i \frac{n}{R} \gamma_5 + m \right] \delta_{n,k} \,.$$

From the above equation, one can extract

$$\begin{aligned} \langle \psi_{L,R}^n \overline{\psi}_{L,R}^n \rangle &= \tfrac{1 \pm \gamma_5}{2} \langle \psi^n \overline{\psi}^n \rangle \tfrac{1 \mp \gamma_5}{2} = \tfrac{i}{p^2 - \left(\frac{n}{R}\right)^2 - m^2} \gamma^\mu p_\mu \,, \\ \langle \psi_{L,R}^n \overline{\psi}_{R,L}^n \rangle &= \tfrac{1 \pm \gamma_5}{2} \langle \psi^n \overline{\psi}^n \rangle \tfrac{1 \pm \gamma_5}{2} = \tfrac{i}{p^2 - \left(\frac{n}{R}\right)^2 - m^2} \left(m \pm i \tfrac{n}{R} \right) \,, \end{aligned} \tag{1.6.3}$$

which matches the above result; one can indeed easily check that

$$\langle \lambda^n \overline{\lambda}^n \rangle = \frac{i}{p^2 - {m_n}^2} \left[\gamma^\mu p_\mu + m_n \right] \,. \tag{1.6.4}$$

1.6.2 Fermions on $\mathcal{M}_4 \times \mathcal{C}_2$

For later pourposes, we will consider in this section $6D$ fermion fields compactified on a general smooth $2D$ manifold $\mathcal{C}_2$, defined as in Sect. 1.1. We will also allow, in this section, the $6D$ fermion to be charged under an $U(1)$ gauge symmetry and a background $A_M = (A_\mu = 0, A_i \neq 0)$ to be present for the gauge connection. A $6D$ fermion $\Psi(x,y)$ has 8 complex components and the $6D$ gamma matrices $\Gamma^A = (\Gamma^\alpha, \Gamma^a)$ can be written as

$$\Gamma^\alpha = \gamma^\alpha \otimes \mathbb{1}_2 \,, \qquad \Gamma^a = i\gamma_5 \otimes \rho^a \,, \tag{1.6.5}$$

in terms of tensor products of the $4D$ Minkowskian gamma matrices γ^α and the $2D$ Euclidean ones ρ^a we choose to be

$$\rho^1 = \sigma_1 \,, \qquad \rho^2 = \sigma_2 \,, \;\Rightarrow\; \rho_3 = i\rho^1\rho^2 = -\sigma_3 \,, \tag{1.6.6}$$

where σ_i are the standard Pauli matrices. The $6D$ chirality matrix $\Gamma_7 \equiv \Gamma^0 \dots \Gamma^5$ is then the tensor product of the $4D$ and $2D$ chiralities:

$$\Gamma_7 = \gamma_5 \otimes \rho_3 \,. \tag{1.6.7}$$

In the following, we will consider a $6D$ chiral (L–handed) fermion Ψ_L. According to the above equation, it is decomposed in terms of chiral $4D$ fields as

$$\Psi_L = \begin{pmatrix} \chi_R \\ \chi_L \end{pmatrix} \,. \tag{1.6.8}$$

Note that now, since we are considering spinors on a non–flat space, it is important to distinguish between the ordinary space–time indices, indicated as $M, N, O, \ldots$ for the $6D$ space, $\mu, \nu, \rho, \ldots$ and $i, j, k, \ldots$ for the $4D$ and $2D$ ones, respectively, and the Local–Lorentz (LL) ones, on the local tangent frame in which the fermion field is defined. We use $A, B, C, \ldots$, $\alpha, \beta, \gamma, \ldots$, $a, b, c, \ldots$ to indicate the $6D$, $4D$ and $2D$ indices. For changing LL in space–time indices, the 6–bein E_M^A must be used which is defined by

$$G_{M,N} = E_M^{\ A} E_N^{\ B} \eta_{AB} \,,$$

with $\eta_{AB} = \mathrm{diag}(+,-,-,-,-,-)$. The 6–bein components on our space with factorized metric as in Eq. (1.1.1) can be chosen to be

$$E_\mu^{\ \alpha} = \delta_\mu^\alpha \,, \qquad E_\mu^{\ a} = E_i^{\ \alpha} = 0 \,, \qquad E_i^{\ a} = e_i^{\ a} \,,$$

where $e_i^{\ a}(y)$ is the 2–bein for the Euclidean space $\mathcal{C}_2$:

$$g_{i,j} = e_i^{\ a} e_j^{\ b} \delta_{ab} \,.$$

The $6D$ Lagrangian for Ψ_L is

$$\mathcal{L}_6 = i\overline{\Psi}_L \Gamma^M D_M \Psi_L = i\overline{\Psi}_L \Gamma^M \left(\partial_M + \frac{i}{2} \Omega_M^{\ AB} \Sigma_{AB} + i A_M \right) \Psi_L \,, \tag{1.6.9}$$

where $\Gamma^M = E^M_{\ A} \Gamma^A$, A_M is the gauge field background, $\Sigma_{AB} = \frac{i}{4} [\Gamma_A, \Gamma_B]$ is the generator of the 6–dimensional LL group and $\Omega_M^{\ AB} = -\Omega_M^{\ BA}$ are the spin connection components. For a Levi–Civita connection, $\Omega_M^{\ AB}$ can be extracted from the equation

$$d\hat{\Theta}^A + \Omega^A_{\ B} \wedge \hat{\Theta}^B = 0 \,,$$

written in terms of the 6–bein 1–form $\hat{\Theta}^A \equiv E_M^{\ A} dX^M$ and the connection 1–form $\Omega^{AB} \equiv \Omega_M^{\ AB} dX^M$. From the above equation, it is clear that $\Omega^{\alpha\beta} = \Omega^{\alpha a} = 0$ and that the only non–vanishing components are $\Omega^{ab} = \omega_i^{\ ab}(y) dy^i$, where $\omega_{i\ ab} \equiv \omega_i \epsilon_{ab}$ ($\epsilon_{12} = 1$) is the 2 dimensional connection on $\mathcal{C}_2$, defined by

$$d\hat{\theta}^a + \epsilon^a_{\ b} \omega \wedge \hat{\theta}^b = 0 \,, \tag{1.6.10}$$

with $\hat{\theta}^a \equiv e_i^{\ a} dy^i$ and $\omega \equiv \omega_i dy^i$. Since $\Sigma^{ab} = -\frac{i}{4} \mathbb{1} \otimes \left[\rho^a, \rho^b\right]$, Eq. (1.6.9) becomes

$$\mathcal{L}_6 = i\overline{\Psi}_L \left(\gamma^\mu \partial_\mu\right) \otimes \mathbb{1} \Psi_L + i\overline{\Psi}_L \gamma_5 \otimes \left(i\rho^i D_i\right) \Psi_L \,, \tag{1.6.11}$$

where

$$D_i = \partial_i + \frac{i}{2} \sigma_3 \omega_i + i A_i \,,$$

is the $2D$ covariant derivative on $\mathcal{C}_2$. According to Eq. (1.6.8), we expand the $6D$ field as

$$\Psi_L(x,y) = \sum_n \left[\chi_L^n(x) \otimes \psi_L^n(y) + \chi_R^n(x) \otimes \psi_R^n(y)\right] ,$$

where $\psi_{L,R}^n$ are the $L-$ and R–handed components of a $2D$ Dirac field $\psi^n \equiv \psi_L^n + \psi_R^n$ and $\chi_{L,R}^n(x)$ are the $4D$ chiral degrees of freedom. The functions ψ^n are chosen to be the solutions of the $2D$ Dirac equation

$$i\rho^i D_i \psi^n = m_n \psi^n \quad \Rightarrow \quad \begin{cases} i\rho^i D_i \psi_R^n = m_n \psi_L^n \\ i\rho^i D_i \psi_L^n = m_n \psi_R^n \end{cases} , \tag{1.6.12}$$

for all possible values of m_n real and positive. The ψ^n's form a complete set and, due to the identities

$$m_k^2 \int_{\mathcal{C}_2} dy \sqrt{g} \psi_L^{n\dagger} \psi_L^k = m_n m_k \int_{\mathcal{C}_2} dy \sqrt{g} \psi_R^{n\dagger} \psi_R^k = m_n^2 \int_{\mathcal{C}_2} dy \sqrt{g} \psi_L^{n\dagger} \psi_L^k ,$$

which are easily proven by repetitively using Eq. (1.6.12) and integrating by parts, $\psi_{L,R}^n$ and $\psi_{L,R}^k$ are orthogonal if $m_n \neq m_k$. For each mass level, degenerate wave functions can be made orthogonal and one can choose the normalization so that

$$\int_{\mathcal{C}_2} dy \sqrt{g} \psi_L^{n\dagger} \psi_L^k = \int_{\mathcal{C}_2} dy \sqrt{g} \psi_R^{n\dagger} \psi_R^k = \delta_{n,k} .$$

The $4D$ effective Lagrangian is then

$$\begin{aligned} \mathcal{L}_4 = \textstyle\sum_n \big[& \overline{\chi}_L^n i\gamma^\mu \partial_\mu \chi_L^n + \overline{\chi}_L^n i\gamma^\mu \partial_\mu \chi_L^n \\ & + i m_n \overline{\chi}_R^n \chi_L^n - i m_n \overline{\chi}_L^n \chi_R^n \big] , \end{aligned} \tag{1.6.13}$$

so that the Dirac fields $\chi^n \equiv \chi_R^n + i\chi_L^n$ describe a Kaluza–Klein tower of spinors of mass m_n.

In summary, we have shown how the study of $6D$ chiral fields compactified on a general $2D$ smooth manifold $\mathcal{C}_2$ can be translated into the study of the $2D$ Euclidean Dirac equation (1.6.12) on $\mathcal{C}_2$. This result has particularly important consequences for what concerns the massless fermion content of the resulting $4D$ theory. For $m_n = 0$, Eq. (1.6.12) separates in two independent equations for the $L-$ and R–handed components of the spinor. In general, one finds n_L L–moving and n_R R–moving independent solutions, corresponding to the presence of $n_{L,R}$ $L,R-$ handed massless fermions in the effective $4D$ theory. The asymmetry in the number of $L-$ and R–handed solutions to Eq. (1.6.12) is given by the Atiyah–Singer index theorem

$$n_L - n_R = \mathcal{I} = \frac{1}{2\pi} \int_{\mathcal{C}_2} F , \tag{1.6.14}$$

with $F = dA$. The index only depends, in $2D$, on the gauge background A. Obtaining a chiral $4D$ spectrum (*i.e.* $\mathcal{I} \neq 0$) is very important for phenomenological pourposes, but not so easy. The simple T^2 compactification (or the S^1 one, as we explicitly checked in the above section) does not lead to a chiral spectrum and one has to consider, for instance, the T^2 torus with a magnetic flux (see *e.g.* [46]) or the S^2 sphere with monopole background (see *e.g.* [19]). In both cases, however, it becomes technically involved to deal with the resulting theory, so that chiral compactifications on smooth spaces are not so commonly employed for model building. On the contrary, orbifolds are commonly used from which, as we will better discuss in the following chapter, chiral spectra can be obtained in a very simple way.

1.6.3 Fermions on T^2

The torus T^2 with no gauge background is a trivial application of the above section. It will be better, however, to perform a little change in our notations when dealing with this case. The fields are more conveniently expanded as

$$\chi_R = \sum_{\vec{n}} \chi_R^{\vec{n}} f_{\vec{n}}\,, \qquad \chi_L = \sum_{\vec{n}} \chi_L^{\vec{n}} f_{\vec{n}}\,, \tag{1.6.15}$$

with $f_{\vec{n}}$ as in Eq. (1.3.2), so that Feynman rules for $\chi_{L,R}^{\vec{n}}$ interactions, when the fermion will be coupled to other fields such as gauge bosons, can be extracted from the $6D$ ones with the usual prescription. The wave functions in Eq. (1.6.15) cannot be matched with those defined by Eq. (1.6.12) by the trivial identification. One has

$$\psi^{\vec{n}} = \begin{pmatrix} e^{i\alpha} f_{n} \\ e^{-i\alpha} f_{\vec{n}} \end{pmatrix}\,, \tag{1.6.16}$$

with $e^{-i\alpha}\lambda_{\vec{n}} = e^{i\alpha}|\lambda_{\vec{n}}|$, so that

$$i\rho^i \partial_i \psi^{\vec{n}} = \sqrt{2} \begin{pmatrix} 0 & \partial_z \\ \partial_{\bar{z}} & 0 \end{pmatrix} \begin{pmatrix} e^{i\alpha} f_{n} \\ e^{-i\alpha} f_{\vec{n}} \end{pmatrix} = m_{\vec{n}} \psi^{\vec{n}}\,, \tag{1.6.17}$$

where $\partial_z = \frac{1}{\sqrt{2}}(\partial_1 - i\partial_2)$, $\partial_{\bar{z}} = \frac{1}{\sqrt{2}}(\partial_1 + i\partial_2)$ and $m_{\vec{n}} = |\lambda_{\vec{n}}|$. As expected, the theory describes a tower of spinors with mass $m_{\vec{n}}$ as in Eq. (1.3.4), with $\vec{n} \in \mathbb{Z}^2$. Clearly, one L– and one R–handed zero mode are present, since the index $\mathcal{I}$ vanishes.

Chapter 2

Orbifolds

Let us consider a general d–dimensional manifold $\mathcal{C}_d$ as in Sect. 1.1 and a discrete N–element group $\mathcal{G}_N$ of isometries acting non–freely on it. The $\mathcal{C}_d/\mathcal{G}_N$ orbifold is obtained by modding out $\mathcal{G}_N$ from $\mathcal{C}_d$, *i.e.* by identifying points $y \in \mathcal{C}_d$ connected by the $\mathcal{G}_N$ action: $y \sim g \cdot y$, with $g \in \mathcal{G}_N$. The $\mathcal{G}_N$ group acting non–freely on $\mathcal{C}_d$, *i.e.* the existence of fixed points $y_i \in \mathcal{C}_d$ such that $g \cdot y_i = y_i$ for some g, is essential in the definition. Field theories on $\mathcal{M}_4 \times \mathcal{C}_d/\mathcal{G}_N$ are obtained from field theories on $\mathcal{M}_4 \times \mathcal{C}_d$ endowed with $\mathcal{G}_N$ invariance. Consider a field $\Phi(x,y)$ on $\mathcal{M}_4 \times \mathcal{C}_d$, the action of $g \in \mathcal{G}_N$ on it [1]

$$\Phi(x,y) \;\rightarrow\; \Phi^g(x,y) = G(g)\Phi(x, g^{-1}\cdot y)\,, \tag{2.0.1}$$

being a symmetry of the $\mathcal{M}_4 \times \mathcal{C}_d$ theory. The orbifold model is defined by gauging away the $\mathcal{G}_N$ action in Eq. (2.0.1), *i.e.* by eliminating from the theory quantum fluctuations which are not invariant under the symmetry transformations. In practice, one restricts to field configurations which are invariant under the $\mathcal{G}_N$ action:

$$\Phi(x, g\cdot y) = G(g)\Phi(x,y)\,, \tag{2.0.2}$$

for any $g \in \mathcal{G}_N$. Physically, the above condition is very clear. Since the point y is really the same point as $g \cdot y$, fields at the two points must be equivalent, so that they must be related by a symmetry transformation as in Eq. (2.0.2). The need for the transformations (2.0.1) to form a representation of the $\mathcal{G}_N$ group, which simply means $G(g)$ to be a representation, is also clear from Eq. (2.0.2). If $g_3 = g_1 \cdot g_2$, $g_{1,2,3} \in \mathcal{G}_N$, we get from Eq. (2.0.2),

$$\Phi(x, g_3\cdot y) = G(g_3)\Phi(x,y) = \Phi(x, g_1\cdot g_2 \cdot y) = G(g_1)\cdot G(g_2)\Phi(x,y)\,,$$

which, in general, would imply $\Phi(x,y)$ to vanish identically if $G(g_3) \neq G(g_1)\cdot G(g_2)$.

[1] We are neglecting here the case, which however may occur, in which $G = G(y)$ in Eq. (2.0.1).

2.1 The S^1/Z_2 Orbifold

The simplest orbifold, $S^1/\mathbf{Z}_2$, is obtained from the circle S^1 by modding out the 2–element $\mathbf{Z}_2 \equiv \{\mathbb{1}, z_2\}$ group of parity, whose only non–trivial element z_2 (${z_2}^2 = \mathbb{1}$) acts as $z \cdot y = -y$ on the coordinate $y \in [-\pi R, \pi R)$ which describes the circle. This is clearly a symmetry operation on S^1 and it has two fixed points $y_1 = 0$ and $y_2 = \pi R$ on it. The fundamental domain is the segment $[0, \pi R]$ and the two extremes, the fixed points, are not identified. The $S^1/\mathbf{Z}_2$ orbifold is then just a line segment, whose boundaries are the fixed points. Consider a field Φ on $\mathcal{M}_4 \times S^1/\mathbf{Z}_2$ and general Scherk–Schwarz periodicity conditions as in Eq. (1.2.1). If we have to construct an orbifold theory, an action $Z_2 \in \mathbf{Z}_2$ (such that ${Z_2}^2 = \mathbb{1}$, since it must provide a representation of $\mathbf{Z}_2$) on Φ must be defined

$$\Phi(x, y) \;\longrightarrow\; \Phi^{z_2}(x, y) = Z_2 \Phi(x, -y)\,, \tag{2.1.1}$$

so that the S^1 theory is invariant under it. To this end, we have to ensure the Φ Lagrangian to be invariant, but also the transformed field in Eq. (2.1.1) to have the same boundary conditions (1.2.1) as the original one, so that the z_2 action in Eq. (2.1.1) is well defined on the S^1 fields. This implies the consistency condition

$$T Z_2 T = Z_2\,. \tag{2.1.2}$$

As already mentioned, $S^1/\mathbf{Z}_2$ is simply the segment $[0, \pi R]$; Eq. (2.1.1) and (1.2.1) can indeed be translated into boundary conditions. At $y = 0$, Eq. (2.1.1) implies

$$(\mathbb{1} - Z_2)\Phi(x, 0) = 0\,, \qquad (\mathbb{1} + Z_2)\partial_y \Phi(x, 0) = 0\,,$$

so that, since Z_2 can always be diagonalized as $Z_2 = \mathrm{diag}(+1, \ldots, -1, \ldots)$, we have Neumann ($\partial\Phi = 0$) boundary conditions at 0 when ϕ has parity $Z_2 = 1$, Dirichlet ones ($\Phi = 0$) when $Z_2 = -1$. At $y = \pi R$, Eq. (2.1.1) and (1.2.1) imply

$$(\mathbb{1} - T Z_2)\Phi(x, \pi R) = 0\,, \qquad (\mathbb{1} + T Z_2)\partial_y \Phi(x, \pi R) = 0\,.$$

Since, due to Eq. (2.1.2), $(T Z_2)^2 = \mathbb{1}$, $Z_2' \equiv T Z_2$ can be defined as the effective orbifold projection matrix at the πR fixed point. Depending on the sign of $Z_2' = \pm 1$, Neumann or Dirichlet boundary conditions are given to Φ at the second fixed point.

Suppose now $\Phi(x, y)$ to be a scalar field with Scherk–Schwarz $U(1)$ twist as in Eq. (1.2.2). On Φ, Z_2 simply acts as $+1$ or -1, so that two inequivalent orbifold conditions

$$\Phi(x, -y) = \pm \Phi(x, y)\,, \tag{2.1.3}$$

can be imposed. In both cases, however, Eq. (2.1.2), as it is always the case when T and Z_2 are assumed to commute, implies $T^2 = 1$. Consistency then makes not all values of α in Eq. (1.2.2) to be allowed, but only $\alpha = 0$, so that $T = 1$, or $\alpha = 1/2$, so that $T = -1$. The need for α to be quantized can be also understood from its Wilson line interpretation, discussed in Sect.1.2. Performing a non–periodic gauge transformation as in Eq. (1.2.4, 1.2.5), the twist α is removed from the S^1 periodicity of Φ', but it reappears in the orbifold boundary condition of the gauge connection A'_y. As we will better discuss in Sect. 2.2, $A_y(-y) = -A_y$ while, from Eq. (1.2.5)

$$A'_y(x, -y) = -A'_y(x, y) + \frac{2\alpha}{g_5 R}\,. \qquad (2.1.4)$$

The action of the orbifold z_2 transformation on A'_y is then the composition of the parity operation with a gauge transformation of parameter $\beta = \frac{2\alpha}{g_5 R} y$. Correspondingly, the same gauge transformation enters in the z_2 action of Φ' which indeed is

$$\Phi'(x, y) \;\rightarrow\; \Phi'^{z_2}(y) = \pm e^{2i\frac{\alpha y}{R}}\Phi'(x, -y)\,, \qquad (2.1.5)$$

which is only compatible with Φ' to be periodic when $\alpha = 0$ or $\alpha = 1/2$. As for S^1, the Scherk–Schwarz twist on $S^1/\mathbf{Z}_2$ can be interpreted as a Wilson line on the path connecting the two fixed points, which is however a discrete Wilson line since

$$W = e^{-ig_5\int_0^{\pi R} A_y dy} = \pm 1\,.$$

Moreover, as it is possible to see from Eq. (2.1.4) and (2.1.5), the case $W = -1$ ($\alpha = 1/2$) and $W = 1$ ($\alpha = 0$) are realized in two "topologically" different theories, depending on the different choices of the z_2 orbifold action on the fields. This is a crucial difference with the S^1 case, in which all Scherk–Schwarz twists were realized as different vacua of the same theory and the actual value of α was dynamically fixed. Since α is a discrete number now, no dynamics can fix it and taking $W = \pm 1$ is up to our choice in defining the theory. To conclude, we observe that continuous Wilson lines also can be present on the $S^1/\mathbf{Z}_2$ orbifold, but only when T and Z_2 belong to a non–abelian group. The condition (2.1.2) could indeed be satisfied by a continuous set of transformations $T(\alpha)$ which it will be possible to reabsorb, as usual, with a non–periodic gauge transformation, then resulting in a flat background for some non–abelian gauge field. Also in this case, the Scherk–Schwarz symmetry breaking is a Wilson line breaking.

Leaving aside for simplicity the case $\alpha = 1/2$, wave functions for Φ on $S^1/\mathbf{Z}_2$ are easily obtained as linear combinations of the S^1 ones in Eq. (1.2.3) which satisfy the orbifold condition (2.1.3). Normalizing, we find

$$f_n^{\pm}(y) \equiv \frac{\eta_n}{\sqrt{2}} \left(f_n(y) \pm f_n(-y) \right) , \tag{2.1.6}$$

with $\eta_n = 2^{-\delta_{n,0}/2}$. Leaving aside the case $n = 0$, in which f_0^+ only is non–vanishing and must be considered, since $f_n(-y) = f_{-n}(y)$, we have $f_{-n}^{\pm}(y) = \pm f_n^{\pm}(y)$, so that independent wave functions in Eq. (2.1.6) are only labelled by $n = 1, \ldots, \infty$. The $f_n^{\mp}$'s are simply given by the usual sine and cosine functions. As an example of the orbifold compactification procedure, consider the scalar field $\Phi^{\pm}$ with orbifold conditions as in Eq. (2.1.3) and periodic on the circle. It is expanded as

$$\Phi^{\pm}(x, y) = \sum_n \phi_n^{\pm}(x) f_n^{\pm}(y) , \tag{2.1.7}$$

and this expansion must be inserted in the $5D$ Lagrangian

$$\mathcal{L}_5 = \partial_M(\Phi)^{\dagger} \partial^M \Phi + m^2 (\Phi)^{\dagger} \Phi ,$$

and integrated in the extra dimension to get the $4D$ effective Lagrangian. The result is immediately found if observing that the orbifold expansion in Eq. (2.1.7) can be matched with the circle one

$$\Phi(x, y) = \sum_n \tilde{\phi}_n(x) f_n(y) = \tilde{\phi}_0 f_0 + \sum_{n=1}^{\infty} \left(\tilde{\phi}_n f_n + \tilde{\phi}_{-n} f_{-n} \right) ,$$

by constraining the $4D$ S^1 fields with the conditions $\tilde{\phi}_n = \pm\tilde{\phi}_{-n} = \frac{1}{\sqrt{2}} \phi_n^{\pm}$ and requiring $\tilde{\phi}_0 = 0$ for $\pm = -$, $\tilde{\phi}_0 = \phi_0^+$ for $\pm = +$. By imposing this on the $4D$ S^1 effective Lagrangian in Eq. (1.1.5), one finds that of the two degenerate massive scalars of mass $M_n = \sqrt{(\frac{n}{R})^2 + m^2}$ only one survives the orbifold projection while the other disappears. The massless zero–mode, moreover, only survives when $Z = +1$. Note that the presence of two degenerate massive scalars in the S^1 theory, which the orbifold parity interchanges and which are identified by the orbifold condition, is due to the parity invariance of the theory itself.

As already mentioned, orbifolds are particularly important for model–building since they permit to generate a chiral fermion spectrum in $4D$ starting from a (non–chiral) ED theory. To see how this happens, consider a $5D$ fermion Ψ on $S^1/\mathbf{Z}_2$. The parity $y \to -y$ acts on the spinor representation of the $5D$ Lorentz group with the matrix γ_5, so that the orbifold condition on fermions is

$$\Psi(x, -y) = \pm\gamma_5 \Psi(x, y) ,$$

where an additional $\pm$ can be inserted by exploiting the phase transformation invariance of the field. What is important in the above equation is that L– and R–handed fermions are treated differently by the orbifold projection, so that if $\pm = +$ is chosen, Ψ_L is even while Ψ_R is odd. The chiral field are then Fourier–expanded as in Eq. (2.1.7), with $+$ for Ψ_L and $-$ for Ψ_R, the contrary for $\pm = -$. The orbifold spectrum is immediately found from the circle one described in Sect. 1.6.1, in which however $m = 0$ must be set, since a $5D$ mass–term $m\overline{\Psi}\Psi$ is not invariant under the orbifold symmetry. Of each couple of fermions with degenerate mass $m_n = \frac{n}{R}$ $(n = 1, \ldots, \infty)$, only one survives the orbifold projection and of the massless Dirac fermion only one chirality (L–handed for $\pm = +$, R–handed for $\pm = -$) is left. We have then seen how a chiral spectrum is obtained from the very simple $S^1/\mathbf{Z}_2$ compactification.

2.2 Gauge theories on $S^1/\mathbf{Z}_2$

Another reason why orbifolds are so popular is that they can break local or global symmetries. Non–trivial conditions on the fields such as those given in Eq. (2.0.2) or (1.2.1), of the form

$$\Phi(x, y'(y)) = \mathcal{T}\Phi(x, y)\,, \tag{2.2.1}$$

can indeed, in general, restrict the symmetry group of Φ since allowed transformations $\Phi \to \Phi'$ will be required to preserve Eq. (2.2.1) in the sense that

$$\Phi'(x, y'(y)) = \mathcal{T}\Phi'(x, y)\,. \tag{2.2.2}$$

In the case of global transformations, $\Phi' = g\Phi$, only those g will be allowed which commute with $\mathcal{T}$, so that the original symmetry group is restricted to its subgroup which commutes with $\mathcal{T}$. When dealing with local transformations, $\Phi' = g(x, y)\Phi$, the condition coming from Eq. (2.2.2) is

$$g(x, y'(y))\mathcal{T} = \mathcal{T}g(x, y)\,, \tag{2.2.3}$$

and provides a restriction on the allowed local transformations to be performed. In the case in which the condition (2.2.1) is identified with the general orbifold condition coming from Eq. (2.1.1) and the local group is a generic non–abelian Lie group $\mathcal{G}$ with generators t^a so that

$$g(x, y) = e^{i\alpha_a(x,y)t^a}\,,$$

imposing Eq. (2.2.3) means to define the parity of the gauge transformation parameters α^a under $y \to -y$. One has indeed

$$\alpha_a(x,-y)t^a = Z_2 \alpha_a(x,y) t^a {Z_2}^{-1}\,, \tag{2.2.4}$$

and, since ${Z_2}^2 = \mathbb{1}$, the above equation, when it is diagonalized, simply states some combinations of the α's to be even and some others to be odd. As we will better discuss in the following, only the subgroup of $\mathcal{G}$ which is generated by the even t^a's (*i.e.* the ones which commute with Z_2, whose associated transformation parameter α^a is even) will appear as the gauge group of the resulting $4D$ theory. As we discussed in Sect. 1.5, indeed, it is the "zero–mode" of the gauge parameter α^a which corresponds to the unbroken $4D$ $U(1) \subset \mathcal{G}$ which is left by the S^1 compactification, all the others being non–linearly realized.

Consider then, on the orbifold $S^1/\mathbf{Z}_2$, the gauge connection $A_M = A_{M,a}t^a$ associated to the group $\mathcal{G}$, its components being periodic around the circle. The most general orbifold condition one can give to A is

$$A_\mu(x,-y) = Z_2 A_\mu(x,y) {Z_2}^{-1}\,, \qquad A_y(x,-y) = -Z_2 A_y(x,y){Z_2}^{-1}\,, \tag{2.2.5}$$

where the relative minus sign between the μ and the y component is due to the parity action. Note that the matrix Z_2 does not need to be an element of $\mathcal{G}$ for the Lagrangian to be invariant. Clearly, Eq. (2.2.5) matches Eq. (2.2.4) in the sense that the condition (2.2.5) is preserved by gauge transformations as in Eq. (2.2.4). In practice, Eq. (2.2.5) simply states some of the gauge bosons to be even and some others to be odd. To work out the spectrum and the gauge structure of the resulting theory we can then simply consider abelian gauge bosons $A^\pm$ with both possible parities:

$$A_\mu^\pm(x,-y) = \pm A_\mu^\pm(x,y)\,, \qquad A_y^\pm(x,-y) = \mp A_y(x,y)\,. \tag{2.2.6}$$

When $\pm = +$, the fields are expanded as

$$A_\mu^+(x,y) = \sum_n {A^{+n}}_{mu} f_n^+\,, \qquad {A^+}_\mu(x,y) = \sum_n {A^{+n}}_\mu f_n^-\,,$$

which matches the S^1 parametrization (1.4.2) if imposing, for $n \neq 0$, $A_\mu^n = A_\mu^{-n} = \left(A_\mu^n\right)^\dagger = \frac{1}{\sqrt{2}}{A^{+n}}_\mu$ and $A_y^n = -A_y^{-n} = -\left(A_y^n\right)^\dagger = \frac{1}{\sqrt{2}}{A^{+n}}_y$. This means, with the definition of Eq. (1.4.5), taking Y_μ^n and y^n to vanish and ${A^{+n}}_\mu = X_\mu^n$, ${A^{+n}}_y = -ix^n$. For what concerns the zero–modes, the gauge boson A_μ^0 is left while the scalar A_y^0 is removed. We then find that of the two non–linearly realized $U(1)$ symmetries we had on S^1 for any $n > 0$, only one is left, and correspondingly only one massive gauge boson. The unbroken $U(1)$ associated to the zero–mode of A_μ remains, so that we have a massless $4D$ vector boson, while the extra massless scalar A_y^0 is projected out. When taking $\pm = -$ in Eq. (2.2.6), fields are expanded as

$$A^-{}_\mu(x,y) = \sum_n A^-{}_\mu^n f_n^- , \qquad A^-{}_\mu(x,y) = \sum_n A^-{}_\mu^n f_n^+ ,$$

and to match Eq. (1.4.2) we have to require $A_\mu^n = -A_\mu^{-n} = -\left(A_\mu^n\right)^\dagger = \frac{1}{\sqrt{2}} A^-{}_\mu^n$ and $A_y^n = A_y^{-n} = \left(A_y^n\right)^\dagger = \frac{1}{\sqrt{2}} A^-{}_y^n$, which means $A^+{}_\mu^n = iY_\mu^n$, $A^+{}_y^n = y^n$ while X_μ^n and x^n are equal to zero. For what concerns the zero–modes, it is the scalar A_y^0 which is left now, while A_μ^0 is projected out. In this second case, then, there is no track of the unbroken $U(1)$ $4D$ gauge symmetry we had on S^1, which is now explicitly broken, and just one tower of non–linearly realized $U(1)$'s is left. We have then shown that of a $5D$ non–abelian gauge group $\mathcal{G}$, only its subgroup $\mathcal{H}$ which commutes with the orbifold projection Z_2 (whose associated gauge bosons have then parities as in Eq. (2.2.6) with $\pm = +$) survives the compactification, in the sense that in the resulting $4D$ theory we will find only an $\mathcal{H}$ linearly realized gauge group. To conclude, note that all the discussion on the gauge fixing procedure performed in Sect. 1.4 for the S^1 case goes on in the same way for $S^1/\mathbf{Z}_2$ as well. The gauge fixing term is the same as in Eq. (1.4.9) and the ghost action is given by Eq. (1.4.10). The ghost fields, clearly, are subjected to the orbifold condition

$$c(x,-y) = Z_2 c(x,y) Z_2{}^{-1} , \qquad \bar{c}(x,-y) = Z_2 \bar{c}(x,y) Z_2{}^{-1} .$$

In this section, we have described $5D$ scalars, fermion and gauge fields compactified on $S^1/\mathbf{Z}_2$ and we have shown most of the results to be similar to the S^1 ones, and easily derived from those. There is a point, however, in which the orbifold theory appears different, and slightly more complicated then the corresponding flat–space one. If on S^1 (and on T^2 as well) Feynman rules for interacting theories are easily extracted from the ones on the ED Mikowski one, essentially because translational invariance is preserved, this is more difficult on the orbifold, since momentum conservation is violated. One can immediately realize that, if plugging a field expansion like (2.1.7) in any $5D$ interaction Lagrangian, interactions which do not conserve the Kaluza–Klein index n will arise. A method for simply obtaining the Feynman rules on $\mathcal{C}_d/\mathbf{Z}_N$ orbifolds from the corresponding ones on $\mathcal{C}_d$, which is very useful in practical computations, is discussed at the end of this chapter.

2.3 The $T^2/\mathbf{Z}_N$ orbifolds

The T^2 torus is defined from the complex plane $\mathbb{C}$ with the identifications

$$z \sim z + \frac{2\pi R}{\sqrt{2}}, \qquad z \sim z + \frac{2\pi R}{\sqrt{2}} U. \tag{2.3.1}$$

The $T^2/\mathbf{Z}_N$ orbifolds are defined by modding out from the T^2 space the N–element $\mathbf{Z}_N$ group, of elements $\{\mathbb{1}, z_N, z_N^2, \ldots, z_N^{N-1}\}$, with ${z_N}^N = \mathbb{1}$, of $2\pi/N$ rotations around the origin of the complex plane. On $\mathbb{C}$, z_N acts as

$$z \longrightarrow \tau z, \tag{2.3.2}$$

with $\tau = e^{\frac{2\pi i}{N}}$. For this to be possible, however, the z_N action in Eq. (2.3.2) must be well defined on T^2, meaning that points of $\mathbb{C}$ which are identified by the Eq. (2.3.1), so that they are the same T^2 point, must be rotated by (2.3.2) into another couple of identified points. This requirement translates into the conditions

$$\tau = m + nU, \qquad \tau U = m' + n'U, \tag{2.3.3}$$

with m, n, m', n' integers. It turns out that the only values of N for which Eq. (2.3.3) can be satisfied are $N = 2, 3, 4, 6$. For $N = 2$, $\tau = -1$ and Eq. (2.3.3) is trivially satisfied, for any U, when $m = n' = -1$, $m = n = 0$. For $N = 3, 4, 6$, on the contrary, Eq. (2.3.3) only holds when the modular parameter is taken to be equal to the orbifold twist: $U = \tau$, so that orbifolds with $N \geq 3$ are labelled by one parameter only, the overall radius R. For $N = 3$, due to the equation $1 + \tau + \bar{\tau} = 0$, Eq. (2.3.3) is satisfied for $m = 0$, $n = 1$, $m' = n' = -1$. For $N = 4$, $\tau = i$ and $m = 0$, $n = 1$, $m' = -1$ and $n' = 0$ in Eq. (2.3.3). For $N = 6$, finally, the identity $1 - \tau + \tau^2 = 0$ can be used to show that Eq. (2.3.3) works for $m = 0$, $n = 1$, $n' = 1$ and $m' = -1$. Being an orbifold, $T^2/\mathbf{Z}_N$ has fixed points, whose structure is however a bit more complicated then the $S^1/\mathbf{Z}_2$ one. Namely, points exist in the $\mathbf{Z}_4$ and $\mathbf{Z}_6$ cases which are fixed under the action of some element ${z_N}^l \in \mathbf{Z}_N$, but not fixed under some subgroup of $\mathbf{Z}_N$, which interchanges (and then identifies) them. Fixed points are then labelled as $z_{l,i}$ ($i = 1, \ldots, F_l$), where the integer l, which assumes values in the $1, \ldots, [N/2]$ range, is the minimum power of τ for which

$$z_{l,i} = \tau^l z_{l,i} + m_i + n_i U,$$

for some couple of integers (m_i, n_i). In the following, a point $z_{l,i}$ will be called an "l–fixed point". On the fundamental domain of $T^2/\mathbf{Z}_2$, shown in Fig. 2.1, four

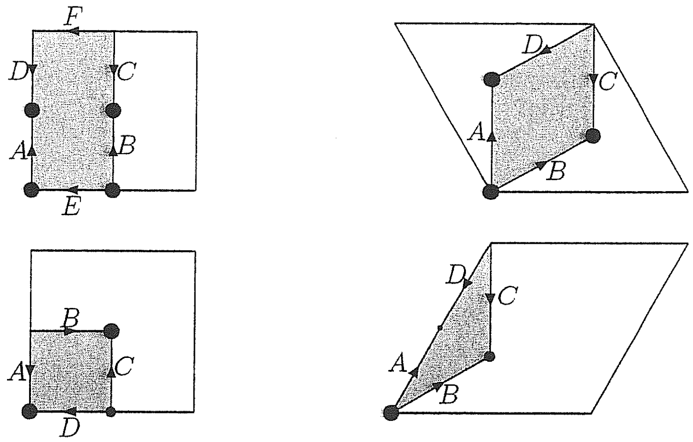

Figure 2.1: The picture shows the $T^2/\mathbf{Z}_2$, $T^2/\mathbf{Z}_3$, $T^2/\mathbf{Z}_4$ and $T^2/\mathbf{Z}_6$ orbifolds and their covering tori. Points of decreasing size indicate the 1–, 2– and 3–fixed points respectively. The Grey region represents the fundamental domain of the orbifolds, and the segments delimiting it must be identified according to: $A \sim D$, $B \sim C$ and, in the $T^2/\mathbf{Z}_2$ case, $E \sim F$.

distinct 1–fixed points are present, with $(n_i, m_i) = (0,0), (1,0), (1,1), (0,1)$ for $i = 1, \ldots, 4$, respectively. On $T^2/\mathbf{Z}_3$, one has three 1–fixed points with $(n_i, m_i) = (0,0), (1,0), (1,1)$ while tw 1–fixed ($(n_i, m_i) = (0,0), (1,0)$) and one 2–fixed ($(n, m) = (1,0)$) points are present on $T^2/\mathbf{Z}_4$. Finally, $T^2/\mathbf{Z}_6$ has one 1–fixed $(0,0)$, one 2–fixed $(1,0)$ and one 3–fixed $(0,1)$ point. In the following, however, it will be also useful to define the numbers N_k of points which are fixed under the action of the ${z_N}^k$ element of $\mathbf{Z}_N$, which are called ${z_N}^k$–fixed points. In N_k, independent ${z_N}^k$–fixed points in one fundamental domain of the T^2 torus are counted. This number is given by

$$N_k = \left[2 \sin \left(\frac{\pi k}{N} \right) \right]^2 , \tag{2.3.4}$$

and must not be confused with the number F_l of l–fixed points. For $N = 4$ and $l = k = 2$, for instance, $F_2 = 1$ while $N_2 = 4$, since the single 2–fixed point of $T^2/\mathbf{Z}_4$ is counted twice in N_2, due to its mirror with which it is identified by the z_4 action, and the 2 1–fixed points are also counted, since they are ${z_4}^2$–fixed also.

Consider now a field Φ with general periodicity on T^2

$$\Phi(x, z + \frac{2\pi R}{\sqrt{2}}) = T_1 \Phi(x, z) , \qquad \Phi(x, z + \frac{2\pi R}{\sqrt{2}} U) = T_2 \Phi(x, z) , \tag{2.3.5}$$

with $[T_1, T_2] = 0$, as shown in Sect. 1.3. The z_N action on Φ

$$\Phi(x, z) \;\longrightarrow\; \Phi(x, z)^{z_N} = Z_N \Phi(x, \tau^{-1} z) ,$$

which is taken to be a symmetry of the Φ Lagrangian, must also be compatible with its periodicity (2.3.5), *i.e.*

$$
\begin{aligned}
Z_N\Phi\left[x,\tau^{-1}\left(z+\tfrac{2\pi R}{\sqrt{2}}\right)\right] &= T_1 Z_N\Phi(x,\tau^{-1}z)\,,\\
Z_N\Phi\left[x,\tau^{-1}\left(z+\tfrac{2\pi R}{\sqrt{2}}U\right)\right] &= T_2 Z_N\Phi(x,\tau^{-1}z)\,,
\end{aligned}
\tag{2.3.6}
$$

for any Φ as in Eq. (2.3.5). For $N=2$, Eq. (2.3.6) becomes

$$
\begin{aligned}
Z_2\Phi(x,-z-\tfrac{2\pi R}{\sqrt{2}}) &= Z_2T_1^{-1}\Phi(x,-z) = T_1Z_2\Phi(x,-z)\,,\\
Z_2\Phi(x,-z-\tfrac{2\pi R}{\sqrt{2}}U) &= Z_2T_2^{-1}\Phi(x,-z) = T_2Z_2\Phi(x,-z)\,,
\end{aligned}
\tag{2.3.7}
$$

which implies

$$
Z_2 = T_i Z_2 T_i\,, \tag{2.3.8}
$$

for $i=1,2$ or, equivalently, $(T_iZ_2)^2 = \mathbb{1}$. This condition is analogous to what found for $S^1/\mathbf{Z}_2$ in Eq. (2.1.2). As for the circle, the general periodicity conditions (Scherk–Schwarz twists) in Eq. (2.3.5) can be reabsorbed (if the T_i's belong to some gauged symmetry group) by local non–periodic transformations, so that they are equivalent to a flat (Wilson loop) gauge background. We have two independent Wilson loops on T^2, wrapping around the two cycles on the torus, which are equivalent to the two Scherk–Schwarz parameters which can be introduced in the periodicity conditions. As for the circle, if T_i and Z_2 are taken to commute in Eq. (2.3.8), we find $T_i^2=\mathbb{1}$ which corresponds the two Wilson lines W_i being discrete. Clearly, the two T_i's can be independently chosen. We will then say that two ($\mathbf{Z}_2$, since $T_i^2 = W_i^2 = \mathbb{1}$) discrete Wilson lines are present on $T^2/\mathbf{Z}_2$. Note that Eq. (2.3.8) does not forbid Wilson lines to be continuous, when Z_2 and T_i belong to some non–abelian group. Also in the continuous case, of course, $W_{1,2}$ are independent on $T^2/\mathbf{Z}_2$. On $T^2/\mathbf{Z}_3$, on the contrary, Eq. (2.3.6) gives

$$
\begin{aligned}
Z_3\Phi(x,\bar\tau z-\tfrac{2\pi R}{\sqrt{2}}(1+\tau)) &= Z_3T_1^{-1}T_2^{-1}\Phi(x,\bar\tau z) = T_1Z_3\Phi(x,\bar\tau z)\,,\\
Z_3\Phi(x,\bar\tau z+\tfrac{2\pi R}{\sqrt{2}}) &= Z_3T_1\Phi(x,\bar\tau z) = T_2Z_3\Phi(x,\bar\tau z)\,,
\end{aligned}
\tag{2.3.9}
$$

where the relation $\bar\tau = -1-\tau$ has been used. The above equation implies the two conditions $Z_3T_1^{-1}T_2^{-1} = T_1Z_3$ and $Z_3T_1 = T_2Z_3$. The two matrices $T_{1,2}$, then, cannot be independently chosen, so that there is only one independent Wilson line on $T^2/\mathbf{Z}_3$. When considering abelian groups, $[T_i, Z_3] = 0$, we find $T_1 = T_2 \equiv T$, $T^3 = \mathbb{1}$, and T is a discrete ($\mathbf{Z}_3$) Wilson line. For $T^2/\mathbf{Z}_4$, similarly, we find from Eq. (2.3.6) that $Z_4T_2^{-1} = T_1Z_4$ and $Z_4T_1 = T_2Z_4$. Also in this case, then, only one independent Wilson line is present which in the abelian case becomes a $\mathbf{Z}_2$ Wilson line, since $T_i = T$ and $T^2 = \mathbb{1}$ when $[T_i, Z_4] = 0$. For $T^2/\mathbf{Z}_6$, making use of the relation $\bar{\tau} = 1 - \tau$, one finds $Z_6 T_1 T_2^{-1} = T_1 Z_6$ and, as before, $Z_6 T_1 = T_2 Z_6$. On $T^2/\mathbf{Z}_6$, no discrete Wilson lines are present, since one finds $T_1 = T_2 = \mathbb{1}$ in the abelian case. All the consistency conditions we have derived for $N = 3, 4, 6$ can be rewritten in the more standard form as

$$(T_i {Z_N}^q)^{N/q} = \mathbb{1}\,, \qquad Z_N T_1 = T_2 Z_N\,, \tag{2.3.10}$$

where $q = 1, \ldots, [N/2]$ is such that N/q is an integer.

2.4 Wave functions on $T^2/\mathbf{Z}_N$

Suppose now Φ^g to be a scalar field on T^2 with trivial periodicity conditions around the cycles of the torus, so that Eq. (2.3.10), since ${Z_N}^N = \mathbb{1}$, is automatically satisfied. The more general orbifold boundary condition is given by

$$\Phi^g(\tau z) = g\Phi^g(z)\,,$$

where we have omitted the indication of the coordinate x (and $\bar{z}$, as usual) for simplicity, and $g^N = 1$. The wave functions on which Φ will be expanded are linear combinations of the T^2 ones in Eq. (1.3.2). They are more easily found by employing the real coordinates $w_{1,2}$ defined in Eq. (1.3.1), which are independently periodic with period $2\pi R$. For $N = 3, 4, 6$, with $U = \tau$, the z_N twist changes the point (w_1, w_2) into the point $(-w_2, w_1 + 2\tau_1 w_2)$, where $\tau_{1,2}$ denotes the real and imaginary parts of τ. For $\mathbf{Z}_2$, one has simply $(w_1, w_2) \to (-w_1, -w_2)$. It will be convenient in the following to introduce a matrix notation, in which the vector $\vec{w}$ is transformed into the vector $Z_N^t \vec{w}$. The matrix Z_N is given by

$$Z_N = \begin{pmatrix} 0 & 1 \\ -1 & 2\tau_1 \end{pmatrix} \tag{2.4.1}$$

for $N = 3, 4, 6$, while $Z_2 = -\mathbb{1}$. By remembering that the basis of periodic functions on T^2 is given by the usual exponential functions $f_{\vec{n}}(\vec{w}) \sim e^{\frac{i}{R}\vec{n}^t \cdot \vec{w}}$ in the $\vec{w}$ coordinates, we find that the effect of rotating $\vec{w}$ with Z_N^t is the same as rotating $\vec{n}$ with Z_N so that, going back to complex coordinates

$$f_{\vec{n}}(\tau^k z) = f_{Z_N^k \vec{n}}(z)\,, \qquad \lambda_{Z_N^k \vec{n}} = \tau^k \lambda_{\vec{n}}\,. \tag{2.4.2}$$

One can easily verify that $Z_N \vec{n} \in \mathbb{Z}^2$ for all allowed values of N and τ. It is now easy to construct $\mathbf{Z}_N$ covariant wave functions on T^2 by applying to the functions

(1.3.2) the orbifold projection weighted by the $\mathbf{Z}_N$ phase g. Defining for convenience the quantity $\eta_{\vec{n}} = N^{-\delta_{\vec{n},\vec{0}}/2}$, those are given by

$$h^g_{\vec{n}}(z) = \frac{\eta_{\vec{n}}}{\sqrt{N}} \sum_{k=0}^{N-1} g^{-k} f_{Z_N^k \vec{n}}(z) \,, \tag{2.4.3}$$

and, thanks to (2.4.2), satisfy the twisted boundary condition

$$h^g_{\vec{n}}(\tau z) = g h^g_{\vec{n}}(z) \,.$$

It is easy to verify that these functions are orthonormal with respect to the Kaluza–Klein momenta $\vec{n}$ and the twist g. However, the functions $h^g_{\vec{n}}(z)$ are not all independent: those with mode vectors connected by the orbifold action are proportional to each other through a phase:

$$h^g_{Z_N^k \vec{n}}(z) = g^k h^g_{\vec{n}}(z) \,. \tag{2.4.4}$$

Correspondingly, the mode vectors $\vec{n}$ are not all independent but restricted to belong to some fundamental domain, which can be determined as follows. The matrix (2.4.1) represents the $\mathbf{Z}_N$ action on the mode vector $\vec{n}$ for the torus wave functions. For $N \neq 2$, it amounts to a rotation with phase τ on the complex plane $u = -n_1 + \tau n_2$. This means that we can divide the space $\mathbb{Z}^2$ of all possible mode vectors $\vec{n}$ into the origin, which is left fixed by Z_N, plus N sectors D_k, with $k = 0, \ldots, N-1$, mapped into each other by Z_N. For $N > 2$, these domains can all be defined as $D_k = \{\vec{n} \in \mathbb{Z}^2 | (Z_N^k \vec{n})_1 < 0, (Z_N^k \vec{n})_2 \geq 0\}$, whereas for $N = 2$, they are given by $D_0 = \{\vec{n} \in \mathbb{Z}^2 | n_1 > 0 \oplus (n_1 = 0, n_2 > 0)\}$, $D_1 = \{\vec{n} \in \mathbb{Z}^2 | n_1 < 0 \oplus (n_1 = 0, n_2 < 0)\}$. The independent wave functions in (2.4.4) are then associated to $\vec{n} \in D_0$ plus the origin if $g = 1$, the ones associated to $\vec{n} \in D_k$ with $k \neq 0$ being the $\mathbf{Z}_N$-transformed of these.

It is now straightforward to characterize the effective $4D$ theory arising from $T^2/\mathbf{Z}_N$ compactification of our scalar Φ. It can be expanded in KK modes as

$$\Phi^g(x, z) = \delta^{g,1} \phi^g{}_{\vec{0}}(x) h^1_{\vec{0}}(z) + \sum_{\vec{n} \in D_0} \phi^g{}_{\vec{n}}(x) h^g_{\vec{n}}(z) \,, \tag{2.4.5}$$

and, similarly to what done for $S^1/\mathbf{Z}_2$, the above expansion can be matched with the T^2 one

$$\Phi(x, z) = \sum_{\vec{n}} \tilde{\phi}_{\vec{n}}(x) f_{\vec{n}}(z) = \tilde{\phi}_0 f_0 + \sum_{\vec{n} \in D_0} \sum_{k=0}^{N-1} \tilde{\phi}_{Z_N{}^k \vec{n}} f_{Z_N{}^k \vec{n}} \,,$$

with the identifications $g^k\tilde{\phi}_{Z_N{}^k\vec{n}} = \tilde{\phi}_{\vec{n}} = \frac{1}{\sqrt{N}}\phi^g{}_{\vec{n}}$ and $\tilde{\phi}_0 = \phi^1{}_{\vec{0}}$ for $g=1$, $\tilde{\phi}_0 = 0$ in all other cases. Note that, due to Eq. (2.4.2), since $m_{\vec{n}} = |\lambda_{\vec{n}}|$, all the N $4D$ fields $\tilde{\phi}_{Z_N{}^k\vec{n}}$ (for $\vec{n} \neq \vec{0}$) which arise from T^2 compactification are degenerate in mass, as a consequence of the $\mathbf{Z}_N$ invariance of the theory. On the orbifold, all of them are removed but one combination, so that the massive spectrum, which is independent on g, consists on a tower of scalars with mass as in Eq. (1.3.4), one for each $\vec{n} \in D_0$. The zero–mode massless scalar, clearly, is present for $g=1$ only.

2.5 Fermions and Gauge fields on $T^2/\mathbf{Z}_N$

Be Ψ, with the conventions of Sect. 1.6, a $6D$ L–handed field on the torus T^2, with trivial periodicities around the cycles. On it, the z_N ($z \to \tau z$) transformation, which is a rotation in the $6D$ Lorentz group, acts as

$$\Psi(z) \;\to\; \Psi^{z_N}(z) = g' R \Psi(\tau^{-1} z)\,, \tag{2.5.1}$$

where g' is an arbitrary $U(1)$ phase and $R = \exp(\frac{2\pi i}{N} J_{56})$ is (up to a minus sign, $-1 = \exp(2\pi i J_{56})$, corresponding to the ambiguity in defining the Lorentz action on spinors) the representation on Ψ of $2\pi/N$ rotations, with $J_{56} = -\frac{i}{2}\Gamma_5\Gamma_6$. Using Eq. (1.6.5) for gamma matrices, one finds, in the 2×2 matrices notation defined by Eq. (1.6.8)

$$J_{56} = -\mathbb{1} \otimes \frac{\sigma_3}{2} \;\;\Rightarrow\;\; R = \begin{pmatrix} \tau^{-1/2} & 0 \\ 0 & \tau^{1/2} \end{pmatrix}. \tag{2.5.2}$$

Note that, as expected since it represents a 2π rotation on fermions, $R^N = -\mathbb{1}$, so that we must take $g' = g\tau^{1/2}$, with $g^N = 1$, to ensure $(g'R)^N = \mathbb{1}$, as required for Eq. (2.5.1) to be $\mathbf{Z}_N$ transformation. The orbifold condition on Ψ then reads

$$\Psi(\tau z) = \begin{pmatrix} \chi_R(\tau z) \\ \chi_L(\tau z) \end{pmatrix} = \begin{pmatrix} g\chi_R(z) \\ g\tau\chi_L(z) \end{pmatrix}. \tag{2.5.3}$$

As for scalars, the $4D$ fermion spectrum arising from Ψ is easily extracted from the known T^2 one. The massive spectrum, again, does not depend on the twist g and consists on a tower of $4D$ Dirac fermions with mass as in Eq. (1.3.4), one for each $\vec{n} \in D_0$, the degeneracy in the spectrum being (partially) removed. For what concerns zero–modes, one R–handed fermion is left for $g=1$, and one L–handed for $g = \bar{\tau}$, so that we can have a chiral spectrum. No zero–modes are present for all other twists.

Let us now consider non–abelian gauge theories on $T^2/\mathbf{Z}_N$. Be Φ a field on $T^2/\mathbf{Z}_N$ transforming in some representation of a non–abelian gauge group $\mathcal{G}$. We take it to be periodic around the cycles of T^2 and with generic orbifold boundary conditions

$$\Phi(\tau z) = Z_N \Phi(z) .$$

The above condition, following the general discussion proposed at the beginning of Sect. 2.2, implies a restriction, summarized in Eq. (2.2.3), on the allowed local transformations $g(z) = e^{i\alpha_a(z)t^a}$ which can act on Φ. In our case, Eq. (2.2.3) implies specific orbifold boundary conditions for the local transformation parameters:

$$\alpha_a(\tau z)t^a = Z_N \alpha_a(z) t^a Z_N^{-1} , \tag{2.5.4}$$

similarly to what found for $S^1/\mathbf{Z}_2$ in Eq. (2.2.4). Let us now diagonalize Eq. (2.5.4). Since ${Z_N}^N = \mathbb{1}$, we can have α_a's of N different kinds, we call them α^g, with orbifold condition

$$\alpha^g(\tau z) = g\alpha^g(z) . \tag{2.5.5}$$

where $g = \tau^k$ and $k = 0, \ldots, N-1$. It is clear from the above equation that, in general, α^g will be a complex transformation parameter obtained as a complex linear combination of the starting α^a's, which are taken to be real in the standard notation. Since the "zero–mode" of α^g is only preserved by Eq. (2.5.5) when $g = 1$, only the subgroup $\mathcal{H}$ of $\mathcal{G}$ generated by "untwisted" generators, *i.e.* the ones which commute with Z_N, whose corresponding α's have $g = 1$, will appear unbroken in the resulting $4D$ theory. To explicitly check this, consider the $6D$ gauge connection $A_M = A_{M,a}t^a$ associated to the group $\mathcal{G}$. Its orbifold boundary condition, compatible with Eq. (2.5.5), is

$$\begin{aligned} A_\mu(\tau z) &= Z_N A_\mu(z) Z_N^{-1} , \\ A_z(\tau z) = \bar{\tau} Z_N A_z(z) Z_N^{-1} , &\quad A_{\bar{z}}(\tau z) = \tau Z_N A_{\bar{z}}(z) Z_N^{-1} . \end{aligned} \tag{2.5.6}$$

Note the $\bar{\tau}$ (τ) factor in the twist of A_z ($A_{\bar{z}}$) coming from the action of $2\pi/N$ Lorentz rotations on the $6D$ gauge field. As for the transformation parameters, Eq. (2.5.6) can be diagonalized and gauge bosons A_M^g, with N different twists can arise, corresponging to the transformation parameter α^g. We are then lead to the study of the $T^2/\mathbf{Z}_N$ compactification of complex gauge bosons A_N^g

$$A_\mu^g(\tau z) = g A_\mu^g(z) , \quad A_z^g(\tau z) = \bar{\tau} g A_z(z) , \quad A_{\bar{z}}^g(\tau z) = \tau g A_{\bar{z}}(z) , \tag{2.5.7}$$

with all possible twists $g = \tau^k$. Note that A_M^g, being a complex field, is the gauge connection of an $U(1) \times U(1)$ gauge symmetry.

As usual, orbifold theories are more easily discussed by starting from the corresponding theory on the covering space. The results of Sect. 1.5, however, were derived for a real gauge boson, so that they cannot be directly applied. Consider then a complex gauge field A_M on T^2. To avoid confusion, since we will be using complex coordinates z and $\bar{z}$, which complex conjugation interchanges, it is better to define $A^+ = A \equiv \frac{1}{\sqrt{2}}(R + iI)$ and $A^- \equiv \frac{1}{\sqrt{2}}(R - iI)$, in terms of the real gauge fields R and I. Note that $(A^-_\mu)^\dagger = A^+_\mu$, $(A^-_z)^\dagger = A^+_{\bar{z}}$ and $(A^-_{\bar{z}})^\dagger = A^+_z$. The Maxwell Lagrangian reads

$$
\begin{aligned}
\mathcal{L}_6 &= -\tfrac{1}{2} F^+{}_{MN} F^{-MN} \\
&= -\tfrac{1}{2} F^+{}_{\mu\nu} F^{-\mu\nu} + F^+{}_{\mu z} F^{-\mu}{}_{\bar{z}} + F^+{}_{\mu\bar{z}} F^{-\mu}{}_{z} + F^+{}_{z\bar{z}} F^-{}_{z\bar{z}} \,,
\end{aligned}
\tag{2.5.8}
$$

with $F^\pm{}_{MN} = \partial_M A^\pm_N - \partial_N A^\pm_M$. After some trivial algebraic manipulation, removing in the end all the A^-'s in favor of the complex conjugates of the A^+'s and omitting the apex "+", expanding the fields as

$$
A_M(x,z) = \sum_{\vec{n}} A^{\vec{n}}_M(x) f_{\vec{n}}(z)\,,
\tag{2.5.9}
$$

the $4D$ effective Lagrangian can be written in the form

$$
\mathcal{L}_4 = \mathcal{L}_4^{\vec{0}} + \sum_{\vec{n}\neq\vec{0}} \mathcal{L}_4^{\vec{n}}\,,
$$

with $\mathcal{L}_4^{\vec{n}}$ as in Eq. (1.5.5), having defined $G_{\vec{n}}$ and $S_{\vec{n}}$ as in Eq. (1.5.3). The only difference with Sect. 1.5 is that all $A^{\vec{n}}_M$ fields, and not just those for positive $\vec{n}$, are independent degrees of freedom now. The theory then describes, for any $\vec{n} \neq 0$, a tower of $U(1)^2$ non–linearly realized gauge symmetries, spontaneously broken at the scale $m_{\vec{n}}$. Moreover, one tower of complex massive scalars are present. At the massless level, we have now two linearly realized $U(1)$'s, and correspondingly two massless gauge bosons, and two massless complex scalars.

Consider now the orbifold theory, with orbifold condition (2.5.7). Orbifold fields will be expanded on the basis of the $h^g_{\vec{n}}$ defined in Sect. 2.4 as

$$
\begin{aligned}
A^g_\mu(x,z) &= \delta^{g,1} A^{g\,\vec{0}}_\mu(x) h^1_{\vec{0}}(z) + \textstyle\sum_{\vec{n}\in D_0} A^{g\,\vec{n}}_\mu(x) h^g_{\vec{n}}(z)\,, \\
A^g_z(x,z) &= \delta^{\bar{\tau}g,1} A^{g\,\vec{0}}_z(x) h^1_{\vec{0}}(z) + \textstyle\sum_{\vec{n}\in D_0} A^{g\,\vec{n}}_z h^{\bar{\tau}g}_{\vec{n}}(z)\,, \\
A^g_{\bar{z}}(x,z) &= \delta^{\tau g,1} A^{g\,\vec{0}}_{\bar{z}}(x) h^1_{\vec{0}}(z) + \textstyle\sum_{\vec{n}\in D_0} A^{g\,\vec{n}}_{\bar{z}} h^{\tau g}_{\vec{n}}(z)\,,
\end{aligned}
\tag{2.5.10}
$$

which matches the T^2 expansion (2.5.9) by identifying, at the massive level,

$$
\begin{aligned}
g^k A^{Z_N{}^k\vec{n}}_\mu &= A^{\vec{n}}_\mu = \tfrac{1}{\sqrt{N}} A^{g\,\vec{n}}_\mu\,, \\
(\bar{\tau}g)^k A^{Z_N{}^k\vec{n}}_z &= A^{\vec{n}}_z = \tfrac{1}{\sqrt{N}} A^{g\,\vec{n}}_z\,, \\
(\tau g)^k A^{Z_N{}^k\vec{n}}_{\bar{z}} &= A^{\vec{n}}_{\bar{z}} = \tfrac{1}{\sqrt{N}} A^{g\,\vec{n}}_{\bar{z}}\,,
\end{aligned}
\tag{2.5.11}
$$

for $k = 0, \dots N-1$. For the scalars defined in Eq. (1.5.3), the above identifications imply $g^k G^{Z_N{}^k} = G^{\vec{n}} \equiv \frac{1}{\sqrt{N}} G^{\vec{n}}_g$ and $g^k S^{Z_N{}^k} = S^{\vec{n}} \equiv \frac{1}{\sqrt{N}} S^{\vec{n}}_g$, which are the same as for the $4D$ gauge bosons. For all g, then, of the N "degenerate" (*i.e.*, broken at the same scale $m_{\vec{n}}$) non–linearly realized $U(1)^2$ symmetries, only one survives in the orbifold theory, so that we have in the spectrum one complex massive gauge boson only for any $\vec{n} \in D_0$. The same happens for the scalars $S^{\vec{n}}$. The big difference among the various values of g comes however in the massless sector. When $g = 1$ and just in that case, the linearly realized $U(1)$ survives, together with its massless gauge boson, while both scalars are removed from the theory. When $g = \tau$, the zero–mode scalar associated to A_z survives, the one coming from $A_{\bar{z}}$ when $g = \bar{\tau}$. For $T^2/\mathbf{Z}_2$ we have both, and we have no zero–modes at all in the other cases. Note that, for $g \neq 1$, when the $4D$ gauge boson is absent, the linearly realized $U(1)$ symmetry is explicitly broken by the orbifold.

For what concerns gauge–fixing problems, all the discussion of Sect. 1.5 can be applied the same way to the orbifold case. The gauge–fixing Lagrangian reads, as usual

$$\mathcal{L}_6^{g-f} = -\frac{1}{\xi} \mathrm{Tr}\left[\partial_\mu A^\mu - \xi(\partial_z A_{\bar{z}} + \partial_{\bar{z}} A_z)\right] , \qquad (2.5.12)$$

and the ghost action is like in Eq. (1.5.8). The ghost fields are subject to the orbifold condition

$$c(\tau z) = Z_N c Z_N^{-1} , \qquad \bar{c}(\tau z) = Z_N \bar{c} Z_N^{-1} .$$

For $\xi = 1$, as usual, the $6D$ Feynman gauge is recovered, but extracting the Feynman rules from the $6D$ one is not as trivial as in the T^2 (or S^1) case considered in the previous section. As already mentioned, this depends on the fact that translation invariance is broken on the orbifold, so that if $6D$ fields are expanded on the basis of orbifold wave functions, their interactions will not, in general, conserve the Kaluza–Klein index. Propagators are, on the contrary, diagonal. In the following section, along the lines of [25], a different parametrization of the orbifold fields will be discussed in which interactions verteces are Kaluza–Klein conserving, while the propagators are not. A simple prescription will be provided for obtaining orbifold Feynman rules from the ones on the corresponding covering space. This reveals to be an extremely useful tool when performing quantum computations in orbifold theories.

2.6 Feynman rules on orbifolds

Let us consider, as at the beginning of this chapter, a generic $\mathcal{C}_d/\mathcal{G}_N$ orbifold, restricting however to the case in which the N–element group $\mathcal{G}_N$ is a $\mathbf{Z}_N$ group. This is enough to cover all $T^2/\mathbf{Z}_N$'s and $S^1/\mathbf{Z}_2$ orbifolds we have treated in this chapter. Be Φ a generic field on $\mathcal{M}_4 \times \mathcal{C}_d$, on which the z_N orbifold $\mathbf{Z}_N$ symmetry acts as

$$\Phi(x,y) \;\rightarrow\; \mathcal{Z}_N\left[\Phi(x,y)\right] \equiv Z_N \Phi(x, {z_N}^{-1}\cdot y)\,,$$

with ${Z_N}^N = \mathbb{1}$, so that ${\mathcal{Z}_N}^N = \mathbb{1}$. The orbifold theory will be obtained from the $\mathcal{C}_d$ one by restricting Φ to be z_N–invariant which means

$$\Phi(x,y) = \mathcal{Z}_N\left[\Phi(x,y)\right]\,.$$

It is convenient [47] (see also [23]) to express Φ in terms of an unconstrained field $\tilde{\Phi}$ on $\mathcal{C}_d$ with the same quantum numbers as Φ , so that the above orbifold condition is automatically satisfied:

$$\Phi \equiv \frac{1}{N}\sum_{k=0}^{N-1} {\mathcal{Z}_N}^k\left[\tilde{\Phi}(x,y)\right] \equiv \mathcal{P}\left[\tilde{\Phi}(x,y)\right]\,, \tag{2.6.1}$$

where the $\mathcal{P}$ operator is a projector, meaning that $\mathcal{P}^2 = \mathbb{1}$, from the space of unconstrained $\mathcal{C}_d$ field $\tilde{\Phi}$ on the orbifold subspace. Orbifold correlators are obtained, in a functional approach, by integrating the $\mathcal{C}_d$ action on orbifold fields only

$$\langle \Phi \ldots \Phi^\dagger \rangle = \frac{1}{Z[0]}\int_{\mathcal{Z}_N[\Phi]=\Phi} \mathcal{D}\Phi\mathcal{D}\Phi^\dagger \Phi \ldots \Phi^\dagger e^{iS[\Phi]}\,.$$

In perturbation theory, all correlators are obtained from the free propagator through the Wick theorem, interactions coming from the power–expansion of the exponential of the action. Note that the action for the orbifold theory in the above equation is equal to the one on the covering space so that the Wick expansion is the same in the two cases, meaning that we have the same verteces in configuration space. The difference comes from the free propagator which, on the orbifold, is [2]

$$\langle \Phi\Phi^\dagger \rangle = \frac{1}{Z[0]}\int_{\mathcal{Z}_N(\Phi)=\Phi} \mathcal{D}\Phi\mathcal{D}\Phi^\dagger \Phi\Phi^\dagger e^{iS_0[\Phi]}\,, \tag{2.6.2}$$

[2]We write the propagator in the form of a correlator among Φ and its hermitian conjugate $\Phi^\dagger$, but our formalism clearly applies to real fields as well.

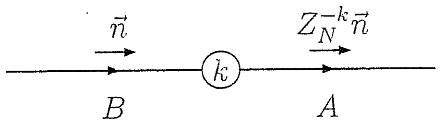

$$= \frac{1}{N}\left[{Z_N}^k \cdot \tilde{G}_{\vec{n}}\right]_{AB}$$

Figure 2.2: Feynman rule for the propagators on an orbifold. In the figure, A, B are a generic set of indices labelling the state and $k = 0, \dots, N-1$ is the possible twist of the propagator.

where $S_0 = (\Phi^\dagger, O \cdot \Phi)$ is the quadratic part of the action. The above equation can be rewritten as

$$\langle \Phi\Phi^\dagger \rangle = \frac{1}{Z[0]} \int \mathcal{D}\tilde{\Phi}\mathcal{D}\tilde{\Phi}^\dagger \mathcal{P}\left[\tilde{\Phi}\right] \mathcal{P}\left[\tilde{\Phi}\right]^\dagger e^{iS_0[\tilde{\Phi}]}, \tag{2.6.3}$$

where the integration variable $\tilde{\Phi}$ is a field on $\mathcal{C}_d$. This is easily proven by changing variables in the above integral, splitting the $\tilde{\Phi}$ field as $\tilde{\Phi} = \Phi + \tilde{\Phi}'$, where $\mathcal{P}[\tilde{\Phi}'] = 0$ and $\Phi = \mathcal{P}\left[\tilde{\Phi}\right]$ as in Eq. (2.6.1). By using the fact that, due to the z_N invariance of the $\mathcal{C}_d$ theory,

$$(\tilde{\Phi}^\dagger, O \cdot \tilde{\Phi}) = (\Phi^\dagger, O \cdot \Phi) + (\Phi'^\dagger, O \cdot \Phi'),$$

the Φ' integration can be performed and one comes back to Eq. (2.6.2). We have shown that the propagator of Φ can be written in terms of the propagator of $\tilde{\Phi}$ on the covering space $\mathcal{C}_d$, as

$$\langle \Phi(y_1)\Phi^\dagger(y_2) \rangle = \langle \mathcal{P}\left[\tilde{\Phi}(y_1)\right] \left(\mathcal{P}\left[\tilde{\Phi}(y_2)\right]\right)^\dagger \rangle \tag{2.6.4}$$

$$= \frac{1}{N^2} \sum_{k,l=0}^{N-1} {Z_N}^k \langle \tilde{\Phi}({z_N}^{-k} \cdot y_1)\tilde{\Phi}^\dagger({z_N}^{-l} y_2)\rangle ({Z_N}^\dagger)^l$$

$$= \frac{1}{N} \sum_{k=0}^{N-1} {Z_N}^k \langle \tilde{\Phi}({z_N}^{-k} \cdot y_1)\tilde{\Phi}^\dagger(y_2)\rangle, \tag{2.6.5}$$

where the last simplification in the above expression comes form the $\mathbf{Z}_N$ invariance of the $\mathcal{C}_d$ theory.

The previous result is particularly useful when the covering space $\mathcal{C}_d$ is a flat momentum–conserving space such as the circle or the torus. In that case, indeed, Feynman rules on $\mathcal{C}_d$ are easily obtained from the corresponding Minkowski space ones, as we already discussed in detail, so that the orbifold propagator in Eq. (2.6.5) can be also obtained. The propagator of $\tilde{\Phi}$ can be written, in terms of the wave functions $f_{\vec{n}}$ given in Eq. (1.3.5), as

$$\langle \tilde{\Phi}(y_1)\tilde{\Phi}^\dagger(y_2)\rangle \equiv \sum_{\vec{n}} \tilde{G}_{\vec{n}}\, f_{\vec{n}}(y_1 - y_2)\,,$$

where $\tilde{G}_{\vec{n}}$ denotes the standard form of the propagator in momentum space, and the torus or circle periodicity conditions result only in the quantization of the KK momenta in the internal directions. For $T^2/\mathbf{Z}_{3,4,6}$, the orbifold transformation acts on the KK momenta as in Eq. (2.4.2), while on $S^1/\mathbf{Z}_2$, and on $T^2/\mathbf{Z}_2$ as well, it simply changes its sign. In all cases, we find

$$\langle \Phi(y_1)\Phi^\dagger(y_2)\rangle = \frac{1}{N}\sum_{k=0}^{N-1}\sum_{\vec{n}} Z_N{}^k\, \tilde{G}_{\vec{n}}\, f_{Z_N^{-k}\vec{n}}(y_1) f^\dagger_{\vec{n}}(y_2)\,. \qquad (2.6.6)$$

By expanding the orbifold field on the covering space basis

$$\Phi(y) = \sum_n \Phi_n f_n(y)\,, \qquad (2.6.7)$$

with f_n as in Eq. (1.2.3) or Eq. (1.3.2), we find

$$\langle \Phi_{\vec{m}}\Phi_{\vec{n}}{}^\dagger\rangle = \frac{1}{N}\sum_{k=0}^{N-1} Z_N{}^k \tilde{G}_{\vec{n}}\, \delta_{\vec{m},Z_N^{-k}\vec{n}}\,. \qquad (2.6.8)$$

The above equation shows that the propagator on an orbifold can be written as the sum of N propagators, of which all but the first violate momentum conservation. Any internal line of a Feynman diagram is then the sum of the "k" propagators shown in Fig. 2.2, in which an incoming momentum $\vec{n}$ is changed into an outgoing one $Z_N^{-k}\vec{n}$. When using the Feynman rule shown in Fig. 2.2, an orientation of the propagator is needed so as to distinguish incoming and outgoing lines. If the field is complex this orientation is naturally provided; if it is real, one orientation has to be chosen to apply the rule of Fig. 2.2, but clearly the result does not depend on this choice.

For what concerns interactions, since we have shown configuration space Feynman rules for the verteces to be the same as the covering space ones and the field Φ has been Fourier–transformed with the $f_{\vec{n}}$'s, momentum space Feynman rules will be also equal. In this approach, the Feynman rules on S^1 or T^2 will be used for verteces and the orbifold propagator shown in Fig. 2.2 will be used for internal lines.

Computations are futher simplified by noting that any interaction vertex has to be z_N-invariant. Its action on a set of K fields, with modes $\Phi_{\vec{n}_f}$ ($f = 1, \ldots, K$),

$$V = \mathcal{V}_{\{A_1,\vec{n}_1\},\dots,\{A_K,\vec{n}_K\}}\Phi_{\{A_1,\vec{n}_1\}}\cdots\Phi_{\{A_K,\vec{n}_K\}} \quad \sim$$

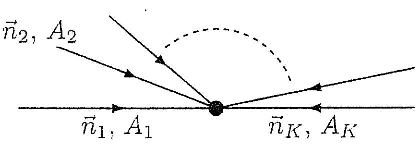

Figure 2.3: The diagrammatic representation of a generic effective vertex V.

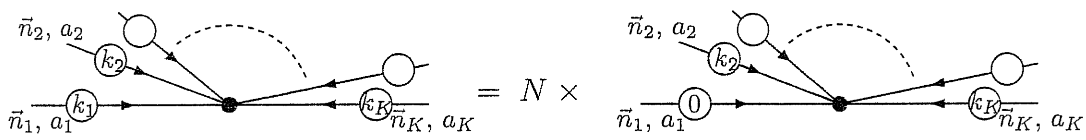

Figure 2.4: Equivalence between interaction vertices on a $\mathbf{Z}_N$ orbifold.

is $\Phi_{\vec{n}_f} \to Z_N{}_f^k \Phi_{Z_N^k \vec{n}_f}$. This leads to the following relation, valid for any interaction vertex $\mathcal{V}$ (see Fig. 2.3):

$$\mathcal{V}_{\{B_1, Z_N^{-k}\vec{n}_1\},\dots,\{B_K, Z_N^{-k}\vec{n}_K\}} \left[Z_N{}_1^k\right]_{B_1 A_1} \cdots \left[Z_N{}_K^k\right]_{B_K A_K} = \mathcal{V}_{\{A_1,\vec{n}_1\},\dots,\{A_K,\vec{n}_K\}}\,, \qquad (2.6.9)$$

where A_f, B_f can represent Lorentz and/or gauge indices of the various fields. Thanks to (2.6.9), we notice that (see Fig. 2.4) if K propagators are attached to a vertex, we do not have to sum over all their K independent twists, as one of them can be set to zero, simply giving an extra factor of N. Notice that there is no need for the vertex V to be elementary, *i.e.* to appear in the tree-level action.

Chapter 3

Gauge–Higgs Unification in Orbifold models

In this chapter, the possibility is discussed of building realistic models of EWSB in which the Little Hierarchy Problem is solved through the implementation, in the framework of flat ED, of the Gauge–Higgs Unification mechanism. [1] In the first paragraph, making also use of explicit simple examples, a short introduction to the mechanism underlying these constructions is provided and the problems one encounters when trying to formulate a realistic model are discussed, together with their solutions. This leads us to a simple interesting model [24], formulated on the $S^1/\mathbf{Z}_2$ orbifold, with all the qualitative features of the SM, which however fails at the quantitative level being the Higgs mass predicted to be smaller then the W boson one. In the rest of the chapter, the possibility is discussed [25] of solving this problem by considering $6D$ models on the $T^2/\mathbf{Z}_N$ orbifolds. In Sect. 3.2, GHU models on $T^2/\mathbf{Z}_N$, based on an $SU(3)$ gauge group, are discussed. The more general orbifold projection which realizes the breaking of $SU(3) \rightarrow SU(2) \times U(1)$ is found and the resulting Higgs fields content of the theory is worked out. Projections giving rise to a single Higgs doublet are found to exist for $N > 2$. In the remainder of the chapter we focus on these single–Higgs projections, which are shown in Sect. 3.3 to give rise, through the presence of a tree–level quartic Higgs coupling, to an Higgs mass which is twice the W boson one. As discussed in the Introduction, a dangerous tadpole operator can arise in $6D$ and destabilize the EWSB scale. This operator is discussed in Sect. 3.4 and its one–loop coefficients computed for all orbifolds and for any content of scalar and fermion fields. The phenomenological possibilities of

[1] For the warped case see *e.g.* [12, 48].

single–Higgs $6D$ GHU models are discussed in Sect. 3.5. Particular attention is devoted to the case in which the tadpole operator is globally vanishing and the EWSB scale and the Higgs mass are not destabilized.

3.1 The Gauge–Higgs Unification mechanism

The Gauge–Higgs unification mechanism consists on identifying the Higgs $4D$ scalar field as the components in the internal space of an ED gauge field. At the conceptual level, GHU models are very interesting since, through compactification, the standard $4D$ electroweak gauge bosons associated to the $SU(2) \times U(1)_Y$ symmetry group and the $4D$ scalar responsible for its breaking both arise from the ED gauge connection, so that they have a unified origin. At a more practical level, $4D$ scalars A_y coming from an extra–dimensional gauge connection A_μ have a very constrained (and protected) quantum dynamics. Infact, they are connected at high energy, through Lorentz symmetry transformations, to $4D$ gauge bosons A_μ with the same quantum numbers, whose dynamics is strongly constrained by the gauge symmetry. Quadratic divergences in the one–loop scalar mass terms, for instance, which are generically expected for $4D$ scalars, are avoided in these models very much the same way they are cancelled in supersymmetric models. At energy scales Λ above the compactification scale, or the inverse curvature radius in the case of non–flat compactifications, Lorentz invariance and ED gauge symmetry are locally restored, so that the high–energy contribution to the 2-point correlator $\langle A_y A_y \rangle$ is part of the $\langle A_M A_N \rangle$ Lorentz multiplet. Since ED gauge invariance forbids high energy contributions to the gauge boson mass term, these are absent from the scalar correlator as well. The mass term for A_y will then in general be insensitive to the high energy cut–off and its size of the order of the compactification scale, since the integral on the momenta is naturally cut–off at that scale. At a more technical level, this depends on the fact that allowed local operators to be used like counter–terms, in which quantum divergences appear, are strongly constrained by ED gauge invariance. In most cases, local operators which are quadratic in A_y, so that they give rise to scalar mass terms in $4D$, are not allowed at all, and the mass term is finite. In the following, we will show this mechanism to be at work in a simple example if a consistent regularization prescription is employed. Note that, as we will see in an explicit example, the above argument only applies to compactifications on smooth spaces. On orbifolds, there are in general curvature and field–strength singularities localized at the fixed points, so that ED gauge invariance and Lorentz symmetry are never restored at those points. This is to say that in an effective field theory approach to the orbifold model, in which the singularity is unresolved up to the cut–off scale Λ, local operators localized at the fixed points can arise, and act as counter–terms, whose symmetry is reduced w.r.t. the "bulk" ED one. [2] Such operators can contain scalar mass–terms and reintroduce the one–loop quadratic sensitivity to the cut–off.

Let us consider now, along the lines of [20], a 5–dimensional $U(1)$ gauge field A_M compactified on the S^1 circle, coupled to a fermion Ψ of mass m and unitary $U(1)$ charge. As shown in Sect. 1.4, the massless tree–level bosonic spectrum consists on a $4D$ $U(1)$ gauge field A^0_μ and one real scalar A^0_y, while at the massive level we have a tower of massive gauge bosons corresponding to a tower of non–linearly realized $U(1)$'s. The A^0_y field is then massless at the tree–level, its one–loop mass is given by the (connected, amputated) 2–point function at zero external $4D$ momentum. As discussed in the first chapter, Feynman rules for this theory are easily found from the usual Minkowski ones. Gauge fields do not contribute at one–loop and the only diagram to be considered is the fermion one. Note that the sum on the internal line ED momenta $p_{y,n} = \frac{n}{R}$ must be performed, together with the $4D$ loop integral. One finds

$$m_H{}^2 = -i\langle A^0_y(0)A^0_y(0)\rangle = 4\frac{g_5{}^2}{2\pi R}\int\frac{d^4p}{(2\pi)^4}\sum_n\frac{p^2 - p_{y,n}{}^2 + m^2}{[p^2 + p_{y,n}{}^2 + m^2]^2}\,, \qquad (3.1.1)$$

where g_5 is the $5D$ gauge coupling and we have Wick rotated the $4D$ momentum, so that p is Euclidean in the above equation. We see that each term in the sum of Eq. (3.1.1) is quadratically divergent, so that there is no hope to get a finite result in any regularization in which the Kaluza–Klein sum is truncated at some point $n = N$ and the d^4p integral treated in some other manner. This was to be expected, since in the truncated $4D$ effective theory the scalar A^0_y is Yukawa–coupled to the N $4D$ fermions of the Kaluza–Klein tower of Ψ, and each fermion contributes to the loop with a quadratic divergency. There is no apparent reason why a big number of fermions (for $N \to \infty$) should improve the situation. From the general discussion above, however, it is clear that a cut–off in the Kaulza–Klein sum is not the right regularization procedure, since the expected finiteness of m_H is due to the $5D$ gauge and Lorentz invariance at high energies. Our regularization, to be compatible with this, must treat symmetrically, in the UV, all the 5 dimensions so that putting a cut–off in the ED momentum $p_{y,n}$ only is not acceptable. The right regularization

[2] The arising, at the quantum level, of localized operator in ED effective field theories was explicitly shown in [47]. See also [49] for a discussion of the role, in the context of $4D$ Casimir effect, of operators localized at the boundaries of a segment.

prescription, in particular, should make Eq. (3.1.1) vanish as the limit $R \to \infty$ is taken, since the $5D$ Minkowsky space gauge theory is reproduced, on which m_H vanishes by gauge invariance. In the limit, the sum is changed in a p_y integral and, exploiting the assumed symmetry in the integration variables, we can change the ${p_y}^2$ term in the numerator in ${p_5}^2/5$, where ${p_5}^2 = p^2 + {p_y}^2$. We then get

$$m_H{}^2(R \to \infty) = \frac{4}{5} {g_5}^2 \left[3 - 2m^2 \frac{\partial}{\partial m^2}\right] \int \frac{d^5p}{(2\pi)^5} \frac{1}{{p_5}^2 + m^2} \,,$$

which is known to vanish in any gauge invariant regularization, such as the Pauli–Villard or the lattice ones. [3] Having assumed our regularization to be such that the above integral vanishes, we can subtract it from Eq. (3.1.1) and get

$$m_H{}^2 = -4{g_4}^2 \int \frac{d^4p}{(2\pi)^4} (1 + \rho\partial_\rho) \left[\sum_n \frac{1}{\left(\frac{n}{R}\right)^2 + \rho^2} - 2\pi R \int \frac{dp_y}{2\pi} \frac{1}{{p_y}^2 + \rho^2}\right] \,, \quad (3.1.2)$$

where g_4 is the $4D$ gauge coupling as in Eq. (1.4.11) and $\rho^2 \equiv p^2 + m^2$. Using the identity

$$\sum_n \frac{1}{\left(\frac{n}{R}\right)^2 + \rho^2} - 2\pi R \int \frac{dp_y}{2\pi} \frac{1}{{p_y}^2 + \rho^2} = \frac{2\pi R}{2\rho} \left[\tanh(2\pi R\rho) - 1\right] \,,$$

we see that the argument of the integral in Eq. (3.1.2) is exponentially suppressed at large p, like $e^{-2\pi R p}$. As expected, then, the mass of the scalar A_y^0 is finite, and exponentially UV insensitive. Due to the exponential factor, indeed, the integral does not effectively receives contributions from momenta higher then the inverse compactification radius, which acts as a cut–off.

As already mentioned, the finiteness of m_H comes from the fact that local $5D$ gauge–invariant operators containing a mass–term for A_y^0 do not exist. This is particularly clear in the present case, since, as discussed in Sect. 1.4, a constant background for A_y^0 corresponds to a flat gauge background, so that the only gauge invariant operator which is sensitive to it is the non–local Wilson loop (1.2.6) wrapping around the circle. Therefore, no local operators exist which can contribute to the A_y^0 effective potential, which is then completely finite [44] at any order in perturbation theory. This is a common, and extremely interesting, feature of all GHU models in which the scalar field can be interpreted as a Wilson line. In these

[3] The lattice–regularized version of this model, with the appropriate link variables required to preserve gauge invariance, was considered in [50] and shown to be equivalent to a strongly–coupled $4D$ Moose theory.

models, the Higgs mass not only is stabilized, *i.e.* protected by large quantum corrections, but also predicted in terms of the microscopic parameters of the theory. In the $6D$ framework discussed in the following paragraphs, however, this Wilson line interpretation will be absent.

Of course, a lot of work must be done for getting a realistic model of EWSB out of the simple S^1 model described above. First of all, for the scalar field to resemble the Higgs, we want it to be in the right representation (the $\mathbf{2}_{\frac{1}{2}}$) of the $SU(2)\times U(1)_Y$ EW gauge group. Therefore, since the Higgs comes from ED fields in the adjoint representation, enlarged groups must be considered, so that the $\mathbf{2}_{\frac{1}{2}}$ is found when decomposing the adjoint in representations of the $SU(2)\times U(1)_Y$ subgroup. The ED gauge group, then, must be broken by compactification, and at the same time scalar zero–modes in the right representations must be left. One finds that this cannot be achieved if considering S^1 or T^2 compactifications. In that cases, indeed, one always find the zero–mode scalars in the adjoint representation of the linearly realized $4D$ group. On orbifolds, on the contrary, there is the possibility of building such a model. Orbifold projections like those in Eq. (2.2.5) can indeed break the ED gauge group, preserving at the same time scalar zero–modes which are not in the adjoint of the surviving group, since "μ" and "y" components of the gauge bosons are treated differently by the projection. For example, consider [28, 24] (see [51] for the study of this model at finite–temperature) an $SU(3)$ gauge theory on $S^1/\mathbf{Z}_2$, the connection having orbifold parities as in Eq. (2.2.5) with

$$Z_2 = e^{2\pi i\sqrt{3}t^8}\begin{pmatrix} -1 & 0 & 0 \\ 0 & -1 & 0 \\ 0 & 0 & 1 \end{pmatrix}, \qquad (3.1.3)$$

where the t^a's are the usual $SU(3)$ generators in the fundamental representation, normalized to $\mathrm{Tr}(t^a t^b) = \frac{1}{2}\delta^{ab}$. The adjoint representation decomposes as $\mathbf{8}\to \mathbf{3}_0\oplus\mathbf{1}_0\oplus\mathbf{2}_{\frac{\sqrt{3}}{2}}\oplus\mathbf{2}_{-\frac{\sqrt{3}}{2}}$ under the $SU(2)\times U(1)$ subgroup and $U(1)$, whose charge is indicated for the various $SU(2)$ representations, is generated by t^8. Given Eq. (3.1.3) and the above decomposition, the orbifold condition (2.2.5) is found to state the $5D$ gauge bosons in the adjoint $\mathbf{3}_0\oplus\mathbf{1}_0$ of the EW group to be even (*i.e.* we have $+$ in Eq. (2.2.6)) while the other, which form one complex doublet of fields in the $\mathbf{2}_{\frac{\sqrt{3}}{2}}$, are odd. At the massless level, then, the EW gauge bosons associated to the $SU(2)\times U(1)$ linearly realized $4D$ gauge group will survive, together with an Higgs complex doublet of scalars. There is a point, however, in which the above construction is not satisfactory. Since the EW symmetry group originates from the breaking of the simple group $SU(3)$, a single gauge coupling g_5 is present, so that the $U(1)_Y$ coupling g_Y is fixed in term of the $SU(2)$ one g. For what concerns the last one, it is immediately found to be $g = g_5/\sqrt{2\pi R}$, as it comes from $SU(2)$ gauge bosons self–interaction diagrams. To determine g', on the contrary, we have to look at the Higgs interaction with the $U(1)$ boson A^8_μ, which is proportional to the Higgs t^8 charge $\frac{\sqrt{3}}{2}$. Having defined the Higgs hypercharge to be $\frac{1}{2}$ as it should, one finds $g_Y/g = \tan\theta_W = \sqrt{3}$, which is clearly wrong. This is a common problem of all GHU models based on the $SU(3)$ gauge group and it will be also present in the $6D$ case, even though in $D = 6$ the possibility opens up [23] to consider $\mathbf{G}_2$ instead of $SU(3)$, from which a better prediction [17] for θ_W is found. To overcome this difficulty, however, a very nice mechanism have been proposed [24] in which an extra $U(1)'$ is included in the $5D$ gauge group, which is unbroken by the orbifold projection. The physical $U(1)_Y$ is taken to be a linear combination of the two $4D$ surviving $U(1)$'s and the weak angle is adjusted by suitably choosing the $U(1)'$ $5D$ charge g'. Of the two $U(1)$'s the hypercharge only is anomaly free and the anomaly of the other must be cancelled by some generalized version of the Green–Schwarz anomaly cancellation mechanism (see [52] for a comprehensive review of anomalies in ED field theories), which also makes the corresponding gauge boson become massive, and decouple from the theory. Since this mechanism seems to be generalizable to higher dimensions as well, we will forget about this problem in the following sections.

Having found a realistic content of gauge bosons and Higgses is still not enough for a realistic model. First of all, we have to ensure the dynamics of the theory to be such that the Higgs takes a VEV on the vacuum, so that EWSB is achieved. This is to say that the Higgs potential, which is finite due to the Wilson line interpretation of its VEV, must have a non–trivial minimum. [4] Explicit one–loop computations reveal this to be possible. One finds gauge field and ghost contributions to have minimum at zero, while the fermion ones do not. A non–trivial minimum can then always be realized when a sufficient (not so high, infact) number of bulk fermions are present. The Higgs then takes a VEV, and this VEV should, as in the SM, give rise to mass–matrices for the SM fermions, then breaking the flavor symmetry. Flavor appears as a big problem in these models, since $4D$ zero–modes coming from bulk $5D$ fermions from compactification have very constrained Yukawa couplings with the Higgs. These couplings are indeed gauge couplings in $5D$, so that they are completely fixed by the representation of $SU(3)$ in which the SM fermion is

[4]This is an example in which, as mentioned in Sect. 2.1, the condition (2.1.2) is satisfied by a continuous T, which is equivalent to a continuous Wilson line. For an Higgs VEV $\langle A^a_y \rangle = 2\alpha/(g_5 R)\delta^{a7}$ aligned with the down component of the doublet, one finds an equivalent Scherk–Schwarz twist $T(\alpha) = \exp(2\pi i \alpha \lambda_7)$, which indeed solves Eq. (2.1.2) with Z_2 as in Eq. (3.1.3).

embedded and there is no hope of getting the complicate SM flavor structure in this way. Also in this case, orbifolds are extremely useful. At the orbifold fixed points, indeed, the $5D$ Lorentz invariance is explicitly broken, as well as the gauge one. Therefore, localized $4D$ chiral fermion fields in representations of the unbroken $SU(2) \times U(1)_Y$ group can be put at the fixed point. As we will better discuss in the following chapter, such localized fermions which are commonly introduced in orbifold field theories, can be thought to arise as string theory brane fields, the brane being located at the fixed point, or to arise from ED "bulk" fields whose wave function localizes around topological defects [34, 37, 38]. Neglecting for the moment their origin, localized fields can be introduced in our model to represent the SM fermions. Having done this, the problem comes of how to couple these fields to the Higgs, so that they are sensitive to the EWSB. Simple $4D$ localized Yukawa couplings would indeed violate the residual $5D$ gauge symmetry which survives the orbifold projection and in turn reintroduce quadratic divergences. In [24], (see [26] for a different, though substantially equivalent, approach), the problem was solved by introducing mass–terms mixing the SM fields with the $5D$ bulk fermions needed to realize the EWSB. The last ones are taken in pairs of opposite orbifold parities, so that a big bulk mass M can be introduced, which makes them decouple from the low–energy theory. Bulk fermions are charged under $SU(3)$ and then couple to the gauge field background and communicate the breaking to the localized fields which then develop mass–matrices. The many SM parameters for flavor (see [53] for an interesting flavor model formulated in this set–up) are introduced via the mixing mass–terms and the masses of the various bulk fermions. Interestingly, since the EWSB is non–local, the bulk fields have to turn at least ones around the circle for "feeling" the breaking, so that in the tree–level diagram for the SM masses, in which they run as internal lines, an exponential suppression factor $e^{-\pi RM}$ appears. Also this mechanism seems easily generalizable to the $6D$ case, so that in the following paragraphs we will not consider flavor problems any more.

The model [24], though extremely successful in reproducing the qualitative features of the SM, fails at the quantitative level. In particular, it predicts too a small Higgs mass, $m_H \sim 30\text{GeV}$ at most, and requires too a low compactification scale, $1/R \sim 500\text{GeV}$, while the current generical experimental bound on models of this kind is $1/R >$ TeV (see *e.g.* [54]). Both problems come from the smallness of the predicted Higgs quartic coupling, which is one–loop generated. By considering a quartic approximation of the Higgs potential, one comes back to the usual $-\mu^2|h|^2 + \lambda|h|^4$ SM potential whose parameters are estimated, from the above numbers, as $\mu \sim 0.156 g_W/R$ and $\lambda \sim 0.018 g_W{}^2$. Note the small number in front of λ, which basically comes from a loop factor. Let us now modify the relation among λ and g_W in $\lambda \sim \alpha_\lambda g_W{}^2$. One finds now $1/R \sim \sqrt{\alpha_\lambda}/(0.156)v$ (where $v = 246$GeV is the Higgs VEV) and $m_H/m_W \sim 2\sqrt{2\alpha_\lambda}$, so that both the Higgs mass and the compactification scale would be raised if increasing α_λ. Note that $\alpha_\lambda \sim 1$ would be realistic. In the following, the possibility is explored to solve this problem by considering 6 dimensional models, in which, as suggested by several authors [7, 22], the Higgs field is not a Wilson line and a tree–level quartic coupling arises, so that the loop factor in α_λ disappears, and its size is increased.

3.2 Gauge–Higgs Unification on $T^2/\mathbf{Z}_N$

Let us consider, with the notations of Sect.s 2.3, 2.4, 2.5, a $6D$ gauge theory compactified on the orbifolds $T^2/\mathbf{Z}_N$. The Lagrangian of the orbifold theory is the sum of a bulk contribution, which must be invariant under the full gauge group, and a set of contributions localized at the fixed points of the orbifold, which have to be invariant only under the gauge group surviving at these points. Remembering the definition of $z_N{}^k$–fixed points given in Sect. 2.3, and observing that physically distinct and relevant sectors are only labelled by $k = 1, \dots, [N/2]$, where $[\dots]$ denotes the integer part, the general form of the effective Lagrangian can be parametrized as

$$\mathcal{L} = \mathcal{L}_6 + \sum_{k=1}^{[N/2]} \sum_{i_k=1}^{N_k} \delta^{(2)}(z - z_{i_k}) \mathcal{L}_{4,i_k} \,, \qquad (3.2.1)$$

where $\mathcal{L}_6$ represents the bulk $6D$ Lagrangian and $\mathcal{L}_{4,i_k}$ the localized Lagrangians at the N_k $z_N{}^k$–fixed points, with N_k as in Eq. (2.3.4). Since $\mathcal{L}$ has to be invariant under the z_N orbifold action, and z_N acts non-trivially on some fixed points, there are in general various non-trivial constraints among the $\mathcal{L}_{4,i_k}$'s. Moreover, the orbifold structure respects a discrete translational symmetry mapping z_N–fixed points onto z_N–fixed points. [5] This implies that the Lagrangians $\mathcal{L}_{4,i_k}$ are constrained to be all equal at fixed k and hence there are only $[N/2]$ independent localized terms appearing in (3.2.1).

In the following, we shall restrict our study to the prototype models of gauge–Higgs unification with a gauge group $G = SU(3)$ that is broken to $H = SU(2) \times U(1)$ by the z_N orbifold projection, with the mechanism discussed in Sect. 2.5. We denote

[5] This is true only in the absence of localized matter that is not uniformly distributed over the fixed points or of discrete Wilson lines.

by t^a the $SU(3)$ generators with the standard normalization $\mathrm{Tr}\, t^a t^b = \frac{1}{2}\delta^{ab}$ in the fundamental representation. The unbroken generators in $SU(2)$ and $U(1)$ are $t^{1,2,3}$ and t^8. The broken generators in $SU(3)/[SU(2) \times U(1)]$ are instead $t^{4,5,6,7}$, and can be conveniently grouped into the usual raising and lowering combinations $t^{\pm 1} = \frac{1}{\sqrt{2}}(t^4 \pm i t^5)$ and $t^{\pm 2} = \frac{1}{\sqrt{2}}(t^6 \pm i t^7)$. In this basis, the group metric in the sector $\pm i, \pm j$ is given by $h_{+i,-j} = h^{+i,-j} = \delta^{ij}$. The most general way to realize the above breaking is obtained by realizing the orbifold action on the gauge field in Eq. (2.5.6) through the matrix

$$Z_N = \tau^{2\,n_p(\frac{1}{3} + \frac{1}{\sqrt{3}} t^8)} = \begin{pmatrix} \tau^{n_p} & 0 & 0 \\ 0 & \tau^{n_p} & 0 \\ 0 & 0 & 1 \end{pmatrix}. \tag{3.2.2}$$

The number n_p must be an integer and is defined only modulo N, so that there are a priori $N-1$ inequivalent possibilities.

The geometric part of the z_N action on a field is fixed, as it clear from Eq.s (2.5.1, 2.5.6), by the decomposition of its representation under the $6D$ $SO(1,5)$ Lorentz group in terms of $SO(1,3) \times SO(2)$, where $SO(1,3)$ is the $4D$ Lorentz group and $SO(2) \simeq U(1)$ is the group of internal rotations. The gauge part of the action on a field in a representation $\mathcal{R}$ of $SU(3)$ is instead given by the twist matrix Z_N in Eq. (3.2.2) generalized to the representation $\mathcal{R}$. This fixes the z_N transformation of any field, up to an arbitrary overall phase g, such that the N-th power of the z_N action is trivial on all the components of the field. The orbifold boundary condition of a generic bosonic or fermionic field component Φ, with $U(1)$ charge s under internal rotations and in the representation $\mathcal{R}$ of $SU(3)$, is then given by

$$\Phi(\tau z) = g_{B,F}\, R_s\, Z_{\mathcal{R}} \Phi(z)\,. \tag{3.2.3}$$

In this equation, $Z_{\mathcal{R}}$ denotes the twist matrix Z_N in the representation $\mathcal{R}$ and $R_s = \tau^s$ is the Lorentz rotation associated to the geometric action of the twist. The overall phases $g_{B,F}$ are such that $g_B^N = 1$ for bosons and $g_F^N = -1$ for fermions, since $R_s^N = \pm 1$ in the two cases. It is convenient to define $g_F = g\tau^{\frac{1}{2}}$, $g_B = g$, so that g is an N-th root of unity for both bosons and fermions. Correspondingly, there are in general N different boundary conditions, associated to the N possible choices of g. The expression of $Z_{\mathcal{R}}$ can be conveniently written as

$$Z_{\mathcal{R}} = \tau^{2\,n_p(\frac{n_{\mathcal{R}}}{3} + \frac{1}{\sqrt{3}} t^8_{\mathcal{R}})}\,, \tag{3.2.4}$$

where $t^8_{\mathcal{R}}$ is the Cartan generator t^8 in the representation $\mathcal{R}$ and $n_{\mathcal{R}}$ is an integer number such that ${Z_{\mathcal{R}}}^N = 1$. It can be written as $n_{\mathcal{R}} = n_1 - n_2$, where n_1 and n_2 are the two Dynkin labels of the representation $\mathcal{R}$. Since the canonically normalized (so that the Higgs field has $\frac{1}{2}$ hypercharge) abelian generator surviving the projection is $Q_{\mathcal{R}} = \frac{1}{\sqrt{3}} t^8_{\mathcal{R}}$, the matrix (3.2.4) gives a phase $\tau^{2\,n_p(\frac{n_{\mathcal{R}}}{3}+q)}$ on a component with $U(1)$ charge q under the decomposition of the representation $\mathcal{R}$ under $SU(3) \to SU(2) \times U(1)$. The relevant informations are listed in Table 3.1 for the first few representations. In the following two subsections, we consider in some more detail the decomposition of gauge and matter fields, as given by (3.2.3).

$\mathcal{R}$	Decomposition of $\mathcal{R}$	$n_{\mathcal{R}}$
3	$\mathbf{2}_{\frac{1}{6}} \oplus \mathbf{1}_{-\frac{1}{3}}$	1
6	$\mathbf{3}_{\frac{1}{3}} \oplus \mathbf{2}_{-\frac{1}{6}} \oplus \mathbf{1}_{-\frac{2}{3}}$	2
8	$\mathbf{3}_0 \oplus \mathbf{2}_{\frac{1}{2}} \oplus \mathbf{2}_{-\frac{1}{2}} \oplus \mathbf{1}_0$	0
10	$\mathbf{4}_{\frac{1}{2}} \oplus \mathbf{3}_0 \oplus \mathbf{2}_{-\frac{1}{2}} \oplus \mathbf{1}_{-1}$	3

Table 3.1: Decomposition of the most relevant $SU(3)$ representations.

3.2.1 Gauge fields

The gauge fields A_M transform as vectors under $SO(1,5)$ rotations and in the adjoint representation under gauge transformations. In complex coordinates, the decomposition of A_M under $SO(1,3) \times U(1)$ is very simple: we get a $4D$ vector field A_μ with charge $s=0$ and two $4D$ scalars A_z and $A_{\bar{z}}$ with charges $s=-1$ and $s=1$ respectively, consistently with Eq. (2.5.6). The boundary conditions can be obtained from Eq. (3.2.3) with $g=1$. The gauge part of the orbifold twist is diagonal if one switches from the standard basis with components A_{Ma} to the creation–annihilation basis with components $A_{M1,2,3,8}$, $A_{M\pm 1} = \frac{1}{\sqrt{2}}(A_{M4} \mp i A_{M5})$ and $A_{M\pm 2} = \frac{1}{\sqrt{2}}(A_{M6} \mp i A_{M7})$. The final result is that the various components of the gauge field $A_M = \sum_a A_{Ma} t^a$ satisfy twisted boundary conditions with the following phases:

$$A_{\mu 1,2,3,8} : 1\,,\ A_{z1,2,3,8} : \tau^{-1}\,,\ A_{\bar{z}1,2,3,8} : \tau^{+1}\,, \tag{3.2.5}$$

$$A_{\mu\pm i} : \tau^{\pm n_p}\,,\ A_{z\pm i} : \tau^{-1\pm n_p}\,,\ A_{\bar{z}\pm i} : \tau^{+1\pm n_p}\,. \tag{3.2.6}$$

The light modes of untwisted fields consist of the gauge bosons $A_{\mu 1,2,3,8}$ forming the adjoint of the surviving gauge group, the scalar fields A_{z+i} with their complex conjugates $A_{\bar{z}-i}$ forming a charged Higgs doublet under this group if $n_p = 1 \bmod N$, and the scalar fields A_{z-i} with their complex conjugate $A_{\bar{z}+i}$ forming a conjugate charged Higgs doublet if $n_p = -1 \mod N$. Referring to the decomposition reported in Table 3.1, the projection keeps the $\mathbf{3}_0$ and $\mathbf{1}_0$ components for $4D$ indices and some numbers n and n_c of the $\mathbf{2}_{\frac{1}{2}}$ and the $\bar{\mathbf{2}}_{-\frac{1}{2}}$ components for internal indices, depending on N and $n_p = 1, \ldots, N-1$. The possibilities for the numbers (n, n_c) for the consistent constructions labelled by the integers (N, n_p) are the following:

$$(n, n_c) = (1, 1): \text{ for } (N, n_p) = (2, 1)\,; \tag{3.2.7}$$

$$(n, n_c) = (1, 0): \text{ for } (N, n_p) = (3, 1), (4, 1), (6, 1)\,; \tag{3.2.8}$$

$$(n, n_c) = (0, 1): \text{ for } (N, n_p) = (3, 2), (4, 3), (6, 5)\,; \tag{3.2.9}$$

$$(n, n_c) = (0, 0): \text{ for } (N, n_p) = (4, 2), (6, 2), (6, 3), (6, 4)\,. \tag{3.2.10}$$

It is therefore possible to construct models with two conjugate Higgs doublets ($\mathbf{Z}_2$), a single Higgs doublet ($\mathbf{Z}_3$, $\mathbf{Z}_4$, $\mathbf{Z}_6$) or no Higgs doublets at all ($\mathbf{Z}_4$, $\mathbf{Z}_6$).

3.2.2 Matter fields

A $6D$ Weyl fermion $\Psi_\pm$ of definite $6D$ chirality decomposes under $SO(1,3) \times U(1)$ into two $4D$ chiral fermions with charges $s = \pm\frac{1}{2}$: $\Psi_\pm = (\psi_{L,R})_{s=\frac{1}{2}} \oplus (\chi_{R,L})_{s=-\frac{1}{2}}$, where L, R denote the $4D$ chiralities. We thus see from (3.2.3) that any $6D$ Weyl spinor gives rise to two $4D$ fermions of opposite $4D$ chiralities, twisted by g and $g\tau$ as in Eq. (2.5.3), times the gauge part of the twist. More generally, a $6D$ spinor field $\Psi_{\mathcal{R},\chi_6}$ of $6D$ chirality $\chi_6 = \pm 1$ transforming in a representation $\mathcal{R}$ of the gauge group, gives rise to different $4D$ spinor components ψ_{q,χ_4} with $U(1)$ charge q and $4D$ chirality $\chi_4 = \pm 1$, twisted by a phase:

$$\psi_{q,\chi_4} : g\,\tau^{\frac{1-\chi_4\chi_6}{2}}\,\tau^{2\,n_p(\frac{n_\mathcal{R}}{3}+q)}\,. \tag{3.2.11}$$

Depending on N and n_p, the various possible choices for g allow the zero modes of different subsets of components to be preserved. We will not list here the many possibilities, since they can be easily derived from the data reported in Table 3.1.

For scalar fields the analysis is simpler, since they are singlets under Lorentz transformations and thus $s = 0$ in (3.2.3). The twist of a scalar field $\phi_\mathcal{R}$ in a representation $\mathcal{R}$ of the gauge group is only given by its gauge decomposition. For a generic component ϕ_q with $U(1)$ charge q, one has

$$\phi_{\mathcal{R},q} : g\,\tau^{2\,n_p(\frac{n_\mathcal{R}}{3}+q)}\,. \tag{3.2.12}$$

Notice that there is a one-to-one correspondence between the case of scalars and that of spinors, since the additional phase $\tau^{\frac{1-\chi_4\chi_6}{2}}$ arising for the latter is always an

N-th root of unity and can therefore be compensated by a different choice of g. It is easy to verify that the zero mode of any component can always be preserved with a suitable and unique choice of the phase g, both for scalars and for fermions. This is an important property for model building.

3.3 Higgs potential

Having defined a class of $6D$ GHU models, let us now see if, as expected, realistic EWSB and Higgs masses can arise, due to the aforementioned tree–level quartic coupling. In the literature, $6D$ Gauge–Higgs unification has been studied already [22, 23] (see also [55]). Most of the models discussed so far, however, were based on $\mathbf{Z}_2$ orbifold constructions that necessarily lead to two charged Higgs doublets. In this case, the tree-level quartic term has a flat direction, just as in the MSSM, and therefore fluctuations along this direction only have radiatively induced masses, which in general tend to be too small. We then focus our attention on $T^2/\mathbf{Z}_N$ orbifold constructions with $N > 2$ leading to one Higgs doublet. As we shall show below, these models have a non-vanishing quartic tree-level potential, in contrast to the $S^1/\mathbf{Z}_2$ orbifold. As already discussed, this term is responsible for an important distinction between the interpretation of EWSB in $T^2/\mathbf{Z}_N$ and $S^1/\mathbf{Z}_2$ orbifolds. In the $5D$ model, the VEV of the Higgs field is a flat direction of the classical potential and corresponds to a Wilson loop, which is also equivalent to a twist in the boundary conditions around S^1. In $6D$ models, on the contrary, the VEV of the Higgs field is *not* a flat direction of the classical potential, and such interpretation is missing. Indeed, there exist no continuous families of solutions to the usual orbifold consistency conditions for Wilson loops (2.3.10) in the case of $SU(3)$ gauge theories on $T^2/\mathbf{Z}_N$ with $N > 2$. Only discrete Wilson loops are allowed. Nevertheless, the $5D$ and $6D$ models share the interesting property that the Higgs dynamics is much more constrained than what is just implied by the surviving gauge symmetry. This is a consequence of the non-linearly realized remnant of the higher-dimensional gauge symmetry associated to parameters depending on the internal coordinates, under which the Higgs field transforms inhomogeneously [56].

Let us now compute the classical Higgs potential that arises for the single Higgs models on $T^2/\mathbf{Z}_N$ with $N = 3, 4, 6$. We choose $n_p = 1$, but the case $n_p = N - 1$ is perfectly similar up to an overall conjugation and therefore physically equivalent. The classical Lagrangian of the $6D$ theory is given simply by $L = -\frac{1}{2}\mathrm{tr}F_{MN}^2$, where $F_{MN} = \partial_M A_N - \partial_N A_M - ig_6\,[A_M, A_N]$. The Lagrangian for the zero modes A_μ^0, A_z^0

and $A^0_{\bar z}$ is easily obtained by integrating over the internal torus. The result is given by

$$L = -\frac{1}{2}\,\mathrm{tr}\,F^{02}_{\mu\nu} + 2\,\mathrm{tr}\,|D_\mu A^0_z|^2 - g_4^2\,\mathrm{tr}\,[A^0_z, A^0_{\bar z}]^2\,, \tag{3.3.1}$$

where $g_4 = g_6/\sqrt{V}$, as in Eq. (1.5.9), is the gauge coupling of the $4D$ effective theory below the compactification scale, $F^0_{\mu\nu} = \partial_\mu A^0_\nu - \partial_\nu A^0_\mu - ig_4[A^0_\mu, A^0_\nu]$ is the field strength of the massless $4D$ gauge bosons, and $D_\mu A^0_{z,\bar z} = \partial_\mu A^0_{z,\bar z} - ig_4[A^0_\mu, A^0_{z,\bar z}]$ is the covariant derivative on the Higgs field. The three weak gauge bosons and the hypercharge gauge boson are identified as $W_{\mu a} = A^0_{\mu a}$ for $a = 1,2,3$ and $B_\mu = A^0_{\mu 8}$. The zero modes of $A_\mu = \sum_a A_{\mu a} t^a$, where $a = 1,2,3,8$, are then given by

$$A^0_\mu = \frac{1}{2}\begin{pmatrix} W^3_\mu + \frac{1}{\sqrt{3}}B_\mu & \sqrt{2}W^+_\mu & 0 \\ \sqrt{2}W^-_\mu & -W^3_\mu + \frac{1}{\sqrt{3}}B_\mu & 0 \\ 0 & 0 & -\frac{2}{\sqrt{3}}B_\mu \end{pmatrix}\,. \tag{3.3.2}$$

Similarly, the two complex components of the Higgs doublet are $h_u = A^0_{z+1}$ and $h_d = A^0_{z+2}$, and their complex conjugates are given by $h^*_u = A^0_{\bar z-1}$ and $h^*_d = A^0_{\bar z-2}$. The zero modes of $A_z = \sum_i A_{z+i}t^{+i}$ and $A_{\bar z} = \sum_i A_{\bar z-i}t^{-i}$ are thus given by

$$A^0_z = \frac{1}{\sqrt{2}}\begin{pmatrix} 0 & 0 & h_u \\ 0 & 0 & h_d \\ 0 & 0 & 0 \end{pmatrix}\,,\quad A^0_{\bar z} = \frac{1}{\sqrt{2}}\begin{pmatrix} 0 & 0 & 0 \\ 0 & 0 & 0 \\ h^*_u & h^*_d & 0 \end{pmatrix}\,. \tag{3.3.3}$$

Substituting these expressions in the Lagrangian, and switching from the $SU(3)$ to an $SU(2)$ notation, we finally find:

$$L = -\frac{1}{2}\,\mathrm{tr}\,F^{W2}_{\mu\nu} - \frac{1}{4}F^{B2}_{\mu\nu} + \left|\left(\partial_\mu - ig_4 W_{\mu a}\frac{\tau_a}{2} - ig_4\tan\theta_W\frac{1}{2}B_\mu\right)h\right|^2 - V_{\mathrm{class}}(h) \tag{3.3.4}$$

where $\tan\theta_W = \sqrt{3}$, as for the $S^1/\mathbf{Z}_2$ case discussed in the previous section and

$$V_{\mathrm{class}}(h) = \frac{g_4^2}{2}|h|^4\,. \tag{3.3.5}$$

Quantum fluctuations induce a correction to the classical potential (3.3.5) and can trigger radiative symmetry breaking. The quantum effective potential can only depend on gauge-invariant quantities. These can be local or non-local in the compact dimensions. Non-local operators involve Wilson lines wrapping around the internal space and are generated with finite coefficients whose size is controlled by the compactification scale $1/R$. The local and potentially divergent operators contributing to the Higgs potential arise from the non-derivative part of $F_{z\bar z}$, like the classical quartic term. Gauge invariance allows two possible classes of local operators of this kind: even powers of F_{MN} in the bulk or arbitrary powers of $F_{z\bar{z}}$ localized at the orbifold fixed points. In general, such terms will be generated at the quantum level with divergent coefficients. At one-loop order, the bulk operators that can lead to divergences in the Higgs potential are the gauge kinetic term F_{MN}^2 and a quartic coupling F_{MN}^4, leading to quadratic and logarithmic divergences to $V(h)$ respectively. Localized operators are of the form $g_4^{2p} F_{z\bar{z}}^p$, where p is any positive integer. Quadratic and logarithmic divergences can arise from the tadpole operator $p = 1$ and the kinetic operator $p = 2$ respectively. Since the quadratic bulk divergence gives rise only to a wave-function renormalization, we see that the only quadratic divergence to the Higgs potential comes from the localized tadpole operator $F_{z\bar{z}}$. In general, the latter induces a modification to the background and, in its non-abelian part, possible mixings between the Higgs and its KK modes, aside from a quadratically divergent mass term for the Higgs field h. In the rough approximation of neglecting the backreaction induced by the modified background and the KK mixings, effects that we will consider in section 3.5, and also neglecting all the logarithmic divergences, we see that the leading terms in the one-loop effective potential for the Higgs are

$$V_{\text{quant}}(h) = -\mu^2 |h|^2 + \lambda |h|^4 \,, \tag{3.3.6}$$

where μ^2 is a radiatively generated and possibly divergent mass term and $\lambda = g^2/2$ is the tree-level quartic term. Assuming $\mu^2 > 0$ so that EWSB can occur, we have $\langle |h| \rangle = v/\sqrt{2}$ with $v = \mu/\sqrt{\lambda}$. At the minimum,

$$\begin{aligned} m_H &= \sqrt{2}\,\mu = \sqrt{2}\,v\,\sqrt{\lambda} \\ m_W &= \frac{1}{2}\,g\,v \,. \end{aligned} \tag{3.3.7}$$

The ratio between m_H and m_W is therefore predicted in a completely model-independent way to be

$$\frac{m_H}{m_W} = \frac{2\sqrt{2\lambda}}{g} = 2 \,. \tag{3.3.8}$$

Extra $U(1)$ fields, possibly needed to fix the weak-mixing angle to the correct value, do not modify Eq. (3.3.8). The main radiative correction to Eq. (3.3.8) arises from the Higgs wave-function distortion induced by the tadpole operator $F_{z\bar{z}}$, as explained in section 3.5. This effect can be estimated by Naïve Dimensional Analysis (NDA) to give $O(1)$ corrections to Eq. (3.3.8). In spite of this, the value of the Higgs mass is significantly increased with respect to the previously considered $5D$ models or $\mathbb{Z}_2$ orbifold constructions.

3.4 Divergent localized tadpole

We have seen that gauge invariance allows a localized interaction that is linear in the field strength, in addition to the universally allowed higher-order interactions involving even powers of the field strength. The localized interaction is particularly relevant, since it involves a mass term for the Higgs fields [30]. It has the form[6]

$$\mathcal{L}_{\text{tad}} = -i \sum_{k=1}^{[N/2]} \frac{\mathcal{C}_k}{N_k} \sum_{i_k=1}^{N_k} \delta^{(2)}(z - z_{i_k}) F^8_{z\bar{z}}(z) \,, \tag{3.4.1}$$

where $\mathcal{C}_k$ are real coefficients of mass dimension 1 and $F^8_{z\bar{z}}$ is the field strength of the $U(1)$ component left unbroken by the orbifold breaking, which in terms of $6D$ fields reads

$$F^8_{z\bar{z}} = \partial_z A^8_{\bar{z}} - \partial_{\bar{z}} A^8_z + g_6 f^{8bc} A_{z\,b} A_{\bar{z}\,c} \,. \tag{3.4.2}$$

The operator in Eq. (3.4.1) is clearly compatible with the gauge symmetry since (see Eq. (2.5.4) with Z_N as in Eq. (3.2.2)) allowed local $SU(3)$ transformations are, at the orbifold fixed points, in the $SU(2) \times U(1)$ subgroup, so that the abelian $U(1)$ generator is gauge–invariant. In $\mathbf{Z}_2$ orbifold models, the parity symmetry $z \leftrightarrow \bar{z}$ can be implemented and it forbids the appearance of the tadpole, which is odd under this discrete symmetry [23, 30]. This parity can be generalized to $\mathbf{Z}_N$ orbifolds, with $N > 2$, only if the twist matrix Z_N is such that ${Z_N}^2 = \mathbb{1}$. The allowed form of the tadpole operator is then $\operatorname{Im}\operatorname{Tr} Z_N F_{z\bar{z}}$, which automatically vanishes whenever ${Z_N}^2 = \mathbb{1}$. More precisely, we will see that the term associated to k in (3.4.1) can be written as $\operatorname{Im}\operatorname{Tr} {Z_N}^k F_{z\bar{z}}$, implying that the tadpole vanishes in the sectors k such that ${Z_N}^{2k} = \mathbb{1}$, when the above $\mathbf{Z}_2$ symmetry can be implemented. Notice that projections that leave only one Higgs doublet do not satisfy ${Z_N}^2 = \mathbb{1}$ and hence are generally affected by tadpoles. We verify this statement by performing a detailed calculation of the coefficients $\mathcal{C}_k$ for all $\mathbf{Z}_N$ models at one-loop order. In particular we compute the contribution to the tadpole arising from gauge (and ghost) fields, and from an arbitrary bulk scalar or fermion in a representation $\mathcal{R}$ of $SU(3)$. Possible localized boundary fields cannot minimally couple to the fields appearing in (3.4.2), because of the residual non-linearly realized gauge symmetries that are unbroken at the orbifold fixed points [56]. We therefore consider in the following $6D$ bulk fields only. This computation is also useful to understand whether and under what circumstances an accidental one-loop cancellation is possible.

[6] Abelian gauge fields that are present already before the orbifold projection and are unbroken can also develop a localized divergence term as in (3.4.1), but in this case the associated divergent mass term for even scalars, the last factor in (3.4.2), is absent.

As shown in Sect. 2.6, the computation of Feynman diagrams on an orbifold can be nicely mapped to that on the corresponding covering torus by using a mode decomposition such that the effect of the orbifold projection amounts only to a non-conservation of the KK momentum in *non-diagonal* propagators, all vertices being momentum–conserving. In the present case, computations are drastically simplified by this technique. We extract the coefficients C_k by computing the 1-point function of all the KK modes of $A^8_{\bar{z}}$. We then work out also the 2-point function for the zero-mode h of the Higgs field, defined as in (3.3.3), to extract its finite non-local mass terms and to check the 1-point function computation. In order to find an expression that can be directly compared with the computation of 1– and 2–point functions for KK modes, we need to work out more explicitly Eq. (3.4.1). Using the T^2 mode expansion, as discussed in Sect. 2.6, we easily find:

$$\int \mathrm{d}z^2 \mathcal{L}_{\rm tad} = -\sum_{k=1}^{[N/2]} C_k \Bigg[\sum_{\vec{n}} \frac{1}{N_k} \sum_{i_k=1}^{N_k} f_{\vec{n}}(z_{i_k}) \Big(p_{z,\vec{n}} A^8_{\bar{z},\vec{n}} - p_{\bar{z},\vec{n}} A^8_{z,\vec{n}} \Big) + \frac{g_4}{\sqrt{V}} \Big(i f^{8+i-j} \Big) h_i h_j^\dagger \Bigg] + \dots , \tag{3.4.3}$$

where $p_{z,\vec{m}} = \frac{i}{\sqrt{2}} \lambda_{\vec{m}}$, $p_{\bar{z},\vec{m}} = -\frac{i}{\sqrt{2}} \bar{\lambda}_{\vec{m}}$ are the internal KK momenta, with $\lambda_{\vec{m}}$, $\bar{\lambda}_{\vec{m}}$ as in (1.3.3), and the dots stand for all the remaining quadratic couplings between all the KK excitations of $A_{z,+i}$ and $A_{\bar{z},-j}$. Using the identity

$$\frac{1}{N_k} \sum_{i_k=1}^{N_k} f_{\vec{n}}(z_{i_k}) = \frac{1}{\sqrt{V}} \delta_{(1-Z_N^k)^{-1}\vec{n} \in \mathbb{Z}^2} , \tag{3.4.4}$$

valid for all the $T^2/\mathbf{Z}_N$ orbifolds, the contributions of the two terms in (3.4.3) to the 1- and 2-point functions are found to be

$$\langle A^8_{z,\vec{n}} \rangle = i p_{\bar{z},\vec{n}} \sum_{k=1}^{[N/2]} \frac{C_k}{\sqrt{V}} \delta_{(1-Z_N^k)^{-1}\vec{n} \in \mathbb{Z}^2} , \tag{3.4.5}$$

$$\langle h_i h_j^\dagger \rangle = g_4 f^{8+i-j} \sum_{k=1}^{[N/2]} \frac{C_k}{\sqrt{V}} . \tag{3.4.6}$$

Notice that the Higgs mass term arising from (3.4.6) is sensible only to the sum of the tadpole coefficients C_k.

3.4.1 1-point function

According to the considerations of Sect. 2.6, all the Feynman rules for the verteces are the standard ones, whereas the propagator has to be replaced (see Fig. 3.1) by

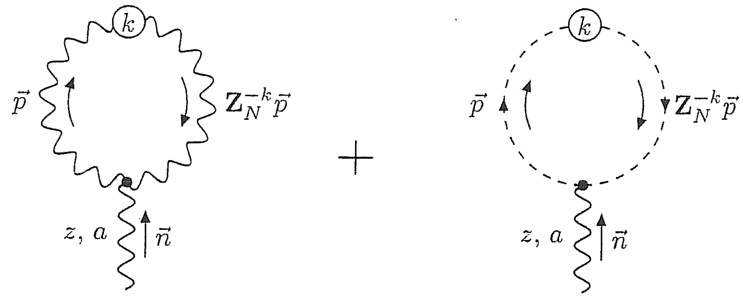

Figure 3.1: The gauge and ghost contributions to the 1-point function $\langle A^a_{z,\vec{n}}\rangle$.

its twisted version, as in Fig. 2.2. In the following we adopt the Feynman gauge, obtained through the choice $\xi = 1$ in the general gauge-fixing term in Eq. (2.5.12). By $4D$ Lorentz invariance, a tadpole can be generated only for the field components A^a_z and $A^a_{\bar{z}}$. An explicit computation of this tadpole shows that it has the form:

$$\langle A^a_{z,\vec{n}}\rangle = g_4 \sum_{k=0}^{N-1} \hat{\xi}^a_k \sum_{\vec{m}} \int \frac{d^4p}{(2\pi)^4} \frac{p_{\bar{z},\vec{m}}}{p^2 - 2\,|p_{z,\vec{m}}|^2}\delta_{\vec{n},(1-Z_N^{-k})\vec{m}}\,, \tag{3.4.7}$$

where $\hat{\xi}^a_k$ are numerical coefficients depending on the kind of field running in the loop and $p^2 = p_\mu p^\mu$ is the $4D$ momentum squared. The sector $k = 0$ never contributes. For the sectors $k \neq 0$, the δ-function in KK space relates the internal momenta of the virtual state to that of the external particle: $p_{\bar{z},\vec{m}} = (1-\tau^k)^{-1} p_{\bar{z},\vec{n}}$. We can then perform the sum over m, and we are left with the condition $(1 - Z_N^{-k})^{-1}\vec{n} \in \mathbb{Z}^2$. Therefore, the quadratically divergent part of Eq. (3.4.7) has the form of Eq. (3.4.5). This condition can easily be shown to be equivalent to $(1 - Z_N^{k-N})^{-1}\vec{n} \in \mathbb{Z}^2$, so that in Eq. (3.4.7) the sector $N - k$ contributes just as the sector k. The two contributions of these conjugate sectors can be paired, as expected, and simply yield twice the real part of one of them (with the obvious exception of the sector $k = N/2$ that, if present, must be counted only once). Finally, defining the new coefficients $\xi^a_k = -2^{1-\delta_{k,N/2}}\tau^{-k/2} N_k^{-1/2}\hat{\xi}^a_k$, Eq. (3.4.7) can be rewritten in the more suggestive form

$$\langle A^a_{z,\vec{n}}\rangle = -g_4 D(\Lambda) \sum_{k=1}^{[N/2]} p_{\bar{z},\vec{n}}\,\delta_{(1-Z_N^k)^{-1}\vec{n}\in\mathbb{Z}^2}\,\mathrm{Im}\,\xi^a_k + \dots\,, \tag{3.4.8}$$

where

$$D(\Lambda) = i\int \frac{d^4p}{(2\pi)^4}\frac{1}{p^2} = \frac{1}{16\pi^2}\Lambda^2\,. \tag{3.4.9}$$

The dots in (3.4.8) stand for additional logarithmically divergent and finite subleading corrections. These corrections are very similar to those found in [57] for the FI term in $5D$ SUSY theories on $S^1/(\mathbf{Z}_2 \times \mathbf{Z}_2')$, and are associated to interactions involving additional internal derivatives $\partial_z \partial_{\bar{z}}$ acting on $F^8_{z\bar{z}}$. Notice also that in the presence of an additional bulk mass term M for the fields running in the loop, which is possible for instance for scalar fields, Eq. (3.4.9) gets modified through the simple substitution $\Lambda^2 \to \Lambda^2 - 2\, M^2 \ln(\Lambda/M)$.

The contributions to ξ_a^k of the gauge and ghost fields in the adjoint representation, and of complex scalar or Weyl spinor fields in an arbitrary representation $\mathcal{R}$ and with overall twist g, are found to be:

$$(\xi_k^a)_{\rm gauge} = \frac{-1}{N N_k^{1/2}} \left[5(\tau^{\frac{k}{2}} + \tau^{-\frac{k}{2}}) - (\tau^{\frac{3k}{2}} + \tau^{-\frac{3k}{2}}) \right] {\rm Tr}_{\rm adj} \left[{Z_N}^k\, t^a \right], \quad (3.4.10)$$

$$(\xi_k^a)_{\rm scalar} = \frac{-2}{N N_k^{1/2}}\, g^k\, (\tau^{\frac{k}{2}} + \tau^{-\frac{k}{2}}) {\rm Tr}_{\mathcal{R}} \left[{Z_N}^k\, t^a \right], \quad (3.4.11)$$

$$(\xi_k^a)_{\rm fermion} = (4) \frac{2^{1-\delta_{k.N/2}}}{N N_k^{1/2}}\, (g \tau^{\frac{1}{2}})^k\, {\rm Tr}_{\mathcal{R}} \left[{Z_N}^k\, t^a \right], \quad (3.4.12)$$

where $(\xi_k^a)_{\rm gauge}$ also contains the ghost contribution. The gauge trace appearing in the above coefficients is as expected to differ from zero only for $a = 8$, reflecting the fact that only a $U(1)$ tadpole is allowed by the gauge symmetry. It is easily evaluated by recalling the definition of the twist matrix $P_{\mathcal{R}}$, Eq. (3.2.4), and exploiting the decomposition of the representation $\mathcal{R}$ under $SU(3) \to SU(2) \times U(1)$. Denoting by $d_{\mathcal{R}_r}$ and $q_{\mathcal{R}_r}$ the dimensionality and the charge under $Q_{\mathcal{R}} = \frac{1}{\sqrt{3}} t^8_{\mathcal{R}}$ of the r-th component $\mathcal{R}_r$ in the decomposition $\mathcal{R} \to \oplus_r \mathcal{R}_r$, we find:

$$ {\rm Tr}_{\mathcal{R}} \left[P^k t^8 \right] = \sqrt{3} \sum_{\mathcal{R}_r} d_{\mathcal{R}_r} q_{R_r} \tau^{2 n_p (\frac{n_{\mathcal{R}}}{3} + q_{\mathcal{R}_r}) k} \,. \quad (3.4.13)$$

Notice that the gauge contribution to the tadpole vanishes at 1-loop order for the $\mathbf{Z}_2$ case. The same happens for any scalar or fermion contribution in a real representation. This can be seen by using the relation (valid for any $\mathbf{Z}_N$ orbifold):[7]

$$ {\rm Tr}_{\mathcal{R}} \left[P^k t^8 \right] = -{\rm Tr}_{\mathcal{R}} \left[P^{-k} t^8 \right], \quad \text{if } \mathcal{R} \text{ real}. \quad (3.4.14)$$

This result is in agreement with that found in [30], where it was also generalized to the 2-loop case. On the contrary, for $N = 3, 4, 6$, there is always some tadpole

[7] Actually the scalar contribution in the $\mathbf{Z}_2$ model vanishes for any representation, not only for real ones.

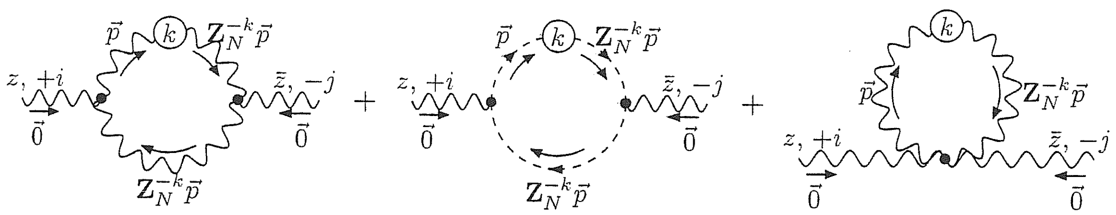

Figure 3.2: The gauge and ghost contributions to the 2-point function $\langle h_i h_j^\dagger \rangle$.

coefficient that is non-vanishing for the single-Higgs projections. The tadpole can only vanish for the zero-Higgs cases $N = 4$, $n_p = 2$ and $N = 6$, $n_p = 3$, since they correspond to vanishing Im $\mathrm{Tr}_{\mathrm{adj}}\left[P^k t^a\right]$.

In order to relate the coefficients ξ_k^8 to the coefficients $\mathcal{C}_k$ appearing in (3.4.1), we must compare Eq. (3.4.8) with Eq. (3.4.5), which have as expected the same structure. The result is

$$\mathcal{C}_k = g_4 \sqrt{V} D(\Lambda) \,\mathrm{Im}\, \xi_k^8 \,. \tag{3.4.15}$$

We summarize in Table 3.2 the contribution of a Weyl fermion to $\mathcal{C}_k$ for all possible twists and for the first few $SU(3)$ representations. Notice that the contribution of a fermion with twist g in the conjugate representation $\bar{\mathcal{R}}$ is equal to that of a fermion twisted by $\bar{g}\bar{\tau}$ in the representation $\mathcal{R}$. Similarly, a scalar in the $\bar{\mathcal{R}}$ with twist g contributes as one in the $\mathcal{R}$ with conjugate twist $\bar{g}$. The sum over all possible twists for any scalar or fermion contribution always vanishes, since in this case one reconstructs the matter content that would appear on the covering torus, which cannot give rise to any localized divergence. We see that for $N = 3, 4, 6$ and for any choice of fermion representations, it is impossible to cancel the total (gauge+ghost+fermion) one-loop contribution to each tadpole coefficient, although one can obtain their global cancellation, namely the cancellation of their integral over the compact space $\sum_k \mathcal{C}_k = 0$. This seems to be possible, without scalars, only for $\mathbf{Z}_4$ with an odd number of $6D$ Weyl fermions in suitable representations. If one includes scalars, an accidental local one-loop cancellation of the tadpole is possible, but in this case one needs a symmetry to protect the mass M of the $6D$ scalars, which is otherwise expected to be at the cut-off scale Λ, and reintroduce a quadratic sensitivity to the latter.

$\mathbf{Z}_2$	1	τ
$c_1(\mathbf{3})$	−4	4
$c_1(\mathbf{6})$	4	−4
$c_1(\mathbf{8})$	0	0
$c_1(\mathbf{10})$	−12	12

$\mathbf{Z}_3$	1	τ	τ^2
$c_1(\mathbf{3})$	−4	−4	8
$c_1(\mathbf{6})$	−20	16	4
$c_1(\mathbf{8})$	12	−24	12
$c_1(\mathbf{10})$	12	12	−24

$\mathbf{Z}_4$	1	τ	τ^2	τ^3
$c_1(\mathbf{3})$	0	−8	0	8
$c_1(\mathbf{6})$	−24	−16	24	16
$c_1(\mathbf{8})$	24	−24	−24	24
$c_1(\mathbf{10})$	−48	24	48	−24
$c_2(\mathbf{3})$	−4	4	−4	4
$c_2(\mathbf{6})$	4	−4	4	−4
$c_2(\mathbf{8})$	0	0	0	0
$c_2(\mathbf{10})$	−12	12	−12	12

$\mathbf{Z}_6$	1	τ	τ^2	τ^3	τ^4	τ^5
$c_1(\mathbf{3})$	4	−4	−8	−4	4	8
$c_1(\mathbf{6})$	−4	−32	−28	4	32	28
$c_1(\mathbf{8})$	36	0	−36	−36	0	36
$c_1(\mathbf{10})$	−60	−84	−24	60	84	24
$c_2(\mathbf{3})$	−4	−4	8	−4	−4	8
$c_2(\mathbf{6})$	−20	16	4	−20	16	4
$c_2(\mathbf{8})$	12	−24	12	12	−24	12
$c_2(\mathbf{10})$	12	12	−24	12	12	−24
$c_3(\mathbf{3})$	−4	4	−4	4	−4	4
$c_3(\mathbf{6})$	4	−4	4	−4	4	−4
$c_3(\mathbf{8})$	0	0	0	0	0	0
$c_3(\mathbf{10})$	−12	12	−12	12	−12	12

Table 3.2: The contribution to the tadpole coefficients $\mathcal{C}_k$ from Weyl fermions for various representations and all choices of the phase g. We report the quantity $c_k = \sqrt{3}\,N\,\mathrm{Im}[\xi_k^8]$, which for the gauge contribution is given by $c_1 = 0$ for $\mathbf{Z}_2$, $c_1 = -21$ for $\mathbf{Z}_3$, $c_1 = -36$ and $c_2 = 0$ for $\mathbf{Z}_4$, and $c_1 = -45$, $c_2 = -21$ and $c_3 = 0$ for $\mathbf{Z}_6$. In all cases, we are considering the projection with $n_p = 1$, giving single-Higgs models for $N \neq 2$.

3.4.2 2-point function

We now compute the one-loop 2-point function for the Higgs field, at zero external $4D$ and KK momentum. Contrarily to the 1-point function, which we have computed for any external KK momentum, this correlation gives us information only on the form of the operator (3.4.1) integrated over the compact space (see Eq. (3.4.6)). Nevertheless, it provides an important independent check of the 1-point function computation and also allows the extraction of the finite non-local contributions to the Higgs mass.

Thanks to the property displayed in Fig. 2.4, each of the diagrams contributing to the one-loop Higgs mass contains only one twisted propagator with twist k. The diagrams with $k = 0$ give a finite contribution, which reproduces up to a $1/N$

factor the result that would be obtained for a theory on the covering torus T^2. The remaining contributions arising from the diagrams with the insertion of a propagator with $k \neq 0$ are instead divergent. Owing to momentum conservation at the verteces, the internal KK momentum in the twisted internal lines has to vanish (see Fig. 3.2). The general structure of the Higgs 2-point function is then given by:[8]

$$\langle h_i h_j^\dagger \rangle = g_4^2 f_8{}^{+i-j} \xi_{\rm div}^8 \, D(\Lambda) + i g_4^2 \, \delta_{ij} \, \xi_{\rm fin}^8 \, F(R) \,, \tag{3.4.16}$$

with $D(\Lambda)$ as in (3.4.9) and

$$F(R) = i \int \frac{d^4 p_4}{(2\pi)^4} \sum_{\vec n \in \mathbb{Z}^2} \frac{p^2}{(p^2 - 2|p_{z,\vec n}|^2)^2} = \frac{U_2}{4\pi^5 R^2} \sum_{\vec n \neq \vec 0} |n_1 + U n_2|^{-4} \,. \tag{3.4.17}$$

It is straightforward to compute the diagrams controlling the divergent part. Note that ghosts do not contribute, because their coupling to the Higgs is proportional to the KK momentum. Thanks to the identities

$$\begin{aligned} {\rm Tr}_{\mathcal{R}} \left[t^{+i} t^{-j} Z_N{}^k \right] &= \tau^l {\rm Tr}_{\mathcal{R}} \left[t^{-j} t^{+i} Z_N{}^k \right] \,, \\ {\rm Tr}_{\mathcal{R}} \left[t^{-j} t^{+i} Z_N{}^k \right] &= -i f_8{}^{+i-j} \frac{1}{1-\tau^l} {\rm Tr}_{\mathcal{R}} \left[t^8 Z_N{}^k \right] \,, \end{aligned} \tag{3.4.18}$$

the result can be rewritten as

$$\xi_{\rm div}^8 = \sum_{k=1}^{[N/2]} {\rm Im}\, \xi_k^8 \,, \tag{3.4.19}$$

where the ξ_k^8's turn out to precisely match the expressions (3.4.10)–(3.4.12) extracted from the 1-point function computation. This result represents a non-trivial check of that computation. Indeed, comparing Eq. (3.4.16) with Eq. (3.4.6), we deduce that

$$\sum_{k=1}^{[N/2]} C_k = g_4 \sqrt{V} D(\Lambda) \, \xi_{\rm div}^8 \tag{3.4.20}$$

which is compatible with the result in Eq. (3.4.15) thanks to the relation (3.4.19).

The diagrams contributing to the finite part can be computed as well, and the coefficients of the finite part are found to be given by:

$$(\xi_{\rm fin}^8)_{\rm gauge} = 2 \frac{4}{N} C({\rm Adj}) \,, \tag{3.4.21}$$

$$(\xi_{\rm fin}^8)_{\rm scalar} = \frac{4}{N} C(\mathcal{R}) \,, \tag{3.4.22}$$

$$(\xi_{\rm fin}^8)_{\rm fermion} = -2 \frac{4}{N} C(\mathcal{R}) \,, \tag{3.4.23}$$

[8]Equation (3.4.16) is valid also for the $\mathbf{Z}_2$ model, where two Higgs fields are present. In this case, there are additional 2-point correlators that we neglect. See *e.g.* [22].

in terms of the quadratic Casimir $C(\mathcal{R})$ of the representation $\mathcal{R}$, defined by the relation $\mathrm{Tr}_{\mathcal{R}}\left[t^a t^b\right] = C(\mathcal{R})\delta^{ab}$, so that $C(\mathrm{Fund}) = \frac{1}{2}$ and $C(\mathrm{Adj}) = 3$.

3.5 Phenomenological implications

In sections 3.3 and 3.4 we have shown how $6D$ gauge theories on orbifold models can lead to a beautiful prediction for the Higgs mass, but at the same time they are affected by a quadratic divergence arising from a localized tadpole term. It is thus natural to try to understand whether and to what extent such models can be considered for realistic model building.

As already mentioned, it seems straightforward to introduce SM fermions and to break the flavor symmetry in this modes, by generalizing to $6D$ the construction of [24]. Moreover, fixing the weak mixing angle to its true value seems possible by introducing additional $U(1)$ gauge fields in the bulk, again generalizing [24].

The real issue, however, is that the presence of the quadratically divergent term (3.4.1) can destabilize the electroweak scale. It must therefore be understood how much (if any) progress has been achieved with respect to the SM, as far as the little hierarchy problem is concerned. The abelian and non-abelian components of the localized operator (3.4.1) induce respectively a non-trivial background for the field A_z^8 and a mass term for the Higgs doublet A_z^{-i}. The latter can generate not only a mass term for the $4D$ Higgs field, but also mixings between all its KK partners. These mixings can be neglected only if their magnitude is much smaller than $1/R$, the typical mass of KK modes. In our case, $\mathcal{C}_k > 1/R$ (see below) and the effect of all these mixings, as well as that of the non-trivial background for A_z^8, must be taken into account. In order to see if and how much the EWSB scale is sensitive to this divergence, one has to compute the background value of A_z^8 and study the quantum fluctuations around it, to get the physical masses of the various fields, in particular for A_z^{-i}. A similar analysis has already been performed in [32], where the effect of localized FI terms in $6D$ orbifold models has been studied (see also [58]). As already mentioned, the tadpole (3.4.1) can be interpreted as a FI term in SUSY theories; this suggests a correspondence that allows a study of its physical consequences even in our non-SUSY set-up. The background induced by the tadpole can be explicitly found as follows. If one sets to zero all $4D$ gauge fields, the effective potential one obtains for the scalar fields A_z^a, in the unitary gauge $\xi \to \infty$ in (2.5.12), can be written, up to some irrelevant constant terms, as

$$V = \frac{1}{2}\sum_{a=1}^{3}|F_{z\bar{z}}^{a}|^2 + |F_{z\bar{z}}^{-i}|^2 + \frac{1}{2}\Big|F_{z\bar{z}}^{8} - i\sum_{k=1}^{[N/2]}\frac{C_k}{N_k}\sum_{i_k=1}^{N_k}\delta^{(2)}(z - z_{i_k})\Big|^2 . \quad (3.5.1)$$

The potential (3.5.1) is a sum of squares and thus, as it happens for the D-term potential of SUSY theories, configurations where it vanishes are automatically consistent classical backgrounds. In the particular case where the tadpole globally vanishes, that is $\sum_k C_k = 0$, the background value of the fields can be easily determined. By taking an ansatz in which all fields $A_{z,1,2,3}$ and $A_{z,\pm i}$ vanish and the only non–trivial background is given to $A_{z,8}$, which is neutral under the $SU(2) \times U(1)_Y$ EW group, all terms vanish in Eq. (3.5.1) but the last one. A global minimum ($V = 0$) of the potential is found if

$$F_{z\bar{z}} = -2\partial_{\bar{z}}A_z^8 = i\sum_{k=1}^{[N/2]}\frac{C_k}{N_k}\sum_{i_k=1}^{N_k}\delta^{(2)}(z - z_{i_k}) \equiv -i\sum_i \xi_i\delta^{(2)}(z - z_i)\,, \quad (3.5.2)$$

where the sum in the last term runs on the distinct fixed points z_i on one fundamental domain of the covering T^2 and ξ_i is the appropriate combination of the tadpole coefficients C_k. To be precise, if we want, as we will, to think the A_z^8 T^2 field to be a field on $\mathbb{C}$ with suitable periodicity conditions, the l.h.s. of Eq. (3.5.2) must be extended by periodicity to the whole complex plane. The unitary gauge condition $\partial_z A_{\bar{z}}^8 = -\partial_{\bar{z}}A_z^8$ has been used in Eq. (3.5.2). By defining $A_z^8 = i\partial_z W$, Eq. (3.5.2) reads

$$\partial\bar{\partial}W = \frac{1}{2}\sum_i \xi_i\delta^{(2)}(z - z_i)\,, \quad (3.5.3)$$

which is basically a generalized form of the equation for the $2D$ propagator on the complex plane $\mathbb{C}$.

Solutions to Eq. (3.5.3), for any $\mathbf{Z}_N$ orbifold model, are easily constructed as ratios and products of the four Jacobi theta functions $\theta_{1,2,3,4}$, defined as in Appendix A. Let us consider now, for definiteness, the case of $T^2/\mathbf{Z}_4$, in which (see Fig. 2.1), 4 fixed points are present. Of those, two are 1–fixed ($z_1 = 0$ and $z_2 = \frac{\pi R}{\sqrt{2}}(1+i)$), while the others ($z_3 = \frac{\pi R}{\sqrt{2}}$ and $z_3 = \frac{\pi R}{\sqrt{2}}i$) are 2–fixed, and are identified by the orbifold symmetry, so that the tadpole coefficients $\xi_{3,4}$ at those points are equal. The function W solving Eq. (3.5.3) is found to be

$$W = \frac{1}{4\pi}\log\left(\prod_{i=1}^{4}|\theta_i(\frac{z}{\sqrt{2}\pi R}|i)|^{2\xi_i}\right) . \quad (3.5.4)$$

To check this, one has to use the identities in Eq. (A.0.3), with $q = e^{-2\pi}$ for $U = i$ as in our case, showing that the product of theta functions in Eq. (3.5.4) can be written as a product of θ_1 functions with shifted argument. Since the only point at which $\theta_1(z|i)$ vanishes is $z = 0$, where it behaves like z, we see that the only singularities of W in Eq. (3.5.4) are located at the four fixed points. Around each z_i point, W behaves as

$$W \sim \frac{\xi_i}{4\pi} \log(|\frac{z - z_i}{\sqrt{2}\pi R}|^2) + \text{cosnt.}\,,$$

so that, by remembering the relation $\frac{1}{2\pi}\partial\bar{\partial}\log(|z|^2) = \delta^{(2)}(z)$, we have proven Eq. (3.5.3) to be solved by Eq. (3.5.4). Note that we have never used, up to now, our assumption that the tadpole should be globally vanishing. This however turns out to be essential if W has to be periodic on T^2, as it should since A^8_z is periodic. If the periodicity under $z \longrightarrow z + \sqrt{2}\pi R$ is automatic, (see Eq. (A.0.4)), the transformations of the theta functions under $z \longrightarrow z + i$ in Eq. (A.0.5) implies

$$W(z + \frac{2\pi R}{\sqrt{2}} i) = W(z) + (\frac{1}{2} + \text{Im} z) \sum_i \xi_i\,.$$

The tadpole must then be globally vanishing for Eq. (3.5.3) to have a solution compatible with the torus boundary conditions, meaning that a neutral background like the one we are looking for can be obtained only in this case. The last point to be checked is the background we have found to be compatible with the orbifold boundary conditions we have assigned. This is to say that W must be untwisted under $z \longrightarrow iz$, since $A_{z,8}$ has twist $-i$. This is immediately checked to be the case, if, again, the tadpole is globally vanishing, thank to the relations

$$\theta_1(-iz|i) = e^{-i\frac{\pi}{2} + \pi z^2} \theta_1(z|i)\,, \qquad \theta_{2,3,4}(-iz|i) = e^{\pi z^2} \theta_{2,3,4}(z|i)\,,$$

which can be deduced from the modular transformations of the theta functions.

Having found the background, let us consider quantum fluctuations. We are intersted, in particular, to the existence of a zero-mode solution $A^{-i}_{z,0}$ for the field A^{-i}_z, to be identified with the Higgs. By looking at the potential in Eq. (3.5.1), we immediately recognize that a mass–term for A^{-i}_z can only come from the second term, the last one generating the quartic coupling. The wave function for the Higgs field is then found by solving the first-order equation

$$F^{-i}_{\bar{z}z} = 2\Big(\partial_{\bar{z}} + ig_6 \frac{\sqrt{3}}{4} \langle A^8_{\bar{z}} \rangle \Big) A^{-i}_{z,0} = 0\,, \tag{3.5.5}$$

where we have used the unitary gauge condition. The above equation is immediately solved. It is, up to normalization

$$A_{z,0}^{-i} = e^{-\frac{\sqrt{3}g_6}{4}W} \,. \tag{3.5.6}$$

We will not provide here a detailed study of the above function, and we refer the reader to [32]. We just want to observe that, in the presence of the tadpole, the Higgs wave function (3.5.6), behaves at the fixed points as

$$A_{z,0}^{-i} \sim |z - z_i|^{-\frac{\sqrt{3}g_6}{8\pi}\xi_i} \,, \tag{3.5.7}$$

so that not only it will be singular at some points, but may even be not normalizable if ξ_i is positive and large enough. Moreover, there are various integrals involving $A_{z,0}^{-i}$ which are physically relevant. The $4D$ effective Higgs quartic coupling, for instance, is proportional to the integral of the 4–th power of $A_{z,0}^{-i}$ while the Yukawas, since fermions have wave functions which are similar to the Higgs one, arise from cubic integrals. It seems then that in the present situation a complete treatment of the orbifold theory is impossible without referring to an underlying resolution of the orbifold singularity. In [32] a "resolution" of the orbifold singularity was considered, consisting in replacing the delta function with a regular distribution of width r, where r has to be considered as the size of the resolved fixed points. In so doing, Eq. (3.5.6) is replaced with some smoothed version of it, so that it can be normalized and all relevant integrals can be computed. The resulting physical quantities, however, are sensitive to the resolution scale $1/r$ so that, in practice, they are sensible to the UV resolved completion of the orbifold theory. There is also another reason to believe the tadpole operator to be deeply related to the resolution of the orbifold singularities. It is known, and this will be explicitly shown in the next chapter when we will address the problem of orbifold resolution, that localized curvature and field–strength backgrounds are "hidden" inside the fixed points. As shown in Eq. (3.5.2), the effect of the tadpole is precisely to add some localized gauge field–strength to the usual flat background $F = 0$. It then corresponds somehow to renormalize the localized gauge background which is present on the resolved orbifold.

Let us now come back to our GHU model with globally vanishing tadpole. The above reasoning shows that a globally vanishing tadpole does not give rise to any quadratic divergence in the Higgs mass parameter μ^2 appearing in (3.3.6). In other words, a globally vanishing tadpole is harmless for EWSB, which is governed by the finite non-local contributions to the 2-point function, proportional to (3.4.17), which for simplicity we have neglected in these simple lines of arguments. In the presence of globally vanishing one-loop tadpole, the little hierarchy problem is then solved. The non-trivial profile for the Higgs field, however, induces large corrections to (3.3.8), since this ratio depends on the integral of the Higgs profile in the internal directions. As mentioned in Sect. 3.3, such corrections are estimated to be of $O(1)$ and thus might significantly alter the tree-level result (3.3.8). To be more quantitative, we can rely on the higher-dimensional generalization of the NDA [59]. We denote in short by $l_4 = 16\pi^2$ and $l_6 = 128\pi^3$ the $4D$ and $6D$ loop factors. The relation between the cut-off scale Λ and the compactification scale $1/R$ is then estimated to be $\Lambda \sim g_4^{-1}(2\pi R)^{-1}\sqrt{l_6}$, which for the EW coupling yields $\Lambda \sim 10/R$. In this way we obtain an estimate for the tadpole coefficient C_k that is in agreement with the direct one-loop result reported in (3.4.15) and of order $l_6/(2\pi R g_4 l_4) > 1/R$, as mentioned. On the other hand, the value of μ^2 in Eq. (3.3.6) induced by finite non-local corrections is of order $\mu^2 \sim g_4^2/(l_4 R^2)$, and from (3.3.7) one estimates $1/R \sim 1$ TeV and $\Lambda \sim 10$ TeV, which are compatible with present experimental bounds in a natural way. On the other hand, for a globally non-vanishing tadpole, it is reasonable to expect to have effectively $\mu^2 \sim g_4^2\Lambda^2/l_4$. From (3.3.7) one now estimates $\Lambda \sim 1$ TeV, corresponding to $1/R \sim 100$ GeV. The amount of fine-tuning that is needed in this case is about the same as in the SM, and there is no progress concerning the little hierarchy problem.

Chapter 4

Orbifold resolutions and fermion localization

As already discussed in the Introduction, compactification on orbifolds is a particularly useful tool, in the context of extra dimensional field theories. Simple orbifolds, in particular $S^1/\mathbf{Z}_2$ and $T^2/\mathbf{Z}_N$, are frequently employed in model–building, as in the cases considered in the previous chapter, for their capability of breaking symmetries and introducing chirality in the fermion spectrum. As also shown in Sect. 1.6.2, however, chiral fermions also arise in any smooth compactification such that the index of the Dirac operator (see Eq. (1.6.14) for the $6D$ case) is non–vanishing. For what concern symmetry breaking, it clearly can arise on a smooth space if a background of a non–abelian gauge field (like $A_{z,8}$, for the $SU(3)$ case previously discussed) is turned on. Both effects, then, could be also obtained by flux compactification, which consists on considering more complicated non–flat spaces like those described in Sect. 1.1 and 1.6.2, on which background for the gauge (and eventually gravity) field strength is present. The main reason for preferring orbifolds is simplicity; when considering fluxes, indeed, we have seen how it becomes technically much more involved to deal with the resulting theory, while an orbifold model can be studied on the covering space (which is in general trivial and flat such as the circle or the torus) by gauging away the discrete orbifold symmetry. Apart of simplicity, another important reason why orbifolds are so commonly used is the flexibility in their $4D$ field content. At the fixed points, indeed, $4D$ localized fields of any kind are commonly introduced in arbitrary number.

Although their apparent simplicity, orbifolds have singularities at the fixed points, and can be seen as singular limits of smooth resolving spaces. Under this point of view, orbifold compactification is just flux compactification, in the limit in which the fluxes approach a singular profile. In this chapter, which is based on [37] and [38], a resolved version of the $\mathbb{C}/\mathbf{Z}_N$, $T^2/\mathbf{Z}_N$ and $S^1/\mathbf{Z}_2$ orbifolds are constructed, and the free theory of a $6D$ chiral spinor studied on them. We show that each orbifold singularity admits various topologically different resolutions, labelled by an integer monopole charge q one can add at each resolved fixed point. As a consequence of this fact, the index of the Dirac operator on the resolved space, which depends on these monopole charges, can assume different values, so that different fermion zero–mode spectra can arise on the resolved theory. This may appear to be an inconsistency, since in the un–resolved orbifold model, which the resolution should resamble in the suitable limit, the number and chirality of the zero–modes which survive the orbifold projection is fixed. Our study of the resolved Dirac equation reveals, however, a very nice physical interpretation of the extra zero–modes. Their wave function is indeed found to be peaked around the resolved singularity, and their probability density to become a delta–function in the orbifold limit. A certain, quite wide, number of "brane" fermion distributions are then found to originate naturally, as an effect of the resolution, from a single "bulk" $6D$ field.

In Sect. 4.1, a resolved version of the non–compact $\mathbb{C}/\mathbf{Z}_N$ orbifold is constructed, and the free theory of a $6D$ chiral spinor studied on it. This theory represents a resolved version of the fermion orbifold model and, indeed, the usual $4D$ chiral zero modes are reproduced when the orbifold limit is taken. Extra states are found, however, with a profile localized at the resolved fixed point. In Sect. 4.2, the compact $T^2/\mathbf{Z}_N$ case is considered. Resolutions are built for all orbifolds and all possible content of discrete Wilson lines. The number and chiralities of $4D$ localized fermions one can get from a single $6D$ chiral field are classified. In Sect. 4.3, finally, $S^1/\mathbf{Z}_2$ orbifolds are discussed. The case is considered in which $S^1/\mathbf{Z}_2$ can be seen as a degenerate limit of $T^2/\mathbf{Z}_2$, and the resolution is then constructed as the limit of the $T^2/\mathbf{Z}_2$ one. Localized chiral zero–modes are found to arise also in this case and their number and chiralities are classified. Moreover, by also making use of numerical methods when needed, massive states are also considered. The mass–spectrum and the wave functions are shown to correctly reproduce the orbifold ones, when the orbifold limit is taken.

4.1 Resolution of $\mathbb{C}/\mathbf{Z}_N$ orbifolds

As the simplest example of the resolution procedure, let us consider the $\mathbb{C}/\mathbf{Z}_N$ orbifolds, which are the non–compact versions of the $T^2/\mathbf{Z}_N$ ones. As we will see later, $T^2/\mathbf{Z}_N$ is locally equivalent to $\mathbb{C}/\mathbf{Z}_N$, so that constructing a resolved version of it permits us to discuss the resolution of $T^2/\mathbf{Z}_N$ as well. The $\mathbb{C}/\mathbf{Z}_N$ orbifolds are obtained from the complex plane $\mathbb{C}$ with euclidean metric by identifying points connected by a $2\pi/N$ rotation around the origin. The fundamental domain one gets is the $2\pi/N$ plane angle in between the $z = t$ and $z = \tau t$ (t real an positive, $\tau = e^{2\pi i/N}$) lines, which are identified. The plane angle can be deformed isometrically in $\mathbb{R}^3$ until the two extreme lines coincide, the resulting surface, shown in Fig. 4.1, being a cone of angle α, with $\sin\alpha = 1/N$. Let us consider on this space a $6D$ L–handed spinor field Ψ. As discussed in Sect. 1.6.2, the wave functions in the internal space of its $4D$ L– and R–handed components can be combined in a $2D$ Dirac field

$$\psi = \begin{pmatrix} \psi_R \\ \psi_L \end{pmatrix}, \tag{4.1.1}$$

subjected to the $2D$ Dirac Equation (1.6.12). Our field, which is assumed to possess an $U(1)$ phase transformation symmetry, is defined as a field on $\mathbb{C}$ which remains invariant under a $2\pi/N$ rotation around the origin, modulo a suitable phase transformation. Consistently with Eq. (2.5.2), we have

$$\psi(\tau z) = \mathcal{P}\psi(z)\,, \qquad \mathcal{P} = e^{\pi i\left(1-\frac{1}{N}\right)\sigma_3} e^{\frac{\pi i}{N}p}\,, \tag{4.1.2}$$

where p is any integer running from $-N+1$ to $N-1$ at steps of 2. The $U(1)$ phase in Eq. (4.1.2) is chosen to make $\mathcal{P}^N = \mathbb{1}$ and an extra $-1 = e^{\pi i\sigma_3}$ has been included in the Lorentz part of $\mathcal{P}$ for future convenience.

4.1.1 Definition of the resolving space

The $\mathbb{C}/Z_N$ orbifold is a cone of angle α with $\sin\alpha = 1/N$. The line element of this space can be written as

$$ds^2 = d\tau_c^2 + \sin\alpha^2\tau_c^2 d\phi^2\,, \tag{4.1.3}$$

in the polar coordinates (τ_c, ϕ), which are related to the complex plane ones by $z = \tau_c e^{i\frac{\phi}{N}}$. Of course, a space with the metric (4.1.3), if $\sin\alpha \neq 1$, is singular at $\tau_c = 0$, and then needs a resolution. The cone possesses an $O(2)$ isometry group, whose $\mathbb{R}^3$ embedding consists on rotations around its axis ($\phi \to \phi + \lambda$) and reflections orthogonal to any plane which contains it ($\phi \to -\phi + \lambda$). It is very reasonable to assume the resolving space $\mathcal{R}$ to possess the same isometry group of the space it has to resolve. Moreover, only spaces which can be entirely described with a single set of coordinates, and are then topologically trivial, will be considered

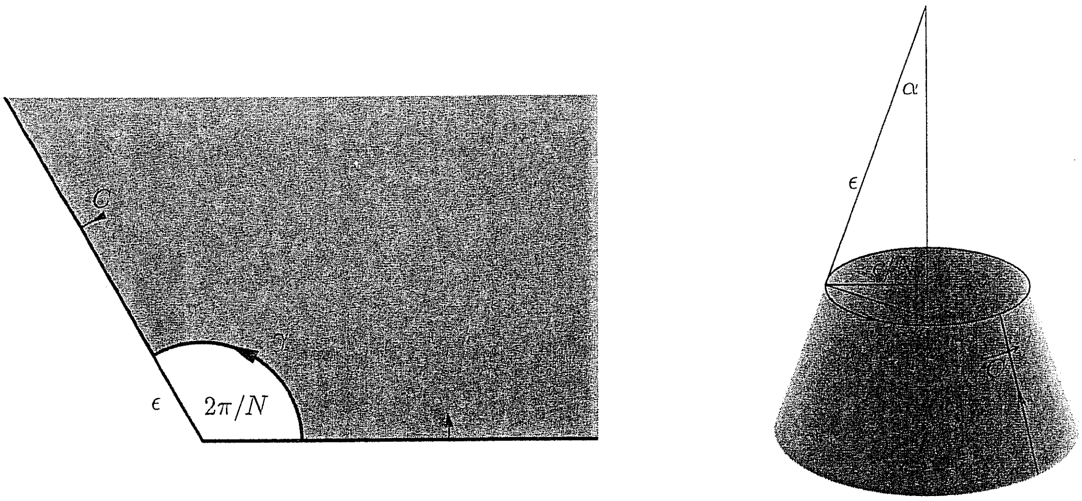

Figure 4.1: The picture in the left shows the fundamental domain of the $\mathbb{C}/\mathbf{Z}_3$ orbifold from which a disk of radius ϵ has been removed. The resulting truncated cone, including the circle γ and the cut which runs along the cone, is shown in the right. The infinitesimal path C, oriented in such a way that the vector product of its direction with the one of the cut is outgoing from the surface, is also shown.

in the following. These assumptions, though very reasonable, exclude of course more complicate resolutions, in which $\mathcal{R}$ breaks the $O(2)$ isometry, which is however restored in the orbifold limit, or it has handles, and then non-trivial topology, but they still leave a very general class of spaces. Topologically trivial smooth $2D$ spaces with $O(2)$ isometry group can be parametrized (see Appendix B) in terms of a single function $\rho(\tau)$, $\tau \in (0, \infty)$, which completely defines the metric, once expressed in the polar coordinates $(\tau,\ \phi)$. In these coordinates

$$ds^2 = d\tau^2 + \rho^2(\tau) d\phi^2\,, \tag{4.1.4}$$

where $\rho(\tau)$ has to satisfy certain constraints (see Eq. (B.0.8)) ensuring that the space so defined is really regular at $\tau = 0$, where polar coordinates are ill-defined. If $\mathcal{R}$ has to reproduce the cone when τ overcomes η, which is defined to be the location of the curve γ in Fig. 4.1, its metric (4.1.4) must reduce to the one in Eq. (4.1.3) up a coordinate change. Therefore, for $\tau \geq \eta$, one requires

$$\rho(\tau) \equiv \sin\alpha(\tau + \tau_c^0)\,, \tag{4.1.5}$$

in such a way that, identifying the coordinate τ_c in Eq. (4.1.3) with $\tau + \tau_c^0 = \tau_c$, $\mathcal{R}$ reproduces, when $\tau > \eta$, a portion ($\tau_c \in (\eta + \tau_c^0, \infty)$) of a cone. Since $\rho \sim \tau$ for $\tau \sim 0$ (see Eq. (B.0.8)), the role of the resolving space is to interpolate a plane at $\tau \sim 0$ with a cone at $\tau \geq \eta$. For $\mathcal{R}$ to be tractable, *i.e.* the tangent plane to be well defined, the first derivative of ρ must be at least continuous. A resolution with $\rho \in \mathcal{C}^1$ at η is called a "$\mathcal{C}^1$ resolution", and an example was provided in [37] consisting in a spherical cap attached to a truncated cone.

4.1.2 Fermions on the resolved orbifold

Let us now define a resolved version of the theory of a free fermion on $\mathbb{C}/\mathbf{Z}_N$. Consider then a $6D$ fermion field on $\mathcal{M}_4 \times \mathcal{R}$. As usual, the wave functions in the internal space of its chiral components are written as a $2D$ Dirac field ψ on $\mathcal{R}$. Apparently, one essential feature for this model to be related with the orbifold one would be that, in the space region where $\mathcal{R}$ coincides with the cone ($\tau > \eta$), the ψ field on $\mathcal{R}$ and the one on $\mathbb{C}/\mathbf{Z}_N$ should share the same boundary conditions, provided by Eq. (4.1.2), under $\phi \to \phi + 2\pi$ ($z \to \tau z$). Note that, however, the boundary conditions alone cannot have any intrinsic meaning. Indeed, as for the $U(1)$ Scherk–Schwarz twist on S^1 discussed in Sect. 1.2, they can be changed and eventually made trivial by field redefinitions, consiting on non-periodic $U(1)$ gauge or Local-Lorentz (LL) transformations which, at the same time, also affect the gauge field and the spin connection, turning on non-trivial (flat) backgrounds A and ω for them. What really matters, on the contrary, is the *holonomy* of the field on circuits surrounding the singularity. To the holonomy, which is gauge invariant, both the boundary conditions and the background of the gauge and spin connections contribute. In the case of trivial boundary conditions, it is expressed by the appropriate Wilson loop. In the case of the orbifold model, in which the connections vanish, the holonomy

$$W = W_{LL} W_{gauge} = \mathcal{P}^{-1} = e^{-\pi i\left(1-\frac{1}{N}\right)\sigma_3} e^{-\frac{\pi i}{N}p}\,, \qquad (4.1.6)$$

comes from the presence of the cut in Fig. 4.1. To be precise, the cut comes from a mismatch in the transition functions at the boundaries of the "big" chart describing the truncated cone, similarly to the Scherk–Schwarz twist discussed in Sect. 1.2.

The resolving space $\mathcal{R}$, on the contrary, is entirely described by a single coordinate set, so that the fields on it are described by single-valued functions. The fermion will then be periodic as $\phi \to \phi + 2\pi$ and backgrounds for A and ω must be present. Note that the presence of a non-trivial LL connection ω is automatic from Eq. (4.1.4) and its form will be shown to be consistent with Eq. (4.1.6). The detailed form of the gauge background A is, on the contrary, arbitrary. The connections A and ω are globally defined ($O(2)$-invariant, consistently with what was assumed to be the isometry group) vector fields on $\mathcal{R}$, with negative intrinsic parity under the $\mathbf{Z}_2$ ($\phi \to -\phi$) action. Note that the coupling of fermions to the A background breaks the parity symmetry (which interchanges $L-$ and $R-$handed fields), while the one to ω does not. This is correct since, as comes from the index theorem (1.6.14), it is the presence of the $U(1)$ gauge background VEV A which can make the fermions violate parity and induce a chiral spectrum. Any globally well defined covariant (pseudo–)vector Ω (see Appendix B) can be parametrized in terms of a single function of τ, its ϕ component Ω_ϕ; Ω_τ being equal to zero. As for $\rho(\tau)$, there are some conditions on Ω_ϕ and its derivatives at $\tau = 0$ (see Eq. (B.0.10)). These conditions are automatically satisfied by the spin connection, once the appropriate local frame has been chosen. Starting from the metric in Eq. (4.1.4), it is straightforward to derive the 2-bein forms $\widehat{\theta}^\alpha$

$$\widehat{\theta}^\alpha = \left(e^{-i\phi\sigma_2}\right)^\alpha_{\ \beta} \widehat{\theta}^\beta_0 = \begin{pmatrix} \cos\phi d\tau - \sin\phi\rho(\tau)d\phi \\ \sin\phi d\tau + \cos\phi\rho(\tau)d\phi \end{pmatrix}, \tag{4.1.7}$$

and, by imposing the torsion-free condition in Eq. (1.6.10), find the associated spin connection

$$\omega = (1 - \dot{\rho}(\tau))d\phi\,. \tag{4.1.8}$$

Note that ω, as expected, becomes a pure gauge ($R = d\omega = 0$) for $\tau \geq \eta$, thanks to the condition (4.1.5). The LL Wilson line W_{LL} on fermions is immediately computed. It is $W_{LL} = e^{-\frac{i}{2}\oint\sigma_3\omega} = e^{-\pi i\sigma_3(1-\sin\alpha)}$, which precisely matches what is needed for reproducing the LL holonomy of the orbifold in Eq. (4.1.6). Since a vanishing field-strength background is present in the bulk, the gauge connection A must become a pure gauge for $\tau \geq \eta$:

$$A(\tau) \equiv \frac{\kappa}{2}(1 - \sin\alpha)d\phi\,, \qquad \kappa = \frac{p + 2Nq}{N-1}\,, \tag{4.1.9}$$

where κ has been chosen so that $W_{gauge} = e^{-i\oint A}$ satisfies Eq. (4.1.6). An arbitrary integer "monopole" charge q, to whose presence the holonomy is insensitive, has been included in Eq. (4.1.9). When a concrete example of resolution will be needed, the gauge connection A will be taken to be proportional to ω: $A = \kappa/2\omega$.

Summarizing, the general resolution of the orbifold model is parametrized by two arbitrary functions, $\rho(\tau)$ and $A_\phi(\tau)$, constrained to satisfy Eq.s (B.0.8), (4.1.5), (B.0.10) and (4.1.9). The resulting space, with its gauge field background, is equivalent by construction to the $\mathbb{C}/\mathbf{Z}_N$ orbifold for $\tau \geq \eta$. The precise relation between fermion fields on $\mathcal{R}$ and the orbifold ones is given by

$$\psi_c(\tau_c, \theta) = e^{\frac{i}{2}(N-1)(\kappa+\sigma_3)\theta}\psi(\tau_c - \tau_c^0, N\theta)\,. \tag{4.1.10}$$

Clearly, Eq. (4.1.10) makes a non–trivial twist under $\theta \to \theta + 2\pi/N$ appear in ψ_c which precisely matches Eq. (4.1.2). Note that all the results of the present section are based on necessity arguments. Some checks have been performed in [38] that the resolved theory really mimic, at energy much below the resolution scale $1/\eta$, the orbifold one.

Given the 2-beins in Eq. (4.1.7), the Dirac equation is easily written

$$\begin{cases} \partial_\tau \psi_L - \frac{i}{\rho(\tau)}\left[\partial_\phi + i(A_\phi - \frac{1}{2}\omega_\phi)\right]\psi_L = -ime^{i\phi}\psi_R \\ \partial_\tau \psi_R + \frac{i}{\rho(\tau)}\left[\partial_\phi + i(A_\phi + \frac{1}{2}\omega_\phi)\right]\psi_R = -ime^{-i\phi}\psi_L \end{cases}, \tag{4.1.11}$$

and displays its invariance under $SO(2)$ Lorentz transformations, acting as

$$\phi \to \phi - \beta\,, \qquad \psi \to e^{\frac{i}{2}\beta\sigma_3}\psi\,. \tag{4.1.12}$$

The operator $i\partial_\phi - \sigma_3/2$, which generates the above symmetry, can be diagonalized with real eigenvalues on the space of solutions to the Dirac equation. Therefore, one can look at solutions of the form

$$\psi_R = e^{in\phi} f_R(\tau)\,, \qquad \psi_L = e^{i(n+1)\phi} f_L(\tau)\,, \tag{4.1.13}$$

with n integer. For $m = 0$, the symmetry of the Dirac equation is enhanced, since it becomes invariant under $\psi \to e^{i\beta\sigma_3}\psi$ transformations also. One can simultaneously diagonalize the σ_3 and $i\partial_\theta$ operators and the ansatz in this case is more general:

$$\psi_{L,R} = f_{L,R}(\tau) e^{in_{L,R}\phi}\,, \tag{4.1.14}$$

with $n_{L,R}$, of course, integers. Let us consider now the massless Dirac equation, whose solutions will provide us the wave function in the internal space of the massless $4D$ zero–modes. With the ansatz (4.1.13), Eq. (4.1.11) becomes

$$\begin{cases} \partial_\tau \log f_R = \frac{1}{\rho(\tau)}\left[n_R + A_\phi + \frac{1}{2}\omega_\phi\right] \\ \partial_\tau \log f_L = -\frac{1}{\rho(\tau)}\left[n_L + A_\phi - \frac{1}{2}\omega_\phi\right] \end{cases}. \tag{4.1.15}$$

It is impossible, of course, to integrate Eq. (4.1.15) without specifying a particular shape of $\rho(\tau)$ and $A_\phi(\tau)$. The behavior of the solutions for $\tau \sim 0$ and $\tau \geq \eta$, however, is universal, since universal is the form of ρ and A_ϕ in these regions. For $\tau \sim 0$, $\rho(\tau) \sim \tau$, $A_\phi(\tau) \sim 0$ and Eq. (4.1.15) approximates the one on the $\mathbb{C}$. The solutions at $\tau \sim 0$ behave then as

$$f_R(\tau) \sim \tau^{n_R}\,, \qquad f_L(\tau) \sim \tau^{-n_L}\,,$$

which means the only well-behaved solutions to be those with

$$n_R \geq 0\,, \qquad n_L \leq 0\,. \tag{4.1.16}$$

In the $\tau \geq \eta$ region, $\rho \equiv \sin\alpha(\tau + \tau_c^0)$, $A_\phi \equiv \kappa/2(1 - \sin\alpha)$. Eq. (4.1.15) then becomes, in the coordinate $\tau_c = \tau + \tau_c^0$, the Dirac equation on the cone, whose solutions are, up to a multiplicative constant

$$f_R = {\tau_c}^{\lambda_R}\,, \qquad f_L = {\tau_c}^{-\lambda_L}\,, \tag{4.1.17}$$

with the integers $\lambda_{L,R}$ defined as

$$\begin{aligned} \lambda_R = \lambda_R(n_R) &= \tfrac{1}{\sin\alpha}(n_R + \tfrac{k+1}{2}(1 - \sin\alpha)) = \tfrac{p+N-1}{2} + N(n_R + q)\,, \\ \lambda_L = \lambda_L(n_L) &= \tfrac{1}{\sin\alpha}(n_L + \tfrac{k-1}{2}(1 - \sin\alpha)) = \tfrac{p-(N-1)}{2} + N(n_L + q)\,, \end{aligned} \tag{4.1.18}$$

where the angular momenta $n_{L,R}$ are subject to the conditions (4.1.16). If we do not impose normalizability to our wave-functions, there are an infinite number of solutions to the Dirac equation, depending on the values of λ_L and λ_R. If we consider those which do not diverge at infinity, one has

$$\begin{aligned} n_L &\geq (\sin\alpha - 1)\frac{\kappa - 1}{2} = -\frac{1}{2N}(p - N + 1) - q\,, \\ n_R &\leq (\sin\alpha - 1)\frac{\kappa + 1}{2} = -\frac{1}{2N}(p + N - 1) - q\,. \end{aligned} \tag{4.1.19}$$

When $n_{L,R}$ reach the bounds of the above inequalities, in the orbifold limit $\eta \longrightarrow 0$, the corresponding wave function is constant on the cone. Constant solutions are peculiar as they correspond to the usual constant zero modes of the $\mathbb{C}/\mathbf{Z}_N$ orbifold; they do not always arise depending on the value of p, as expected from Eq. (4.1.2), but also on the sign of q. The bounds of the inequalities in Eq. (4.1.19) can be reached if $p = N-1$ and $q \geq 0$ for left-handed states or $p = -N+1$ and $q \leq 0$ for right-handed states. These values of p are precisely those required for the orbifold projection given in Eq. (4.1.2) to leave untwisted the left- and right-handed states respectively, in such a way that the corresponding zero mode is present. The non-constant solutions are those for which the strict inequalities are satisfied in Eq. (4.1.19). For $q > 0$, q left-handed states of this kind are present, and no right-handed ones. For $q < 0$, we have $-q$ right-handed states and no left-handed ones. For $q = 0$, no non-constant state can be present.

We see that, as expected, different choices of the integer q, which was not fixed by the general discussion of the previous subsection, correspond to a different number of (non-divergent at infinity) zero modes on the resolution of the orbifold. What is important to notice is that the extra states which are introduced by the presence of the integer q have a power-like divergence at $\tau = \eta$ when the orbifold limit $\eta \to 0$ is taken. Moreover, in any case but when $|p|$ is maximum and q has the "wrong" sign, they are bound states, which can be normalized on the resolved cone. They correspond then to states which are *localized* at the fixed point of the orbifold which, surprisingly enough, *naturally* arise when resolving the singularity.

4.2 Resolution of $T^2/\mathbf{Z}_N$

Let us consider now the compact $T^2/\mathbf{Z}_N$ orbifolds, defined in Sect. 2.3. In this section, a resolved version $\mathcal{R}_N$ of $T^2/\mathbf{Z}_N$ is constructed, and the massless Dirac equation studied on it. Localized states are shown to arise at the resolved fixed points, in a number which depends on the integer monopole charges $q_{l,i}$ one is allowed to put at the resolved fixed points. The resulting bulk–brane field distributions is derived.

4.2.1 The resolving space

As in Sect. 2.3, $T^2/\mathbf{Z}_N$ orbifolds are defined from the complex plane $\mathbb{C}$ by modding out translations and $2\pi/N$ rotations. We will take $R = \frac{1}{\sqrt{2\pi}}$ in Eq. (2.3.1) and consider a spinor field ψ on $T^2/\mathbf{Z}_N$ subjected to the generalized periodicity conditions

$$\psi(z+1) = T_1\psi(z)\,, \qquad \psi(z+U) = T_U\psi(z)\,, \qquad T_{1,U} \equiv e^{\frac{2\pi i}{N}t_{1,U}}\,, \tag{4.2.1}$$

with $T_{1,U} \in U(1)$ are discrete Wilson lines, subjected to Eq.s (2.3.8, 2.3.10) with Z_N replaced by the orbifold twist matrix $\mathcal{P}$ defined by

$$\psi(\tau z) = \mathcal{P}\psi(z)\,, \qquad \mathcal{P} \equiv e^{\pi i(1-\frac{1}{N})\sigma_3}e^{\frac{\pi i}{N}p}\,. \tag{4.2.2}$$

Consistency conditions (2.3.8) and (2.3.10) require constraints on the allowed values of $t_{1,U}$ and p in Eq. (4.2.1) and (4.2.2). For $T^2/\mathbf{Z}_2$ one needs $p = \pm 1$, $t_{1,U} = 0, 1$. For $T^2/\mathbf{Z}_3$, p is in the $-2, 0, 2$ range while $t_1 = t_U = 0, 1, 2$. In the $T^2/\mathbf{Z}_4$ case, one has $p = \pm 3, \pm 1$ and $t_1 = t_U = 0, 1$. For $T^2/\mathbf{Z}_6$, finally, $t_1 = t_U = 0$ and $p = \pm 5, \pm 3, \pm 1$. Consider now the physically distinguished l–fixed points $z_{l,i}$ of $T^2/\mathbf{Z}_N$, with $l = 1, \ldots, [N/2]$ and $i = 1, \ldots, F_l$, with the notation of Sect. 2.3. At each fixed point $z_{l,i}$, the orbifold has a conical $\mathbb{C}/\mathbf{Z}_{N/l}$ singularity, as it can be seen from Fig. 2.1 by computing the deficit angle. The twist matrix which characterizes the singularity is the effective orbifold twist $\mathcal{P}_{l,i}$

$$\begin{aligned}\psi(z_{l,i}+\tau^l z) &= \psi(\tau^l(z_{l,i}+z)+m_i+n_iU)\\ &= T_1^{m_i}T_U^{n_i}\mathcal{P}^l\psi(z_{l,i}+z) \equiv \mathcal{P}_{l,i}\psi(z_{l,i}+z)\,,\end{aligned}$$

i.e. the transformation matrix of orbifold fields under $2\pi l/N$ rotations around $z_{l,i}$. Clearly, ${\mathcal{P}_{l,i}}^{N/l}=1$ by consistency.

A resolution $\mathcal{R}_N$ of each $T^2/\mathbf{Z}_N$ orbifold is easily constructed by removing small disks surrounding the singularities —which correspond, for each $z_{l,i}$ fixed point, to a truncated $\mathbb{C}/\mathbf{Z}_{N/l}$ orbifold with projection matrix $\mathcal{P}_{l,i}$— from the fundamental domain and replacing them with the appropriate resolving space, defined in Sect. 4.1. In this way, the resolution simply consists on a flat region, corresponding to the bulk, which connects various resolved cones that represent the singularities. Note that, since ${\mathcal{P}_{l,i}}^{N/l}=1$, the projection matrices can be written as

$$\mathcal{P}_{l,i} = e^{\pi i\left(1-\frac{l}{N}\right)\sigma_3}e^{\frac{\pi i}{N/l}p_{l,i}}\,,$$

with $p_{l,i}$ running from $-(N/l-1)$ to $N/l-1$ at steps of two. This matches the form (4.1.2) of the projection matrix, so that the results of the above section can be directly applied if identifying N and p with N/l and $p_{l,i}$, respectively. Clearly, as in Eq. (4.1.9), an arbitrary integer monopole charge $q_{l,i}$ can be put at each fixed point. As mentioned in Sect. 4.1, when $|p|$ is maximal the sign of q needs to be the same as p for the resolution correctly reproduce the constant zero–modes of the $\mathbb{C}/\mathbf{Z}_N$ orbifold, so that we will restrict here to this case. For each orbifold, the allowed configurations of effective projections $p_{l,i}$ are easily derived. In the $T^2/\mathbf{Z}_2$ case either, for $t_{1,U}=0$, all fixed points have the same twist $p=\pm1$ or, if at least one of $t_{1,U}$ is different from zero, two fixed points have the opposite twist then the other two. For $T^2/\mathbf{Z}_3$, similarly, either the twist for all fixed points is the same, $p_{1,i}=p=\pm2,0$, or they are all different, $p_{i,i}=(2,0,-2)$ or permutations. In the $T^2/\mathbf{Z}_4$ case one may have $p_{1,2}=p_{1,1}=p=\pm3,\pm1$ and $\mathcal{P}_{2,1}=\mathcal{P}^2$, and then $p_{2,1}=p+2\,\mathrm{Mod}(4)=(-1)^{(p+1)/2}$, or $p_{1,2}=-p_{1,1}=-p=\pm3,\pm1$, and $p_{2,1}=p\,\mathrm{Mod}(4)=(-1)^{(p-1)/2}$. For $T^2/\mathbf{Z}_6$, the only possibility is $p_{1,1}=p=\pm5,\pm3,\pm1$, $p_{2,1}=p+3\,\mathrm{Mod}(6)$ and $p_{1,1}=p\,\mathrm{Mod}(4)=(-1)^{(p-1)/2}$. In the following, the fermion zero–modes spectrum on the resolving space $\mathcal{R}_N$ will be derived. The index of the Dirac operator in Eq. (1.6.14), *i.e.* the number of L– minus the number of R–handed zero–modes, is easily computed on $\mathcal{R}_N$ by means of Eq. (4.1.9). One finds

$$\mathcal{I}\equiv n_L-n_R=\frac{1}{2\pi}\int F=\sum_{l,i}\frac{p_{l,i}}{2N/l}+\sum_{l,i}q_{l,i}\,, \tag{4.2.3}$$

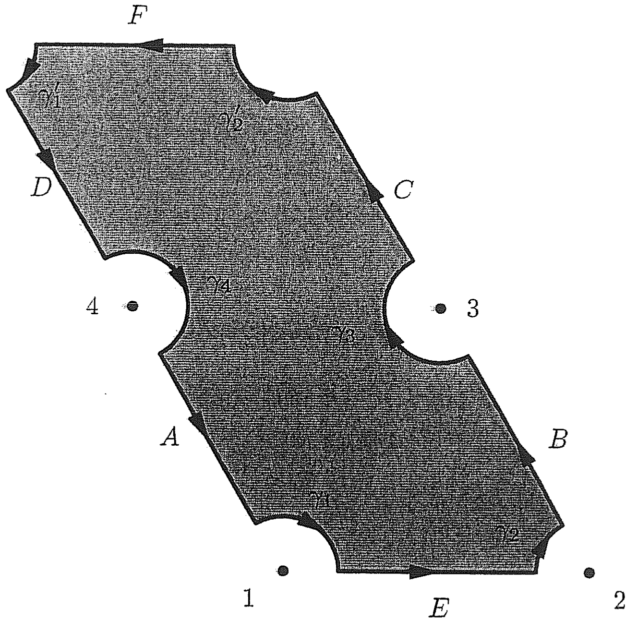

Figure 4.2: The fundamental domain in the complex plane of the $T^2/\mathbf{Z}_2$ orbifold with complex structure $\tau = e^{2\pi i/3}$. The location of the four fixed points is also shown. The fixed points have been removed by cutting infinitesimal disks away from the fundamental domain. Its edges are given by the six oriented lines shown in the figure. Each couple of lines is identified ($A \sim D$, $B \sim C$, $E \sim F$) due to torus+orbifold point identifications. Due to these identifications, the oriented curves γ_3, γ_4, $\gamma_1 + \gamma_1'$ and $\gamma_2 + \gamma_2'$ are closed and represent the boundaries of the "truncated" orbifold.

which is integer, for any allowed choice of $p_{l,i}$. Is worth noticing that the first term in Eq. (4.2.3) counts the orbifold bulk zero–modes, meaning that it is always zero but for $p = \pm(N-1)$ and $t_{1,U} = 0$, in which case its value is ± 1, in accordance with the orbifold projection (4.2.2) which leaves untwisted, respectively, the L–(R–)handed component of the fermion field.

4.2.2 The zero–modes

The fundamental domain of $T^2/\mathbf{Z}_N$ —from which infinitesimal disks have been removed in correspondence with the singularities, as shown in Fig. 4.2 for the $T^2/\mathbf{Z}_2$ case— constitutes the "bulk" of the resolving space $\mathcal{R}_N$ defined in the previous section. The massless Dirac equation in this region simply states (see Eq. (1.6.17)) the wave functions to be holomorphic ($\psi_R(z)$) and anti–holomorphic ($\psi_L(\bar{z})$). Define the circuit Γ, counter–clockwise oriented, as the boundary of the bulk region. It is composed by infinitesimal circular paths $\gamma_{l,i}$ around each $z_{l,i}$ fixed point, and completed by the segments, indicated in Fig.s 4.2 and 2.1 as $A \sim D$, $B \sim C$ (and $E \sim F$ in the $T^2/\mathbf{Z}_2$ case), which delimit the fundamental domain. Note that each segment is covered by Γ in the opposite direction then its "mirror", with which it is identified, and chiral fields at the two identified segments are proportional, as implied by Eq. (4.2.1) and (4.2.2). One then has

$$\frac{1}{2\pi i}\int_{A_2-A_1} dz\partial_z \log\left(\psi_R(z)\right) = -\frac{1}{2\pi i}\int_{A_2-A_1} d\bar{z}\partial_{\bar{z}} \log\left(\psi_L(\bar{z})\right) = 0\,,$$

for $(A_1, A_2) = (A, D), (B, C), (E, F)$. Therefore, if the above contour integral is performed on the whole closed path Γ, it only receives contributions from the $\gamma_{l,i}$ circular paths, which are all oriented clockwise and cover each a $2\pi/(N/l)$ plane angle. [1] At each fixed point $z_{l,i}$, the L– and R–handed wave functions behave as

$$\psi_R(z) \sim (z - z_{l,i})^{\lambda_R^{l,i}}\,, \qquad \psi_L(\bar{z}) \sim (\bar{z} - \bar{z}_{l,i})^{-\lambda_L^{l,i}}\,, \tag{4.2.4}$$

so that (see Eq. (4.1.17)) locally match the massless wave functions —with angular momenta $\lambda_{R,L} = \lambda_{R,L}^{l,i}$— on the resolved $\mathbb{C}/\mathbf{Z}_{(N/l)}$. The allowed values for $\lambda_{R,L}^{l,i}$ are then seen from Eq. (4.1.18) to be

$$\begin{array}{l} \lambda_R^{l,i} = \frac{p_{l,i}+N/l-1}{2} + N/l(n_R^{l,i} + q_{l,i})\,, \\ \lambda_L^{l,i} = \frac{p_{l,i}-(N/l-1)}{2} + N/l(n_L^{l,i} + q_{l,i})\,, \end{array} \tag{4.2.5}$$

with $n_{R,L}^{l,i}$, respectively, arbitrary positive and negative integers. By mean of Eq. (4.2.4), the contour integral on $\gamma_{l,i}$ is immediately computed, and one finds

$$\begin{array}{l} \frac{1}{2\pi i}\oint_\Gamma dz\partial_z \log\left(\psi_R(z)\right) = \frac{1}{2\pi i}\sum_{l,i}\int_{\gamma_{l,i}} dz\left(\frac{\psi_R'(z)}{\psi_R(z)}\right) = -\sum_{l,i}\frac{\lambda_R^{l,i}}{N/l} = b_R\,, \\ -\frac{1}{2\pi i}\oint_\Gamma d\bar{z}\partial_{\bar{z}} \log\left(\psi_L(\bar{z})\right) = -\frac{1}{2\pi i}\sum_{l,i}\int_{\gamma_{l,i}} d\bar{z}\left(\frac{\psi_L'(\bar{z})}{\psi_L(\bar{z})}\right) = \sum_{l,i}\frac{\lambda_L^{l,i}}{N/l} = b_L\,, \end{array} \tag{4.2.6}$$

where the theorem of residuals has been used to write the last equality. Having assumed the wave functions not to have poles in the bulk, the result is entirely given by the number $b_{R,L}$ of zeroes, counted with their multiplicity, of $\psi_{R,L}$ inside Γ. By means of Eq. (4.2.5), the condition (4.2.6) can be expressed as

$$\sum_{l,i} n_R^{l,i} = -b_R - \mathcal{I} - 1\,, \qquad \sum_{l,i} n_L^{l,i} = b_L - \mathcal{I} + 1\,, \tag{4.2.7}$$

with $\mathcal{I}$ as in Eq. (4.2.3). In the following, $b_{L,R} = 0$ will be assumed, and the assumption will be verified at the end, when the number of chiral zero–modes derived

[1] In the case in which two representatives of the same fixed point $z_{l,i}$ are present as two distinct corners of the fundamental domain, $\gamma_{l,i}$ must be thought as the union of two paths, each covering a $\pi/(N/l)$ angle, located at the two corners.

with $b_{L,R} = 0$ will be shown to be consistent with the known value of the index $\mathcal{I}$. If an additional (say, R–handed) state with $b_R > 0$ has to be present, since all $n_R^{l,i}$'s need to be positives, $\mathcal{I}$ would need to be smaller than $-1 - b_R$, which is incompatible with the existence of any "new" L–handed state with $b_L > 0$, whose presence is however required by the index theorem. Consider then Eq. (4.2.7) with $b_{L,R} = 0$. It implies that only L–(R–)handed states can be present on $\mathcal{R}_N$ if $\mathcal{I}$ is positive (negative). No R–handed and $\mathcal{I}$ L–handed states have then to appear if $\mathcal{I}$ is positive, no L–handed and $-\mathcal{I}$ R–handed if it is negative. The distinct solutions to Eq. (4.2.7), however, are much more then $|\mathcal{I}|$, meaning that not all of them are independent. One should be able to write down, for any solution to Eq. (4.2.7), the explicit form of the wave–function, identified by its behavior (4.2.4) at the fixed points, and check that, for any given value of $\mathcal{I}$, only $|\mathcal{I}|$ of them are linearly independent. This can be done in some explicit example for the $T^2/\mathbf{Z}_2$ case, the wave–functions being provided by suitable products and ratios of Jacobi theta functions, as discussed in [37]. Even though a mathematical proof is not available, the general criterion is that linearly independent wave–functions are only labelled by the degree and location of their pole of maximum degree. This is physically very reasonable since, in the orbifold limit, the wave function localizes at its maximum pole, and "local" quantities only, such as the angular momentum $\lambda_{L,R}^{l,i}$, can be relevant to label it. By using the above prescription, the location and number of zero–modes can be derived, for any $T^2/\mathbf{Z}_N$ orbifold and any allowed value of the twists $p_{l,i}$.

As an illustrative example of the procedure, consider the simple $T^2/\mathbf{Z}_2$ case, with $p_{1,i} = +1$ for any $i = 1, \ldots 4$. One has $\mathcal{I} = 1 + \sum_{i=1}^4 q_{1,i} > 0$, since all monopole charges must be positive, and then L–handed state only can appear. In this case Eq. (4.2.5) reads

$$\lambda_L^{1,i} = 2(n_L^{1,i} + q_{1,i})\,,$$

while Eq. (4.2.7) becomes

$$\sum_i (n_L^{1,i} + q_{1,i}) = 0\,. \tag{4.2.8}$$

Consider each fixed point separately; take $i = 1$ for definiteness. A state localized at $i = 1$ is found for any choice of $n_L^{1,i} \leq 0$, satisfying Eq. (4.2.8), such that $\lambda_L^{1,1} > 0$, all the other $\lambda_L^{1,i}$'s being smaller then that. Note that, having fixed a positive value for $\lambda_L^{1,1}$, several choices of $n_L^{2,3,4}$ satisfying the above constraints could be possible. Having assumed the physical states to be only labelled by the location and degree of their higher pole, however, just one must be counted among all these, so all what matters is that at least one of them exists. This is clearly the case for any $n_L^{1,1} = 0, \ldots, -q_{1,1} + 1$ (such that $\lambda_L^{1,1} > 0$) since one could take $\lambda_L^{1,i} = 0$ for $i = 2, 3$

and $\lambda_L^{1,4} = -\lambda_L^{1,1}$. Therefore, $q_{1,1}$ L–handed localized states have been found at $i = 1$ and, since the same holds for any i, $q_{1,i}$ states are found at each fixed point. One independent state only, the bulk one ($\lambda_L^{1,i} = 0$) escaped the above analysis. Note that, even if this does not occur in the present case, states which are *doubly localized* at two fixed points "1" and "2" can appear. States with equal angular momenta at two points $\lambda_L^{1,2} = \lambda_L$ are, in general, linear combination of two states, one localized at "1", the other at "2", with maximum poles of order λ_L. It happens, however, that such "singly" localized states at "1" and at "2" do not exist, for some value of λ_L. When this is the case, a new linearly independent doubly localized zero–mode must be take into account. In a straight–forward, but tedious way, all orbifolds with all twists could be discussed. The number of localized fermions at each fixed point, for different patterns of effective orbifold projections is summarized in Table 4.1 for the $T^2/\mathbf{Z}_{2,3,4}$ orbifolds. In the table, $\mathcal{I} \geq 0$ is assumed, so that all states are L–handed, but the spectrum of R–handed localized states one gets when $\mathcal{I} \leq 0$ is easily obtained by inverting the signs of $p_{l,i}$ and $q_{l,i}$. For $T^2/\mathbf{Z}_2$ and $T^2/\mathbf{Z}_3$, the result for the most general pattern of effective orbifold projection $p_{l,i}$ can be obtained from the table by interchanging the fixed points. For $T^2/\mathbf{Z}_4$, on the contrary, the absence of discrete Wilson line, $T_{1,U} = 1$ in Eq. (4.2.1), is assumed. The case $T_{1,U} = -1$, and the results for the $T^2/\mathbf{Z}_6$ orbifold as well, which are not shown, could be easily worked out. When looking at the table, the index theorem (4.2.3) may sometimes appear not to be respected, one state being missing, even thought the usual bulk zero–modes are correctly added to the counting. When this happens, a doubly localized state —which is not counted in the table— appears and makes the index theorem respected.

4.3 The "resolved" $S^1/\mathbf{Z}_2$ orbifold

The one–dimensional orbifold $S^1/\mathbf{Z}_2$, much more then the two–dimensional ones considered up to now, is of great phenomenological importance, since many models have been formulated in which it has been used to describe the internal dimension. Geometrically, $S^1/\mathbf{Z}_2$ is simply a line segment, and the two points of the circle which are fixed under the $\mathbf{Z}_2$ action are simply *boundaries* and then, differently from the two–dimensional cases considered up to now, are not singular points at all. At the purely geometrical level, therefore, there is no reason for trying to replace $S^1/\mathbf{Z}_2$ with some "smoothed version" of it. Thought doubts could be aroused on the full consistency of field theories on a segment, one may argue that these technicalities

	1	2	3	4
$(1,1,1,1)$	$\lvert q_{1,1}\rvert$	$\lvert q_{1,2}\rvert$	$\lvert q_{1,3}\rvert$	$\lvert q_{1,4}\rvert$
$(1,1,-1,-1)$	$\left[\frac{\mathcal{I}+\lvert q_{1,1}\rvert-\lvert q_{1,2}\rvert-1}{2}\right]_-$	$\left[\frac{\mathcal{I}+\lvert q_{1,2}\rvert-\lvert q_{1,1}\rvert-1}{2}\right]_-$	0	0

$(2,2,2)$	1	2	3
	$\lvert q_{1,1}\rvert$	$\lvert q_{1,2}\rvert$	$\lvert q_{1,3}\rvert$

$(0,0,0)$	1	2	3
$q_{1,1}=\lvert q_{1,1}\rvert$, $q_{1,2}=\lvert q_{1,2}\rvert$, $q_{1,3}=\lvert q_{1,3}\rvert$	$\lvert q_{1,1}\rvert$	$\lvert q_{1,2}\rvert$	$\lvert q_{1,3}\rvert$
$q_{1,1}=\lvert q_{1,1}\rvert$, $q_{1,2}=\lvert q_{1,2}\rvert$, $q_{1,3}=-\lvert q_{1,3}\rvert$	$\left[\frac{\mathcal{I}+\lvert q_{1,1}\rvert-\lvert q_{1,2}\rvert-1}{2}\right]_-$	$\left[\frac{\mathcal{I}+\lvert q_{1,2}\rvert-\lvert q_{1,1}\rvert}{2}\right]_-$	0
$q_{1,1}=\lvert q_{1,1}\rvert$, $q_{1,2}=-\lvert q_{1,2}\rvert$, $q_{1,3}=-\lvert q_{1,3}\rvert$	0	0	$\mathcal{I}$

$(2,0,-2)$	1	2	3
$q_{1,1}=\lvert q_{1,1}\rvert$, $q_{1,2}=\lvert q_{1,2}\rvert$, $q_{1,3}=-\lvert q_{1,3}\rvert$	$\left[\frac{\mathcal{I}+\lvert q_{1,1}\rvert-\lvert q_{1,2}\rvert+1}{2}\right]_-$	$\left[\frac{\mathcal{I}+\lvert q_{1,2}\rvert-\lvert q_{1,1}\rvert-1}{2}\right]_+$	0
$q_{1,1}=\lvert q_{1,1}\rvert$, $q_{1,2}=-\lvert q_{1,2}\rvert$, $q_{1,3}=-\lvert q_{1,3}\rvert$	$\mathcal{I}$	0	0

$(3,3,1)$	$1,1$	$1,2$	$2,1$
	$\lvert q_{1,1}\rvert$	$\lvert q_{1,2}\rvert$	$\lvert q_{2,1}\rvert$

$(1,1,-1)$	$1,1$	$1,2$	$2,1$
$q_{1,1}=\lvert q_{1,1}\rvert$, $q_{1,2}=\lvert q_{1,2}\rvert$, $q_{2,1}=-\lvert q_{2,1}\rvert$	$\left[\frac{\mathcal{I}+\lvert q_{1,1}\rvert-\lvert q_{1,2}\rvert-1}{2}\right]_-$	$\left[\frac{\mathcal{I}+\lvert q_{1,2}\rvert-\lvert q_{1,1}\rvert-1}{2}\right]_-$	0
$q_{1,1}=\lvert q_{1,1}\rvert$, $q_{1,2}=-\lvert q_{1,2}\rvert$, $q_{2,1}=-\lvert q_{2,1}\rvert$	$\mathcal{I}$	0	0

$(-1,-1,1)$	$1,1$	$1,2$	$2,1$
$q_{1,1}=\lvert q_{1,1}\rvert$, $q_{1,2}=\lvert q_{1,2}\rvert$, $q_{2,1}=\lvert q_{2,1}\rvert$	$\lvert q_{1,1}\rvert$	$\lvert q_{1,2}\rvert$	$\lvert q_{2,1}\rvert$
$q_{1,1}=\lvert q_{1,1}\rvert$, $q_{1,2}=-\lvert q_{1,2}\rvert$, $q_{2,1}=\lvert q_{2,1}\rvert$	$\left[\frac{2\mathcal{I}-2\lvert q_{1,1}\rvert+\lvert q_{2,1}\rvert-1}{3}\right]_-$	0	$\left[\frac{\mathcal{I}+2\lvert q_{1,1}\rvert-\lvert q_{2,1}\rvert-2}{3}\right]_-$
$q_{1,1}=-\lvert q_{1,1}\rvert$, $q_{1,2}=-\lvert q_{1,2}\rvert$, $q_{2,1}=\lvert q_{2,1}\rvert$	0	0	$\mathcal{I}$

Table 4.1: Number of fermions localized at the various fixed points for $T^2/\mathbf{Z}_{2,3,4}$. When a number in the table is negative, it has to be replaced with 0, while the other non-vanishing number on the same raw must be replaced with $\mathcal{I}$. The symbols $[\ldots]_\pm$ are used; $[x]_-$ is the usual integer part of x corresponding, when the argument is positive, to the maximum integer which is smaller or equal then x; $[x]_+$, on the contrary, is the minimum integer which is greater or equal then x.

do not signal any physical need of resolving the orbifold effective theory, which may be considered as it is. The approach followed here, however, is weakly related to the above considerations. The resolution may just be seen as a mechanism for the localization of fermions, that will be shown to take place in this case as in the two–dimensional ones. The final result will consist on a list of "special" brane fermion distributions, to be eventually studied in the unresolved orbifold theory, which can be obtained from considering $S^1/\mathbf{Z}_2$ as a limit of a boundaryless $2D$ space. Clearly, introducing one more dimension in the resolving theory slightly restricts the class of $5D$ models one can treat. Only those can be considered whose field content can be interpreted as arising from a $6D$ model. $5D$ Dirac fields will be reproduced by starting from chiral $6D$ spinors.

4.3.1 The resolving space

Let us consider a $T^2/\mathbf{Z}_2$ orbifold with complex structure $U = it$ (t real) and fermions periodic for $z \to z + U$ (*i.e.*, no Wilson line around the U cycle). In the degenerate limit $t \to 0$, this theory degenerates to a one dimensional $S^1/\mathbf{Z}_2$ orbifold with periodic (if $t_1 = 0$ in Eq. (4.2.1)) or anti-periodic (if $t_1 = 1$) fermions on the covering circle S^1. In this limit, the two-dimensional orbifold (see Fig. 4.3) becomes a one-dimensional segment, where the z_1 and z_4, as well as the z_2 and z_3, fixed points collapse to a single point. The space $\mathcal{C}$ which resolves the $S^1/\mathbf{Z}_2$ segment is then taken to be a $2D$ compact "cigar-like" surface (see Fig. 4.3) which resembles, in a certain region, a finite portion of a cylinder of radius r. The cylinder becomes, in the orbifold limit in which r shrinks to zero, a line segment which reproduces the bulk of $S^1/\mathbf{Z}_2$. The rest of the space consists on two disconnected regions and each of them will shrink to a point in the orbifold limit. They provide the resolved description of the orbifold fixed points. The topology of $\mathcal{C}$ is assumed to be as simple as possible, *i.e* the one of the sphere. Namely, each fixed point will be described by a single chart, the overlapping of the two being provided by the cylinder. Moreover, the $O(2)$ isometry group of the cylinder is taken to be the isometry of the whole space. The results of Appendix B can then be applied in each coordinate system, and the metric parametrized as

$$(ds^2)_i = d\tau_i{}^2 + \rho_i{}^2(\tau_i) d\phi_i{}^2 \,, \qquad (4.3.1)$$

where $\phi_{1,2}$ are angles and $\tau_{1,2}$ both run in the $[0, L-\eta]$ interval, being L the total "length" of $\mathcal{C}$, *i.e.* the distance between its two "poles" $\tau_1 = 0$ and $\tau_2 = 0$. The two coordinate systems are related by $\tau_2 = L - \tau_1$ and $\phi_2 = -\phi_1$ in the overlapping

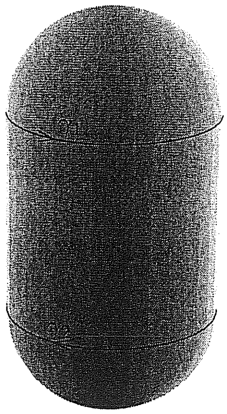

Figure 4.3: The cigar-like surface $\mathcal{C}$, which reproduces the $S^1/\mathbf{Z}_2$ orbifold when the radius r goes to zero. The oriented curves $\gamma_{1,2}$, corresponding to $\tau_{1,2} = \eta$, are also shown.

region $\tau_i \in [\eta, L - \eta]$ which parametrizes the cylinder. The resolved fixed points are described by the two disconnected regions $\tau_{1,2} \in [0, \eta]$, and the orbifold limit consists on taking $\eta \longrightarrow 0$. Since each (τ_i, ϕ_i) coordinate system is ill–defined at $\tau_i = 0$, $\rho_i(\tau_i)$ and its derivatives must satisfy certain conditions at $\tau_i = 0$, summarized in Eq. (B.0.8), ensuring that no physical singularity is present at that point. Moreover, since Eq. (4.3.1) must reduce to the flat cylinder metric: $\rho_{1,2}(\tau_i) \equiv \rho_{1,2}(\eta) \equiv r$ for $\tau_i \geq \eta$. As a particular class of $\mathcal{C}^\infty$ profiles for ρ_i, consider

$$\rho_i(\tau_i) = \int_0^{\tau_i} d\tau \left[e^{\delta^2 \left(\frac{1}{\eta^2} + \frac{1}{\tau^2 - \eta^2} \right)} \right] . \tag{4.3.2}$$

Be ψ a spinor field on $\mathcal{C}$. It will be described, in each coordinate system, by single–valued functions, so that its holonomy on circles wrapping around the cylinder is entirely given by the appropriate Wilson loop. The Local-Lorentz part of the holonomy is easily computed: $W_{LL} = e^{-\pi i \sigma_3} = -1$. The total holonomy needs to be the identity, if some light state has to survive when the orbifold limit is taken. A non trivial gauge background A^i ($i = 1, 2$ labels the two coordinate systems) must then be included to generate a gauge holonomy $W_{gauge} = -1$. This background, as usual, is assumed to be $O(2)$ invariant and then (see Appendix B) it has the form $A^i = A^i_{\phi_i}(\tau_i) d\phi_i$, and is subjected to the conditions (B.0.10) at $\tau_i = 0$. Moreover, A^i must to reduce to a pure gauge for $\tau_i \geq \eta$,

$$A^i = \frac{\tilde{\kappa}_i}{2} d\phi_i \, , \tag{4.3.3}$$

where $\tilde{\kappa}_i$ needs to be an odd integer if requiring $W_{gauge} = e^{-i \oint A} = -1$. Having chosen $A^{1,2}$ in Eq. (4.3.3), the gauge + LL transformations relating, on the cylinder, the representations of the fermion field in the two coordinate systems is fixed to be

$$\psi^2(L-\tau_1,-\phi_1) = e^{i\left(\sigma_3+\frac{\tilde{\kappa}_1+\tilde{\kappa}_2}{2}\right)\phi_1} e^{-i\frac{\pi}{2}\sigma_3}\psi^1(\tau_1,\phi_1)\,. \tag{4.3.4}$$

The Dirac equation on $\mathcal{C}$ is given, in each coordinate system, by Eq. (4.1.11) and, as in Eq. (4.1.13), its $SO(2)$ invariance can be used to parametrize the ϕ_i–dependence of massive states as

$$\psi_R^i = f_R^i(\tau_i)e^{in_i\phi_i}\,, \qquad \psi_L^i = f_L^i(\tau_i)e^{i(n_i+1)\phi_i}\,. \tag{4.3.5}$$

In the massless case, as in Eq. (4.1.14), the ansatz is

$$\psi_{L,R}^i = f_{R,L}^i(\tau_i)e^{in_{L,R}^i\phi_i}\,, \tag{4.3.6}$$

with $n_{L,R}^i$, and n_i, integers.

4.3.2 Zero-modes

With the ansatz (4.3.6), the massless Dirac equation (4.1.11) reads

$$\begin{cases} \partial_{\tau_i}\log f_R^i = \frac{1}{\rho_i(\tau_i)}\left[n_R^i + A_\phi^i + \frac{1}{2}\omega_\phi\right] \\ \partial_{\tau_i}\log f_L^i = -\frac{1}{\rho_i(\tau_i)}\left[n_L^i + A_\phi^i - \frac{1}{2}\omega_\phi\right] \end{cases}. \tag{4.3.7}$$

At $\tau_i \sim 0$ it reduces to the $\mathbb{C}$–plane one. In that limit, the solutions then behave as

$$f_R^i \sim \tau^{n_R^i}\,, \qquad f_L^i \sim \tau^{-n_L^i}\,,$$

meaning that the only states to be considered have $n_R^i \geq 0$ and $n_L^i \leq 0$. Clearly, $n_{L,R}^2$ must be expressed in terms of $n_{L,R}^1$, if the two wave functions $\psi_{L,R}^i$ have to describe, on the cylinder, the same fermion state. According to Eq. (4.3.4), one has

$$n_R^2 = -\left(n_R^1 + \frac{\tilde{\kappa}_1+\tilde{\kappa}_2}{2} + 1\right), \qquad n_L^2 = -\left(n_L^1 + \frac{\tilde{\kappa}_1+\tilde{\kappa}_2}{2} - 1\right).$$

Imposing $n_R^2 \geq 0$, $n_L^2 \leq 0$ then implies an upper bound for the allowed values of n_R^1 and a lower one for n_L^1. Therefore, it is

$$0 \leq n_R^1 \leq -\frac{\tilde{\kappa}_1+\tilde{\kappa}_2}{2} - 1\,, \qquad -\frac{\tilde{\kappa}_1+\tilde{\kappa}_2}{2} + 1 \leq n_L^1 \leq 0\,, \tag{4.3.8}$$

so that $|(\tilde{\kappa}_1+\tilde{\kappa}_2)/2|$ zero modes, L–handed if $(\tilde{\kappa}_1+\tilde{\kappa}_2)/2$ is positive, R–handed if it is negative, are found on $\mathcal{C}$. This is in agreement with what results from applying the Atiyah–Singer index theorem. Besides of the chirality and number of the zero-modes, their wave function on the cylinder (*i.e.* in the bulk) can also be computed, regardless to the detailed profile of $\mathcal{C}$, since the bulk equation is universal. In the $i=1$ coordinate system, for $\tau_1 \geq \eta$, the solutions have the form

$$\left\{ \begin{array}{l} f_R^1(\tau_1) = A_R e^{\frac{\lambda_R^1}{r}\tau_1} \\ f_L^1(\tau_1) = A_L e^{-\frac{\lambda_L^1}{r}\tau_1} \end{array} \right. , \tag{4.3.9}$$

where $\lambda_R^1 = n_R^1 + \frac{1}{2}(\tilde{\kappa}_1 + 1)$, $\lambda_L^1 = n_L^1 + \frac{1}{2}(\tilde{\kappa}_1 - 1)$. The solutions in the $i=2$ coordinates are easily obtained by transforming Eq. (4.3.9) according to Eq. (4.3.4). The bulk profile of the R-handed states, then, is localized at $\tau_1 = \eta$ (the "1" fixed point) if $\lambda_R^1 < 0$, at $\tau_1 = L - \eta$ (the "2" fixed point) if $\lambda_R^1 > 0$. The contrary holds for the L-handed ones. The usual constant orbifold bulk zero mode is obtained for $\lambda_{L,R}^1 = 0$.

The fermion spectrum on $\mathcal{C}$ is summarized in Table 4.2, and agrees with what found in [37] where $\mathcal{C}$ was assumed to be composed by two halves–spheres connected by a cylinder. Note that the presence of one (L– or R–handed) bulk zero mode is not automatic. It only arises when the two gauge fluxes $\tilde{\kappa}_{1,2}$ have the same sign, its chirality depending on this sign. This case is considered in the upper part of Table 4.2 and corresponds, in the orbifold limit, to a model on $S^1/\mathbf{Z}_2$ in which the L–handed component of the spinor is taken to be even (if $\tilde{\kappa}_{1,2} > 0$), or odd (if $\tilde{\kappa}_{1,2} < 0$). In the other case considered in the table, on the contrary, no bulk zero–mode is present. It corresponds then to fermions which are antiperiodic on the S^1 circle. This is the same as considering a fermion on the segment with, at the "1" extreme, Neumann ($\partial\phi = 0$) and Dirichlet ($\phi = 0$) boundary conditions, respectively, for the L– and R–handed components; the opposite at "2". The case $\tilde{\kappa}_1 < 0$, $\tilde{\kappa}_1 > 0$ is obtained from Table 4.2 by interchanging the two fixed points. These correspondences, which can be checked here at the level of bulk zero–modes only, will be verified in the following section, when bulk massive states will be studied. The mass–spectrum and the wave–functions will be shown to reproduce, once the orbifold limit is taken, the ones on the segment with the appropriate boundary conditions.

4.3.3 Massive states

With the ansatz (4.3.5), the Dirac equation becomes

$$\left\{ \begin{array}{l} \partial_{\tau_i}(if_L^i) + \frac{1}{\rho_i(\tau_i)}\left[n_i + 1 + (A_{\phi_i}^i - \frac{1}{2}\omega_{\phi_i}^i)\right](if_L^i) = mf_R^i \\ \partial_{\tau_i}f_R^i - \frac{1}{\rho_i(\tau_i)}\left[n_i + (A_{\phi_i}^i + \frac{1}{2}\omega_{\phi_i}^i)\right]f_R^i = -m(if_L^i) \end{array} \right. , \tag{4.3.10}$$

$\tilde{\kappa}_{1,2} > 0$	$\tilde{\kappa}_{1,2} < 0$
$(\|\tilde{\kappa}_1\| - 1)/2$ L at "1"	$(\|\tilde{\kappa}_1\| - 1)/2$ R at "1"
1 L in the bulk	1 R in the bulk
$(\|\tilde{\kappa}_2\| - 1)/2$ L at "2"	$(\|\tilde{\kappa}_2\| - 1)/2$ R at "2"

$\tilde{\kappa}_1 > 0,\ \tilde{\kappa}_2 < 0$		
$\tilde{\kappa}_1 + \tilde{\kappa}_2 > 0$	$\tilde{\kappa}_1 + \tilde{\kappa}_2 = 0$	$\tilde{\kappa}_1 + \tilde{\kappa}_2 < 0$
$\|\tilde{\kappa}_1 + \tilde{\kappa}_2\|/2$ L at "1"		$\|\tilde{\kappa}_1 + \tilde{\kappa}_2\|/2$ R at "2"

Table 4.2: Fermion zero–modes spectrum on the resolved $S^1/\mathbf{Z}_2$ orbifold for different choices of the gauge fluxes $\tilde{\kappa}_{1,2}$. The chirality and the location of the states are indicated.

and, clearly, cannot be solved until the shape of $\rho_i(\tau_i)$ and $A_{\phi_i}(\tau_i)$ is not specified. At $\tau_i \sim 0$, however, it simply reduces to the $\mathbb{C}$–plane one and its regular solutions can be expressed, for $\tau_1 \ll \eta$, as

$$f_R^i = \mathcal{N}_i\, J_n(m\tau_i)\,, \qquad f_L^i = \mathcal{N}_i\, J_{n+1}(m\tau_i)\,, \tag{4.3.11}$$

where $J_n(z)$ are the first kind Bessell functions, with the conventions of [60]. At $\tau_i \geq \eta$, on the contrary, the equations become those on the cylinder, and the solution assumes the form

$$\begin{aligned} f_R^i &= \alpha_i e^{i\omega_i\tau_i} + \beta_i e^{-i\omega\tau_i}\,, \\ i f_L^i &= \alpha_i \left(\tfrac{\lambda_i}{mr} - \tfrac{i\omega_i}{m}\right) e^{i\omega_i\tau_i} + \beta_i \left(\tfrac{\lambda_i}{mr} + \tfrac{i\omega_i}{m}\right) e^{-i\omega_i\tau_i}\,, \end{aligned} \tag{4.3.12}$$

having defined the integers $\lambda_i = n_i + \frac{(\tilde{\kappa}_i+1)}{2}$ and $\omega_i^2 = m^2 - {\lambda_i}^2/r^2$, which can be either positive or negative, having neglected the case $\omega_i = 0$. The coefficients $\alpha_{1,2}$ and $\beta_{1,2}$ entering in Eq. (4.3.12) are determined by the evolution of the solution, due to Eq. (4.3.10), from the initial condition (4.3.11) at $\tau_i = 0$, to $\tau_i = \eta$. They are then fixed by the $\mathcal{N}_{1,2}$ coefficients appearing in Eq. (4.3.11). A profile–independent approach to the computation of the wave functions cannot be followed and a definite class of "trial" profiles must be used. The C^∞ profiles of Eq. (4.3.2), labelled with the real parameter δ, will be considered, and a gauge connection $A^i = \frac{\kappa_i}{2}\omega^i$ will be employed. The results which follow have been verified to depend weakly on δ, the strict limit $\eta \longrightarrow 0$ being completely resolution–independent. From now on, the case $\delta = \eta$ will be considered. Eq. (4.3.10) is numerically solved from 0 to η, for any given value of the mass–parameter m. The solutions are found in the two coordinate sets, up to the constant multiplicative factors $\mathcal{N}_{1,2}$, by considering Eq. (4.3.11) with

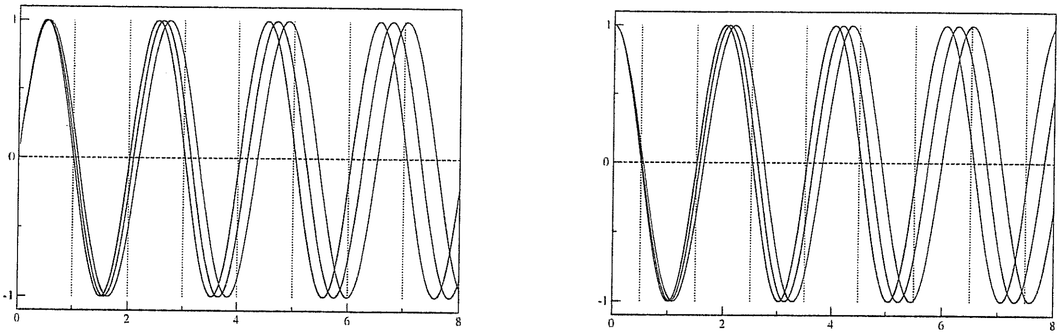

Figure 4.4: The function $\sigma(m)$, whose zeros give the mass–spectrum on $\mathcal{C}$, is plotted versus mL/π. On the left, the case $\tilde{\kappa}_1 = 1$, $\tilde{\kappa}_2 = 3$ and $n_1 = 1$, for three different choices of the resolution parameter $\eta = L/10, L/20, L/100$. On the right, $\tilde{\kappa}_1 = 1$, $\tilde{\kappa}_2 = -3$ and $n_1 = 1$, for $\eta = L/10, L/20, L/100$

$\mathcal{N}_{1,2} = 1$ as the initial condition at $\tau_i = 0$. [2] The parameters $\alpha_{1,2}$ and $\beta_{1,2}$ of Eq. (4.3.12) are then determined by continuity, and the two wave–functions on the cylinder are found. Since the two must describe a single spinor field on $\mathcal{C}$, however, they must be related by Eq. (4.3.4), which implies $n_{1,2}$ to be related as

$$n_2 = -n_1 - 1 - \frac{(\tilde{\kappa}_1 + \tilde{\kappa}_2)}{2}, \tag{4.3.13}$$

and consequently $\lambda_2 = -\lambda_1 \equiv \lambda$, $\omega_1 = \omega_2 \equiv \omega$, but also

$$\begin{aligned} f_R^2(L - \tau_1) &\equiv \gamma f_R^1(\tau_1)\,, \\ i f_L^2(L - \tau_1) &\equiv -\gamma i f_L^1(\tau_1)\,, \end{aligned} \tag{4.3.14}$$

for some proportionality factor γ. Note that, once Eq. (4.3.13) is imposed, the solution in each coordinate system is uniquely determined for any given n_1, up to the rescaling $\mathcal{N}_{1,2}$, which at most can change the value of γ. All what can be done is then to try to check if Eq. (4.3.14) is satisfied. To this end, define

$$\sigma(m) = \frac{1}{|\vec{f}^1(L/2)||\vec{f}^2(L/2)|}\mathrm{Det}\begin{pmatrix} f_R^1(L/2) & -f_R^2(L/2) \\ i f_L^1(L/2) & i f_L^2(L/2) \end{pmatrix},$$

[2] The author thanks M.Neri for her help in implementing the required software. Various routines developed in Numerical Recipes [61] for differential equation solving, numerical integration and computation of Bessell functions have been employed. Clearly, since the differential equation becomes singular at $\tau_i = 0$, this point cannot be used for assigning the initial conditions. The initial condition (4.3.11) has then been imposed at a point $\bar{\tau}_i \ll \eta$, and checks have been performed the results not to depend on $\bar{\tau}_i$, if it is small enough. It has been also verified, by solving the equation from $\bar{\tau}_i$ backwards, that the solution so obtained remains finite when τ_i approaches 0, while divergences are encountered if perturbing the initial conditions, meaning that the regular solution of Eq. (4.3.10) is correctly selected by this procedure.

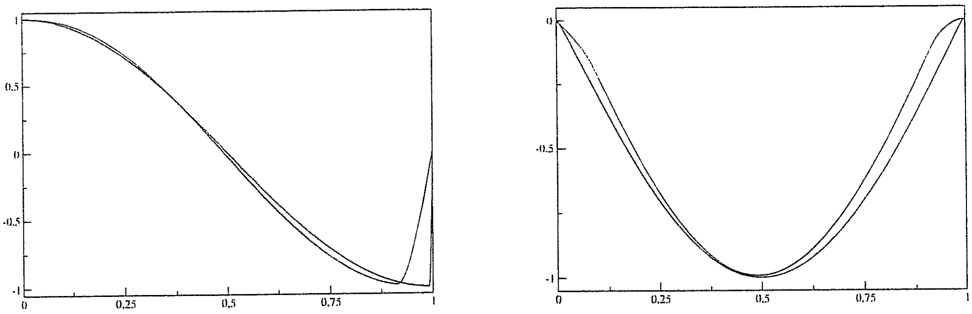

Figure 4.5: The L– and R–handed components of the first Kaluza–Klein mode, for two different values of the resolution parameter $\eta = L/10,\ L/100$, as a function of $\tau/L \in [0, 1]$. The case $\tilde{\kappa}_1 = 1$, $\tilde{\kappa}_2 = 3$ and $n_1 = -1$ is considered in the picture.

where $|\vec{f}^{1,2}(L/2)|$ is the modulus of the $(f_R^{1,2}, \pm i f_L^{1,2})$ vector, so that σ is the sine of the angle between $\vec{f}^1(L/2)$ and $\vec{f}^2(L/2)$. It only vanishes if (4.3.14) is satisfied at $\tau_{1,2} = L/2$. Vanishing of $\sigma(m)$, however, is equivalent to Eq. (4.3.14), since functions in the two sides of Eq. (4.3.14) are solutions, on the cylinder, to the same differential equation and then coincide if they are equal at one point. The mass–spectrum of fermions on $\mathcal{C}$ is given by the values of m for which $\sigma(m)$ vanishes.

As an example, consider the case $\tilde{\kappa}_1 = 1$, $\tilde{\kappa}_2 = 3$. Only for $n_1 = -1$, and then $\lambda = 0$, small masses are obtained, since it happens that $\sigma = 0$ can be only realized when $\omega^2 = m^2 - \lambda^2/r^2$ is positive, the bulk solutions having oscillating behavior. All states with $\lambda \neq 0$ have then mass at the $1/r$ scale, and decouple in the orbifold limit. A plot of $\sigma(m)$ is shown in Fig. 4.4 for different choices of the resolution parameter η. The zeroes of σ are seen to approach, as η decreases, the expected values of $m_k = k\pi/L$. This is consistent with the interpretation of $\mathcal{C}$ as an $S^1/\mathbf{Z}_2$ orbifold with even L–handed fields. Note that smaller values of the orbifold masses are better reproduced for a given resolution parameter η. For the first Kaluza-Klein state the relative errors with respect to the orbifold value π/L are $(0.09, 0.04, 0.009)$, linearly decreasing with $\eta = L/10, L/20, L/100$. For the second Kaluza-Klein state the relative errors are $(0.09, 0.05, 0.008)$, and similarly for the third one: $(0.09, 0.04, 0.009)$. One has, in practice, $\delta m/m \sim \eta/L$. Once the values of the masses are found by computing at the zeroes of $\sigma(m)$, the wave function for each massive state is easily computed. In Fig. 4.5, the L– and R–handed components of the wave function of the first Kaluza–Klein state are plotted, for $\eta = L/10,\ L/100$, as a function of $\tau \in [0, L]$. The wave–functions are given, for $\tau \in [0,\ L-\eta]$, by $f_R^1(\tau)$ and $i f_L^1(\tau)$; by $f_R^2(L-\tau)$ and $-i f_L^1(L-\tau)$, rescaled so that the resulting profile is continuous, in the $[L-\eta,\ L]$ interval. The L–handed component, as shown in the plot, approximates the cosine function with frequency L/π, while the R–handed one resambles a sine with the same frequency and a minus sign in front. This is precisely what expected for the wave function of the first Kaluza–Klein state on $S^1/\mathbf{Z}_2$. To conclude, the case $\tilde{\kappa}_1 = 1$, $\tilde{\kappa}_2 = -3$ can be considered. It should correspond, in the orbifold limit, to a segment with Neumann (Dirichlet) boundary condition for the L–(R–)handed field at the "1" extreme and the contrary at "2". In Fig. 4.4, the profile of $\sigma(m)$ obtained in this case is plotted for $\eta = L/10$, $L/20$, $L/100$. The zeroes approach now, as expected, $m_k = \pi/L(k + 1/2)$. One could also verify that the wave functions are correctly reproduced.

Conclusions

Basically, two main subjects have been treated in this thesis. The first one, discussed in Chapter 3, is the GHU mechanism for stabilizing the EWSB scale and in particular its implementation in $6D$ orbifold models. The second one, to which chapter 4 is devoted, is the arising of localized fermions at the fixed points of resolved orbifolds.

For what concern $6D$ GHU, we explored $SU(3)$ models on $T^2/\mathbf{Z}_N$ orbifolds and discussed the two new features which arise in the $6D$ case as compared to the $5D$ one, briefly reviewed in Sect. 3.1. Firstly, we have shown how the Higgs–W mass–ratio (and the compactification scale $1/R$ as well) is increased in single–Higgs models due to the arising of a tree–level quartic coupling. Secondly, we have addressed the problem of quantum stability of the EWSB scale, which is not any more guaranteed in the $6D$ case, due to the existence of the tadpole operator. We have shown the arising of the tadpole, whose coefficients we explicitly computed at one–loop, to be unavoidable in single–Higgs models. Moreover, an accidental cancellation of the leading divergence in the tadpole coefficients (which would be enough to stabilize the Weak scale) is found to be impossible without introducing fundamental scalars. The tadpole, then, is a serious problem for GHU models in $D \geq 6$. The possibility of cancelling it, with different gauge groups and/or numbers of ED, can be used as a guiding line for GHU model–building, as discussed in [62]. We found, however, that it may not be impossible to "live" with the tadpole in the case in which it is globally vanishing, or at least when the leading divergence in its integral is cancelled, as it is possible to arrange for in the $SU(3)$ $T^2/\mathbf{Z}_4$ case. As discussed in Sect. 3.5, indeed, a globally vanishing tadpole induces a non–trivial (but neutral) background for the A_z^8 field, and it does not trigger EWSB. Moreover, a massless scalar Higgs doublet is present in this background, so that neither the EWSB scale nor the Higgs mass are destabilized by the divergence which arise in the tadpole coefficients. Both quantities are generated by non local quantum correction, as in the $5D$ case. Though technically challenging, a more detailed study of models with globally vanishing tadpole would be extremely interesting. Realistic construction may also come, in

$6D$ orbifold context, from the search of different gauge groups. In the $\mathbf{G}_2$ case, for instance, a single–Higgs projection exists on $T^2/\mathbf{Z}_6$, and a semi–realistic prediction is found for the Weak angle in this case, so that the construction of an electroweak–unifying GHU model could be attempted. A single Higgs projection also exists for $SO(5)$ in $T^2/\mathbf{Z}_4$ and, interestingly, a local accidental cancellation of the tadpole can be achieved in this model. In the $\mathbf{G}_2$ case, however, the tadpole cannot be cancelled, even not globally, while the fermion content required for the cancellation in the $SO(5)$ case gives rise to an irreducible $6D$ gauge anomaly. Other gauge groups could be considered. Note that the possibility of the Higgs field to be a non–abelian continuous Wilson line, even though we discussed the opposite case, is not ruled out. In such a model, of course, no tree–level quartic coupling (and no quantum divergences) would appear, so that one would face again the same problems encountered in the $5D$ case and in the $SU(3)$ $T^2/\mathbf{Z}_2$ one, *i.e.* the smallness of m_H and $1/R$. Since the problem is basically numerical, however, (a factor four in m_H and $1/R$ would be enough) one should not neglect the possibility that different group–theoretical factors might significantly improve the situation.

In the fourth chapter of this thesis, fermion localization from orbifold resolution has been discussed. By studying the Dirac equation on resolved orbifolds, the arising of extra localized states, in a number which depends on the integer monopole charges labelling the resolution, has been demonstrated. We believe this is important for two reasons. Firstly, orbifold resolution is found to be a (very natural) mechanism through which localized fermions can be obtained, without need for any extra dynamics or extra fields than those required by the resolution of the orbifold singularity itself. Secondly, various bulk–brane fermion distributions are found to originate naturally from a single ED field, so that they have an unified origin. Field distributions which admit such a interpretation have been classified; we believe that this might provied a non–trivial constraint for model building.

A very important point is, in this respect, the generality of our results, *i.e.* the possibility that different resolutions might give rise to different brane fermions content. For studying the $\mathbb{C}/\mathbf{Z}_N$ cone (see Sect. 4.1 and Appendix B) we have employed a very general class of resolutions. Namely, we have considered a resolving base space with trivial topology (diffeomorphic to $\mathbb{R}^2$) and the same $O(2)$ isometry group of the corresponding orbifold, but with completely general ($O(2)$–invariant) profile for the gauge and the spin connections. We have shown, by computing it, the localized zero–modes spectrum on $\mathbb{C}/\mathbf{Z}_N$ to be independent on the detailed profile of the resolution. For what concern $T^2/\mathbf{Z}_N$ and $S^1/\mathbf{Z}_2$, on the contrary, we have used general resolutions for the singularities, but assumed the bulk to be described by a flat space to which the resolved singularities are "attached" in a $\mathcal{C}^\infty$ manner. We cannot exclude the possibility that more complicated resolutions, in which the bulk is not flat before the orbifold limit is taken, might give rise to different spectra.

Of course, various generalizations of this analysis should be considered. First of all, non abelian gauge fields should be added, so that one could study the general case of orbifold projections realizing the orbifold breaking $\mathcal{G} \to \mathcal{H} \subset \mathcal{G}$. This generalization is technically straightforward, at least as far as inner automorphisms are concerned, and leads to interesting constraints on the allowed fermion configurations. From the usual orbifold field theory point of view, we have complete freedom of putting at the orbifold fixed points an arbitrary number of $4D$ fermions in arbitrary representations of the surviving group $\mathcal{H}$, regardless of the representation and number of bulk fields. As it will be clear in the following simple example, much of this arbitrariness will be removed when imposing the orbifold model to admit our simple resolution. Consider an $SU(2)$ doublet of Dirac fermions $\psi = (\psi^+,\, \psi^-)^t$ on the $T^2/\mathbf{Z}_2$ orbifold, satisfying the following orbifold+torus boundary conditions:

$$\begin{aligned} \psi(-z) = \mathcal{P}\psi(z)\,, \qquad \mathcal{P} = e^{\frac{\pi i}{2}\sigma_3} e^{\frac{\pi i}{2} J_3}\,, \\ \psi(z+1) = \psi(z)\,, \\ \psi(z+U) = \psi(z)\,, \end{aligned} \tag{4.3.15}$$

where J_l $(l = 1,2,3)$ are the generators of $SU(2)$, normalized such that $J_3 = \mathrm{diag}(1,-1)$. When applied to the $SU(2)$ gauge fields, the boundary conditions (4.3.15) realize the breaking of $SU(2) \to U(1)$. The components $\psi^\pm$ of ψ satisfy the conditions given in Eqs. (4.2.2) and (4.2.1), with $t_{1,U} = 0$ and $p = \pm 1$, respectively. It is clear, from the form of the twist matrix $\mathcal{P}$ in Eq. (4.3.15), that the resolution of this orbifold configuration requires a background gauge field A_i, at each resolved $\mathbb{C}/\mathbf{Z}_2$ singularity, aligned with the J_3 direction: $A_i = A_i^3 J_3$. Each component $\psi^\pm$ of the fermion doublet can be treated, since the gauge background is diagonal, as an $U(1)$ fermion, like those considered in Chapter 4, with $A_i^\pm = \pm A_i^3$, and the spectrum of localized fermions can be read from Table 4.1. For ψ^+, we have $p_{1,i}^+ = +1$ and $q_{1,i}^+ = q_i \geq 0$. For ψ^-, $p_{1,i}^- = +1$ and $q_i^- = -q_{1,i}$. The two monopole charges $q_{1,i}^\pm$ are related by the fact that the $A_i^\pm$ backgrounds really come from the non–abelian gauge background $A_i^3 J_3$. Aside the usual bulk modes (one L–handed and one R–handed), q_i left-handed and an equal number of right-handed localized states are present at the fixed point $z_{1,i}$. All L–handed (R–handed) states have $+1$ (-1) charge under the surviving $U(1)$ gauge symmetry. The index of the Dirac operator is zero, as expected, since $\mathrm{Tr}[F] = 0$ for $SU(2)$. On the contrary, the most general configuration one can have from the point of view of the unresolved orbifold theory, would allow to put at the fixed points an arbitrary number of $4D$ chiral fermions with any charge under the $U(1)$ surviving gauge group.

An other extention which might be considered is the study of other fields, other then fermions, on the resolved orbifolds, in order to see if an analogous localization phenomenon does occur. Moreover, the orbifold resolutions considered in this thesis might be used to study operators localized at the fixed points. In some cases, as for the gauge tadpole discussed in Chapter 3, the consistent treatment of such operators seems indeed to require (see *e.g.* [63] and references therein) a resolution of the orbifold fixed points. In this respect, one remark is in order. Even though orbifold field theories do need a resolution at the level of regularization (*i.e.*, to perform consistent computations) when dealing with localized operators of particular types, there is no true physical need for resolving the singularities. The un–resolved orbifold models can be safely considered as effective field theories, the scale of the resolution (if any) being above (or at) its physical cut–off. It is then important to remark that the phenomenon of fermion localization observed here is completely independent on the resolution scale, which can be arbitrarily high. The allowed brane fermion configurations listed in this thesis can be directly considered in the unresolved orbifold model, as a remnant of the high energy resolution. All other effects related to the finite size of the singularities can be neglected.

Acknowledgements

First of all I warmly thank Marco Serone for these three years of stimulating scientific (and extra–scientific) friendly discussions and for the continuous support and encouragement. I'm also grateful to Luca Silvestrini and Claudio Scrucca, for the fruitful and extremely amusing collaboration, and to Giuliano Panico, for the many discussions we had. I also thank Matteo Salvatori, Giovanni Villadoro and, in particular, Fabio Zwirner. I acknowledge CERN and the university of Rome "La Sapienza", in which part of the work presented in this thesis was done, for hospitality.

A special thank to Marilisa Neri for her invaluable help during these years, and also for the useful informatic support. Let me also thank all friends here at SISSA for their enjoyable company, and my family for patience and support. Special thanks to Luca Mazzucato for his continuous chattering about physics and (mainly) politics.

Appendix A

Theta functions

The theta functions with characteristics $a, b = 0, 1/2$ are defined as follows:

$$\theta\begin{bmatrix} a \\ b \end{bmatrix}(z|U) = \sum_n q^{\frac{1}{2}(n+a)^2} e^{2\pi i(z+b)(n+a)}, \tag{A.0.1}$$

where $q = \exp(2\pi i U)$. Another common and more compact notation is the following:

$$\theta\begin{bmatrix} 1/2 \\ 1/2 \end{bmatrix} = \theta_1\,; \quad \theta\begin{bmatrix} 1/2 \\ 0 \end{bmatrix} = \theta_2\,;$$
$$\theta\begin{bmatrix} 0 \\ 0 \end{bmatrix} = \theta_3\,; \quad \theta\begin{bmatrix} 0 \\ 1/2 \end{bmatrix} = \theta_4\,. \tag{A.0.2}$$

These functions are related by the following identities:

$$\begin{aligned} \theta_2(z) &= \theta_1\Big(z - \frac{1}{2}\Big), \qquad \theta_3(z) = q^{1/8} e^{-i\pi z}\theta_1\Big(z - \frac{1}{2} - \frac{U}{2}\Big), \\ \theta_4(z) &= -iq^{1/8} e^{-i\pi z}\theta_1\Big(z - \frac{U}{2}\Big), \end{aligned} \tag{A.0.3}$$

omitting the dependence on the modular parameter U. They are clearly holomorphic functions, but they are not elliptic functions, since they are not exactly periodic. They satisfy the following periodicity conditions under $z \longrightarrow z+1$:

$$\begin{aligned} \theta_1(z+1|U) &= -\theta_1(z|U), \qquad \theta_2(z+1|U) = -\theta_2(z|U), \\ \theta_3(z+1|U) &= \theta_3(z|U), \qquad \theta_4(z+1|U) = \theta_4(z|U), \end{aligned} \tag{A.0.4}$$

and

$$\begin{aligned} \theta_1(z+U|U) &= -q^{-\frac{1}{2}} e^{-2\pi i z}\theta_1(z|U), \qquad \theta_2(z+U|U) = q^{-\frac{1}{2}} e^{-2\pi i z}\theta_2(z|U), \\ \theta_3(z+U|U) &= q^{-\frac{1}{2}} e^{-2\pi i z}\theta_3(z|U), \qquad \theta_4(z+U|U) = -q^{-\frac{1}{2}} e^{-2\pi i z}\theta_4(z|U), \end{aligned} \tag{A.0.5}$$

under $z \longrightarrow z + U$. One of the most important property of theta functions is that they have only one simple zero and no poles at all inside a fundamental domain $\mathcal{P}$. The zeroes z_i of the 4 theta functions θ_i ($i = 1, 2, 3, 4$) are at $z_1 = 0$, $z_2 = 1/2$, $z_3 = (1 + U)/2$ and $z_4 = U/2$, modulo lattice shifts.

Appendix B

Two dimensional spaces with $O(2)$ isometry group

B.0.4 The metric tensor in polar coordinates

The $O(2)$ group divides in $SO(2) \otimes \mathbf{Z}_2$; it will exist a coordinate system $\{x^i\}$ on which $SO(2)$ acts as rotation, and $\mathbf{Z}_2$ as parity:

$$\begin{aligned} x^i &\longrightarrow (h_\lambda)^i{}_j\, x^j\,, \\ x^i &\longrightarrow (P)^i{}_j\, x^j\,, \end{aligned} \tag{B.0.1}$$

where $h_\lambda = e^{i\lambda\sigma_2}$ and $P = \sigma_3$. The invariance under $O(2)$ of the line element implies for the metric g_{ij} to satisfy

$$\begin{aligned} g_{ij}(h_\lambda x)\,(h_\lambda)^i{}_l\,(h_\lambda)^j{}_k &= g_{lk}(x)\,, \\ g_{ij}(Px)\,(P)^i{}_l\,(P)^j{}_k &= g_{lk}(x)\,. \end{aligned} \tag{B.0.2}$$

In this coordinate system, of course, the metric must be regular ($\mathcal{C}^\infty$, with rank 2 and $(+,+)$ signature) at any point, including the origin $x = 0$, which has however the peculiar property of being fixed under $O(2)$. Take Eq. (B.0.2) at $x = 0$, it states the $O(2)$ invariance of $g_{ij}(0)$, which transforms as 2-tensor (in the $\mathbf{2} \otimes \mathbf{2}$) of $O(2)$. Since the only invariant $O(2)$ tensor is δ_{ij}, g must be proportional to the identity at $x = 0$. Moreover, if d derivatives of Eq. (B.0.2) are taken, one finds that, at $x = 0$, the d-th derivative of g, which is in the $\mathbf{2}^{d+2}$ tensor representation, must be invariant. A non trivial invariant can be only built when d is even, meaning that all odd derivatives of g_{ij} are enforced to vanish at zero.

The space will be more simply described in the polar coordinates $(\tau,\, \phi)$, being ϕ an angle and τ running on the positive real axis. The coordinate transformation reads

$$x^i = (h_\phi)^i{}_j\, v^i(\tau)\,, \tag{B.0.3}$$

being $v(\tau)$ a representative of $\mathbb{R}^2/SO(2)$ which can be chosen to have the form $v^i(\tau) = (r(\tau), 0)^i$, with $r(\tau)$ a smooth positive monotonic function vanishing at $\tau = 0$ and divergent for $\tau \to \infty$. Of course, this coordinate system is not appropriate for describing the origin, Eq. (B.0.3) being not invertible at $x = 0$, which indeed corresponds to $\tau = 0$ for any value of ϕ. In polar coordinates, the action of h_λ is simply a shift $\phi \to \phi + \lambda$. Accordingly, the Killing vector field K associated to $SO(2)$ has components $K^\tau = 0$, $K^\phi = 1$ and the Killing equation $(\mathcal{L}_K(g))_{ij} = 0$ states that

$$\partial_\phi g_{\tau\tau} = \partial_\phi g_{\tau\phi} = \partial_\phi g_{\phi\phi} = 0\,, \tag{B.0.4}$$

meaning that, in polar coordinates, all the components of the metric only depend on τ. Moreover, since the parity $P \in O(2)$ acts as $\phi \to -\phi$ in polar coordinates, $g_{\tau\phi}$ must vanish. The metric, up to now, is parametrized in terms of the two functions of τ, $g_{\tau\tau}$ and $g_{\phi\phi}$. The possibility of choosing $r(\tau)$, however, can be used to fix $g_{\tau\tau}$ to 1. This can be implemented by taking

$$\tau(r) = \int_0^r dr' \sqrt{g_{11}\left[x = (r', 0)\right]}\,, \tag{B.0.5}$$

which is indeed monotonic, invertible and positive.

Summarizing, the line element has the general form

$$ds^2 = d\tau^2 + \rho^2(\tau) d\phi^2\,, \tag{B.0.6}$$

having defined the function

$$\rho(\tau) = \sqrt{g_{\phi\phi}(\tau)} = r(\tau)\sqrt{g_{22}\left[x = (r(\tau), 0)\right]}\,, \tag{B.0.7}$$

which is, of course, undetermined, and encloses all the freedom one has in the definition of $\mathcal{R}$. Note that $\rho(\tau)$ is almost arbitrary, but not completely. At $\tau = 0$, in particular, it must satisfy some consistency conditions which ensure that the space, described in a coordinate system which is ill-defined in the origin, is however regular at that point, and the singularity is entirely due to the coordinate choice. By taking ∂_τ derivatives of Eq. (B.0.7), and remembering that odd derivatives of g_{ij} vanish at zero, one easily realizes that

$$\rho(0) = 0\,, \qquad \frac{d\rho}{d\tau}(\tau = 0) = 1\,, \qquad \frac{d^{2n}}{d\tau^n}\rho(\tau = 0) = 0\,, \tag{B.0.8}$$

for any n positive integer.

B.0.5 Globally defined one-forms

Be Ω a globally defined 1-form field, invariant under the isometry group $O(2)$, with negative intrinsic parity under the $\mathbf{Z}_2 \subset O(2)$. Its components $\Omega_i(x)$ in the "x" coordinate system considered in the previous section, in which $O(2)$ acts as in Eq. (B.0.1) are subjected to the condition

$$\begin{aligned} \Omega_i(h_\lambda x)(h_\lambda)^i{}_j &= \Omega_j(x)\,, \\ \Omega_i(Px)(P)^i{}_j &= -\,\Omega_j(x)\,, \end{aligned} \tag{B.0.9}$$

By looking at Eq. (B.0.9) and its derivatives at $x = 0$, one immediately recognizes that any d-th derivative of Ω_i must vanish at the origin if d is even, since it transforms in the $\mathbf{2}^{d+1}$ of $O(2)$. The Killing equation $\left(\mathcal{L}_K(\Omega)\right)_i = 0$, with K as in the previous section, states that both ϕ and τ components of Ω only depend on τ. Moreover, parity invariance $\phi \to -\phi$ enforces $\Omega_\tau(\tau)$ to be identically zero. The more general $O(2)$ invariant vector field Ω is then parametrized in term of one function of τ only, its ϕ component $\Omega_\phi(\tau)$, which can be expressed as

$$\Omega_\phi(\tau) = \Omega(\partial_\phi) = -r(\tau)\Omega_2\left[x = (r(\tau), 0)\right] \,,$$

in terms of the components $\Omega_i(x)$ of Ω in the "x" coordinates. Taking derivatives of the above equation w.r.t. τ and remembering that Ω_i and its even derivatives need to vanish at the origin, one immediately recognizes that $\Omega_\phi(\tau)$ must satisfy the following consistency conditions at $\tau = 0$

$$\Omega_\phi(\tau = 0) = 0\,, \qquad \frac{d^n}{d\tau^n}\Omega_\phi(\tau = 0) = 0\,, \tag{B.0.10}$$

where n is any odd positive number. Conditions (B.0.10), analogously to those in Eq. (B.0.8), are necessaries to ensure Ω to be well defined at the origin.

Bibliography

[1] R. Barbieri and A. Strumia, Phys. Lett. **B462**, 144 (1999), hep-ph/9905281.

[2] R. Barbieri, (2003), hep-ph/0312253.

[3] S. Weinberg, Phys. Rev. Lett. **59** (1987) 2607.

[4] N. Arkani-Hamed and S. Dimopoulos, JHEP **06**, 073 (2005), hep-th/0405159; G. F. Giudice and A. Romanino, Nucl. Phys. **B699**, 65 (2004), hep-ph/0406088.

[5] S. Weinberg, Phys. Rev. D **19**, 1277 (1979); L. Susskind, Phys. Rev. D **20**, 2619 (1979).

[6] D. B. Kaplan and H. Georgi, Phys. Lett. B **136**, 183 (1984). D. B. Kaplan, H. Georgi and S. Dimopoulos, Phys. Lett. B **136** (1984) 187.

[7] N. Arkani-Hamed, A. G. Cohen, and H. Georgi, Phys. Lett. **B513**, 232 (2001), hep-ph/0105239.

[8] N. Arkani-Hamed *et al.*, JHEP **08**, 021 (2002), hep-ph/0206020; N. Arkani-Hamed, A. G. Cohen, E. Katz, and A. E. Nelson, JHEP **07**, 034 (2002), hep-ph/0206021.

[9] C. Csaki, C. Grojean, L. Pilo, and J. Terning, Phys. Rev. Lett. **92**, 101802 (2004), hep-ph/0308038; C. Csaki, C. Grojean, H. Murayama, L. Pilo, and J. Terning, Phys. Rev. **D69**, 055006 (2004), hep-ph/0305237.

[10] N. Arkani-Hamed, S. Dimopoulos, and G. R. Dvali, Phys. Lett. **B429**, 263 (1998), hep-ph/9803315; I. Antoniadis, N. Arkani-Hamed, S. Dimopoulos, and G. R. Dvali, Phys. Lett. **B436**, 257 (1998), hep-ph/9804398.

[11] L. Randall and R. Sundrum, Phys. Rev. Lett. **83**, 3370 (1999), hep-ph/9905221; *ibid.* **83**, 4690 (1999), hep-th/9906064.

[12] K. Agashe, R. Contino, and A. Pomarol, Nucl. Phys. **B719**, 165 (2005), hep-ph/0412089.

[13] J. M. Maldacena, Adv. Theor. Math. Phys. **2**, 231 (1998) Int. J. Theor. Phys. **38**, 1113 (1999) arXiv:hep-th/9711200; S. S. Gubser, I. R. Klebanov and A. M. Polyakov, Phys. Lett. B **428**, 105 (1998) arXiv:hep-th/9802109; E. Witten, Adv. Theor. Math. Phys. **2**, 253 (1998) arXiv:hep-th/9802150.

[14] I. Antoniadis, Phys. Lett. **B246**, 377 (1990); I. Antoniadis, C. Munoz, and M. Quiros, Nucl. Phys. **B397**, 515 (1993), hep-ph/9211309; A. Delgado, A. Pomarol, and M. Quiros, Phys. Rev. **D60**, 095008 (1999), hep-ph/9812489; I. Antoniadis, S. Dimopoulos, A. Pomarol, and M. Quiros, Nucl. Phys. **B544**, 503 (1999), hep-ph/9810410.

[15] R. Barbieri, L. J. Hall, and Y. Nomura, Phys. Rev. **D63**, 105007 (2001), hep-ph/0011311.

[16] Y. Kawamura, Prog. Theor. Phys. **103**, 613 (2000), hep-ph/9902423; *ibid.* **105**, 999 (2001), hep-ph/0012125; *ibid.* **105**, 691 (2001), hep-ph/0012352; G. Altarelli and F. Feruglio, Phys. Lett. **B511**, 257 (2001), hep-ph/0102301; L. J. Hall and Y. Nomura, Phys. Rev. **D64**, 055003 (2001), hep-ph/0103125; A. Hebecker and J. March-Russell, Nucl. Phys. **B613**, 3 (2001), hep-ph/0106166; *ibid.* **B625**, 128 (2002), hep-ph/0107039.

[17] N. S. Manton, Nucl. Phys. **B158**, 141 (1979).

[18] D. B. Fairlie, Phys. Lett. **B82**, 97 (1979); J. Phys. **G5**, L55 (1979); P. Forgacs and N. S. Manton, Commun. Math. Phys. **72**, 15 (1980); G. Chapline and R. Slansky, Nucl. Phys. **B209**, 461 (1982); N. V. Krasnikov, Phys. Lett. **B273**, 246 (1991).

[19] S. Randjbar-Daemi, A. Salam, and J. A. Strathdee, Nucl. Phys. **B214**, 491 (1983).

[20] H. Hatanaka, T. Inami, and C. S. Lim, Mod. Phys. Lett. **A13**, 2601 (1998), hep-th/9805067.

[21] G. R. Dvali, S. Randjbar-Daemi, and R. Tabbash, Phys. Rev. **D65**, 064021 (2002), hep-ph/0102307.

[22] I. Antoniadis, K. Benakli, and M. Quiros, New J. Phys. **3**, 20 (2001), hep-th/0108005.

[23] C. Csaki, C. Grojean, and H. Murayama, Phys. Rev. **D67**, 085012 (2003), hep-ph/0210133.

[24] C. A. Scrucca, M. Serone, and L. Silvestrini, Nucl. Phys. **B669**, 128 (2003), hep-ph/0304220.

[25] C. A. Scrucca, M. Serone, L. Silvestrini, and A. Wulzer, JHEP **02**, 049 (2004), hep-th/0312267.

[26] G. Burdman and Y. Nomura, Nucl. Phys. **B656**, 3 (2003), hep-ph/0210257.

[27] L. J. Hall, Y. Nomura, and D. R. Smith, Nucl. Phys. **B639**, 307 (2002), hep-ph/0107331; N. Haba and Y. Shimizu, Phys. Rev. **D67**, 095001 (2003), hep-ph/0212166; K.-w. Choi *et al.*, JHEP **02**, 037 (2004), hep-ph/0312178; I. Gogoladze, Y. Mimura, and S. Nandi, Phys. Lett. **B560**, 204 (2003), hep-ph/0301014; *ibid.* **B562**, 307 (2003), hep-ph/0302176; Phys. Rev. **D69**, 075006 (2004), hep-ph/0311127.

[28] I. Antoniadis and K. Benakli, Phys. Lett. **B326**, 69 (1994), hep-th/9310151.

[29] A. Wulzer, "Gauge-Higgs unification in six dimensions," (2004), hep-th/0405168.

[30] G. von Gersdorff, N. Irges, and M. Quiros, Phys. Lett. **B551**, 351 (2003), hep-ph/0210134.

[31] R. Barbieri, R. Contino, P. Creminelli, R. Rattazzi, and C. A. Scrucca, Phys. Rev. **D66**, 024025 (2002), hep-th/0203039; S. Groot Nibbelink, H. P. Nilles, and M. Olechowski, Phys. Lett. **B536**, 270 (2002), hep-th/0203055.

[32] H. M. Lee, H. P. Nilles, and M. Zucker, Nucl. Phys. **B680**, 177 (2004), hep-th/0309195.

[33] L. J. Dixon, J. A. Harvey, C. Vafa, and E. Witten, Nucl. Phys. **B261**, 678 (1985); *ibid.* **B274**, 285 (1986).

[34] R. Jackiw and C. Rebbi, Phys. Rev. **D13**, 3398 (1976); R. Jackiw and P. Rossi, Nucl. Phys. **B190**, 681 (1981); V. A. Rubakov and M. E. Shaposhnikov, Phys. Lett. **B125**, 136 (1983).

[35] B. Bajc and G. Gabadadze, Phys. Lett. **B474**, 282 (2000), hep-th/9912232; I. Oda, Phys. Lett. **B496**, 113 (2000), hep-th/0006203; C. Ringeval, P. Peter, and J.-P. Uzan, Phys. Rev. **D65**, 044016 (2002), hep-th/0109194; H. Abe, T. Kobayashi, N. Maru, and K. Yoshioka, Phys. Rev. **D67**, 045019 (2003), hep-ph/0205344; W. Nahm and D. H. Tchrakian, JHEP **04**, 075 (2004), hep-th/0310231; R. Koley and S. Kar, Class. Quant. Grav. **22**, 753 (2005), hep-th/0407158; Mod. Phys. Lett. **A20**, 363 (2005), hep-th/0407159.

[36] S. Groot Nibbelink, H. P. Nilles, and M. Olechowski, Nucl. Phys. **B640**, 171 (2002), hep-th/0205012.

[37] M. Serone and A. Wulzer, "Orbifold resolutions and fermion localization," (2004), hep-th/0409229.

[38] A. Wulzer, "Orbifold resolutions with general profile," (2005), hep-th/0506210.

[39] G. Nordstrom, IN *APPELQUIST, T. (ED.) ET AL.: MODERN KALUZA-KLEIN THEORIES* 50-56. (PHYS. Z. 15 (1914) 504-506); T. Kaluza, Sitzungsber. Preuss. Akad. Wiss. Berlin (Math. Phys.) **1921**, 966 (1921); O. Klein, Z. Phys. **37**, 895 (1926); Nature **118**, 516 (1926).

[40] E. . Appelquist, T., E. . Chodos, A., and E. . Freund, P. G. O., "Modern Kaluza-Klein Theories,", USA: ADDISON-WESLEY (1987) 619 P. (FRONTIERS IN PHYSICS, 65).

[41] J. Scherk and J. H. Schwarz, Nucl. Phys. **B153**, 61 (1979); Phys. Lett. **B82**, 60 (1979).

[42] Y. Hosotani, Phys. Lett. **B126**, 309 (1983); Ann. Phys. **190**, 233 (1989); N. Haba, M. Harada, Y. Hosotani, and Y. Kawamura, Nucl. Phys. **B657**, 169 (2003), hep-ph/0212035.

[43] E. Witten, Nucl. Phys. **B258**, 75 (1985); L. E. Ibanez, H. P. Nilles, and F. Quevedo, Phys. Lett. **B187**, 25 (1987).

[44] A. Masiero, C. A. Scrucca, M. Serone, and L. Silvestrini, Phys. Rev. Lett. **87**, 251601 (2001), hep-ph/0107201.

[45] M. E. Peskin and D. V. Schroeder, "An Introduction to quantum field theory," USA: Addison-Wesley (1995) 842 p.

[46] D. Cremades, L. E. Ibanez, and F. Marchesano, JHEP **05**, 079 (2004), hep-th/0404229.

[47] H. Georgi, A. K. Grant, and G. Hailu, Phys. Lett. **B506**, 207 (2001), hep-ph/0012379.

[48] R. Contino, Y. Nomura and A. Pomarol, Nucl. Phys. B **671** (2003) 148 arXiv:hep-ph/0306259; K. Oda and A. Weiler, Phys. Lett. B **606** (2005) 408 arXiv:hep-ph/0410061.

[49] K. Symanzik, Nucl. Phys. **B190**, 1 (1981).

[50] N. Arkani-Hamed, A. G. Cohen, and H. Georgi, Phys. Rev. Lett. **86**, 4757 (2001), hep-th/0104005.

[51] G. Panico and M. Serone, JHEP **0505** (2005) 024 arXiv:hep-ph/0502255.

[52] C. A. Scrucca and M. Serone, Int. J. Mod. Phys. **A19**, 2579 (2004), hep-th/0403163.

[53] G. Martinelli, M. Salvatori, C. A. Scrucca and L. Silvestrini, arXiv:hep-ph/0503179.

[54] A. Delgado, A. Pomarol and M. Quiros, JHEP **0001** (2000) 030 arXiv:hep-ph/9911252.

[55] Y. Hosotani, S. Noda, and K. Takenaga, Phys. Rev. **D69**, 125014 (2004), hep-ph/0403106.

[56] G. von Gersdorff, N. Irges, and M. Quiros, (2002), hep-ph/0206029.

[57] C. A. Scrucca, M. Serone, L. Silvestrini, and F. Zwirner, Phys. Lett. **B525**, 169 (2002), hep-th/0110073.

[58] D. M. Ghilencea, S. Groot Nibbelink, and H. P. Nilles, Nucl. Phys. **B619**, 385 (2001), hep-th/0108184; S. Groot Nibbelink, H. P. Nilles, M. Olechowski, and M. G. A. Walter, Nucl. Phys. **B665**, 236 (2003), hep-th/0303101.

[59] Z. Chacko, M. A. Luty, and E. Ponton, JHEP **07**, 036 (2000), hep-ph/9909248.

[60] M. Abramowitz and I. A. Stegun, editors, *Handbook of mathematical functions: with formulas, graphs, and mathematical tables* (New York Dover, 1965).

[61] W. Press, S. Teukolsky, W. Vetterling, and B. Flannery, *Numerical Recipes in Fortran, 2nd ed.* (Cambridge University Press, 1992).

[62] C. Biggio and M. Quiros, Nucl. Phys. **B703**, 199 (2004), hep-ph/0407348.

[63] F. del Aguila, M. Perez-Victoria, and J. Santiago, JHEP **02**, 051 (2003), hep-th/0302023.